



## → GIOVE EXPERIMENTATION RESULTS

*A Success Story*



SP-1320  
October 2011

## → GIOVE EXPERIMENTATION RESULTS

**A Success Story**

## Acknowledgements

The results of the GIOVE experimentation have proved to be of incredible value in steering the Galileo Programme in a positive direction, and have greatly exceeded all expectations.

This report is a tribute to all those whose hard work and ideas have contributed to the GIOVE success story.

In the preparation of this publication, ESA acknowledges the contributions of the following organisations:

ASI  
CNES  
CSA  
DLR  
EADS Astrium  
Geo-Forschungs-Zentrum (GFZ)  
GMV  
INDRA Espacio  
INRiM  
International Laser Ranging Service (ILRS)  
Norspace  
Oerlikon  
RUAG Space  
Science and Technology Facilities Council (STFC)  
Scisys  
Selex Galileo  
Septentrio Satellite Navigation  
Space Engineering  
Space Research Centre (Polish Academy of Science)  
SpectraTime  
Surrey Satellite Technology Limited (SSTL)  
Telespazio  
Thales Alenia Space (TAS)  
VEGA Group

*ESA Galileo Project Office*

October 2011

### An ESA Communications Production

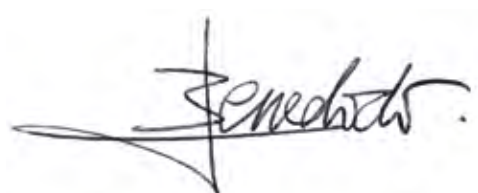
<b>Publication</b>	<i>GIOVE Experimentation Results: A Success Story</i> (ESA SP-1320 October 2011)
<b>Production Editor</b>	K. Fletcher
<b>Technical Editor</b>	S. Binda
<b>Editing/Layout</b>	Contactivity bv, Leiden, the Netherlands
<b>Publisher</b>	ESA Communications ESTEC, PO Box 299, 2200 AG Noordwijk, The Netherlands Tel: +31 71 565 3408 Fax: +31 71 565 5433 <a href="http://www.esa.int">www.esa.int</a>
<b>ISBN</b>	978-92-9221-415-9
<b>ISSN</b>	0379-6566
<b>Copyright</b>	© 2011 European Space Agency

## Foreword

With the launch of the first Galileo In-orbit Validation (IOV) satellites in 2011, and the progress towards the deployment of Full Operational Capability (FOC) starting in late 2012, the GIOVE mission has already demonstrated how Galileo will work in the space environment.

In the years since the launch of GIOVE-A in 2005, and GIOVE-B in 2008, the accumulated results of in-orbit and ground experimentation have confirmed the maturity of the most critical technologies, the validity of the analytical models and ESA's ability to meet the challenges of ensuring the performance of the Galileo system.

GIOVE has exceeded even our own expectations. It is a credit to all the industries involved, ESA, the European Commission and the EU Member States. It is proof of our capacity, but in particular our determination, to ensure that Galileo is a European success.

A handwritten signature in black ink, appearing to read 'J. Benedicto', with a stylized flourish extending to the left.

Javier Benedicto  
Galileo Project Manager, ESA



## Contents

<b>Foreword</b> . . . . .	<b>iii</b>
<b>1. Introduction.</b> . . . . .	<b>1</b>
1.1 GIOVE-A . . . . .	3
1.2 GIOVE-B . . . . .	5
<b>2. GIOVE-A: Satellite and Operations</b> . . . . .	<b>7</b>
2.1 Payload Operations . . . . .	9
2.2 Current Status of GIOVE-A. . . . .	13
<b>3. GIOVE-B: Satellite and Operations</b> . . . . .	<b>15</b>
3.1 Payload Operations . . . . .	17
3.2 The IOT Campaign . . . . .	18
3.3 Current Status of GIOVE-B. . . . .	24
<b>4. GIOVE Mission Segment</b> . . . . .	<b>25</b>
4.1 GPC Operations . . . . .	27
4.2 Evolution of the GIOVE Mission. . . . .	34
4.3 GIOVE Mission in the IOV/FOC context . . . . .	39
<b>5. GIOVE-A: Five Years of Experimentation Results</b> . . . . .	<b>41</b>
5.1 The Observation System . . . . .	43
5.2 Navigation Assessment and Orbit Models . . . . .	47
5.3 GIOVE-A Clock Characterisation . . . . .	54
5.4 IONO and BGD Experimentation . . . . .	59
5.5 Sensor Station Characterisation . . . . .	65
5.6 GPS to Galileo Time Offset (GGTO) Experimentation . . . . .	70
<b>6. GIOVE-B: Three Years of Experimentation Results</b> . . . . .	<b>75</b>
6.1 GIOVE-B Clock Characterisation . . . . .	84
6.2 GIOVE-B MBOC Characterisation . . . . .	87
<b>7. GIOVE: Added Value of the Experimentation and Risk Mitigation for the IOV phase</b> . . . . .	<b>91</b>
7.1 Navigation Assessment and Orbit Models . . . . .	93
7.2 GIOVE Clock Characterisation . . . . .	94
7.3 IONO and BGD Experimentation . . . . .	95
7.4 Sensor Station Characterisation . . . . .	96
7.5 GGTO Experimentation. . . . .	96

<b>8. GIOVE: A Verification Step in the Development of Galileo</b>	<b>99</b>
8.1 Key Performance Parameters	101
8.2 Use of GIOVE Results at the System Level	107
<b>9. Conclusions</b>	<b>111</b>
9.1 GIOVE-A	113
9.2 GIOVE-B	113
9.3 GIOVE Mission Segment	113
9.4 GIOVE-A: Five Years in Orbit	114
9.5 GIOVE-B: Three Years in Orbit	114
9.6 GIOVE: Added Value of the Experimentation and Risk Mitigation for the IOV Phase	114
9.7 A Verification Step in the Development of Galileo	114
<b>Annexes</b>	<b>117</b>
Bibliography	119
Acronyms and Abbreviations	123



# → INTRODUCTION



## 1. Introduction

In the late 1990s the European Space Agency began the development and industrialisation of two onboard clock technologies: the Rubidium Atomic Frequency Standard (RAFS) and the Passive Hydrogen Maser (PHM). This initiative turned out to be a key factor in the subsequent decision to build a European Global Navigation Satellite System. In 2004, the two technologies successfully passed ground environmental qualification tests (including vibration, shock and radiation).

In parallel, in 2002 ESA began the development of an experimental ground mission segment, called the Galileo System Test Bed version 1 (GSTB-V1). Within the GSTB-V1 project, tests of prototype Galileo orbit determination, integrity and time synchronisation algorithms were developed in order to generate navigation and integrity products based on GPS data.

In 2003, in the second step in the development of the Galileo system, the implementation of the GSTB-V2 began with the development of two satellites, the Galileo In-orbit Validation Elements (GIOVEs), GIOVE-A and GIOVE-B. These satellites have allowed the mitigation of a number of programmatic and technical risks during the Galileo IOV phase:

- securing the use of the frequencies allocated by the International Telecommunications Union (ITU) for the Galileo system;
- validating Signal-in-Space performance in representative environmental conditions;
- characterising the onboard clock (RAFS and PHM) technologies in space;
- characterising the radiation environment for the Galileo medium-Earth orbit (MEO);
- collecting the lessons learnt in the development, deployment and validation of the Ground Mission Segment, especially concerning the Galileo Experimental Sensor Stations (GESSs); and
- collecting the lessons learnt regarding the in-orbit performance and operation of the space segment onboard units.

Figure 1.1 shows the overall GIOVE system architecture, and the components necessary to achieve the above-mentioned objectives:

- the space segment, comprising the GIOVE-A and GIOVE-B satellites;
- the Ground Control Segment, comprising the Ground Satellite Control Centres (GSCs) in Guildford (UK) for GIOVE-A and in Fucino (Italy) for GIOVE-B; and
- the GIOVE Mission Segment infrastructure to support the experimentation activities.

This report describes the GIOVE system and summarises the operations and experimentation activities carried out until mid-2011 (unless otherwise stated).

### 1.1 GIOVE-A

GIOVE-A was built by SSTL. This 3-axis-stabilised satellite has a cube-shaped body with dimensions  $1.3 \times 1.8 \times 1.65$  m, a launch mass of 600 kg and a power demand of 700 W satisfied by two wings of Sun-tracking arrays, each 4.54 m long. The satellite has a butane propulsion system with two tanks each holding 25 kg (Figure 1.2, left).

The triply redundant payload transmits Galileo signals in two separate frequency channels. The main elements of the GIOVE-A payload are:

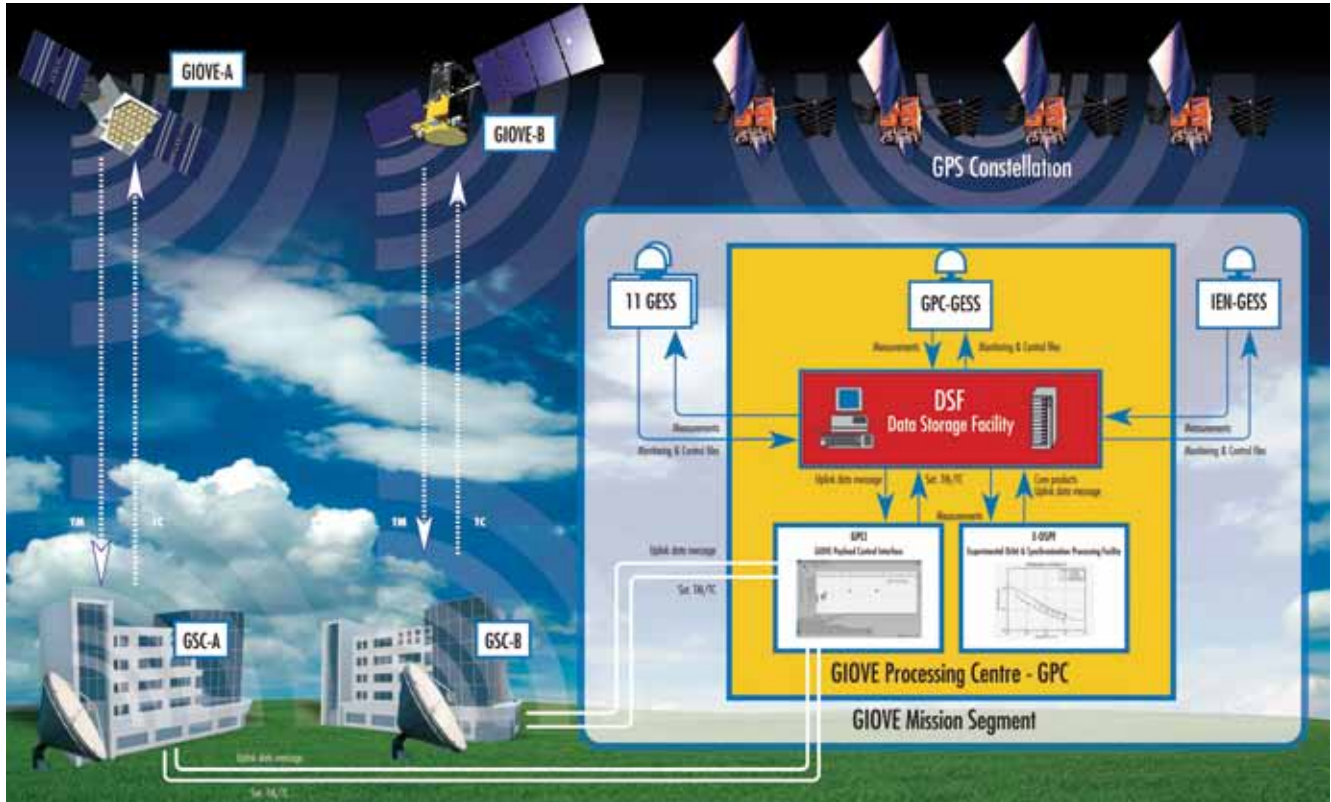


Figure 1.1. GIOVE system architecture.

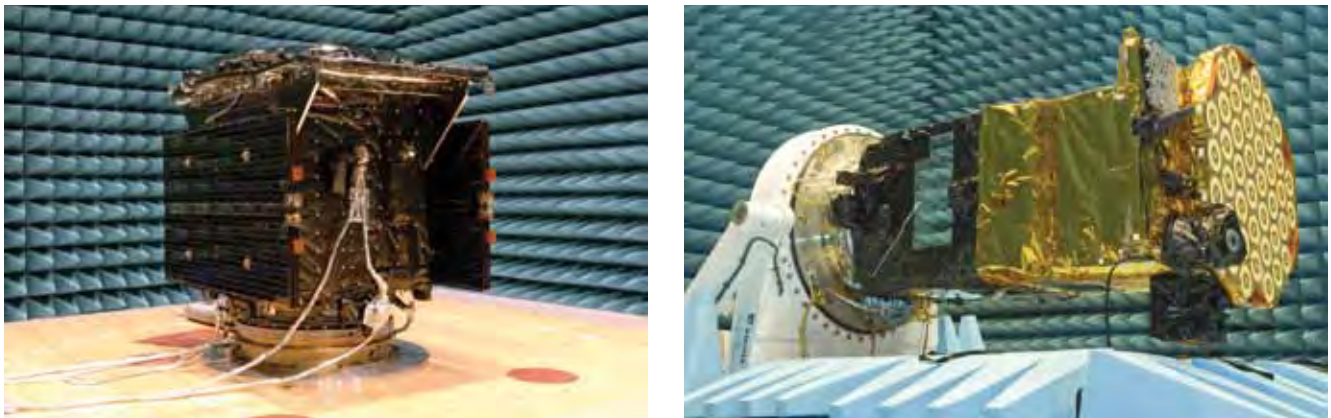


Figure 1.2. GIOVE-A (left) and GIOVE-B (right) during testing.

- the antenna: a phased array of individual L-band elements, illuminating the whole visible Earth below;
- the signal generation units to create representative Galileo signals;
- the clocks: two cold redundant, compact RAFS clocks with a stability of 10 ns per day, that are the result of ESA developments;
- two types of radiation monitor to characterise the MEO environment; and
- a GPS navigation receiver to experiment with autonomous localisation in MEO orbit.

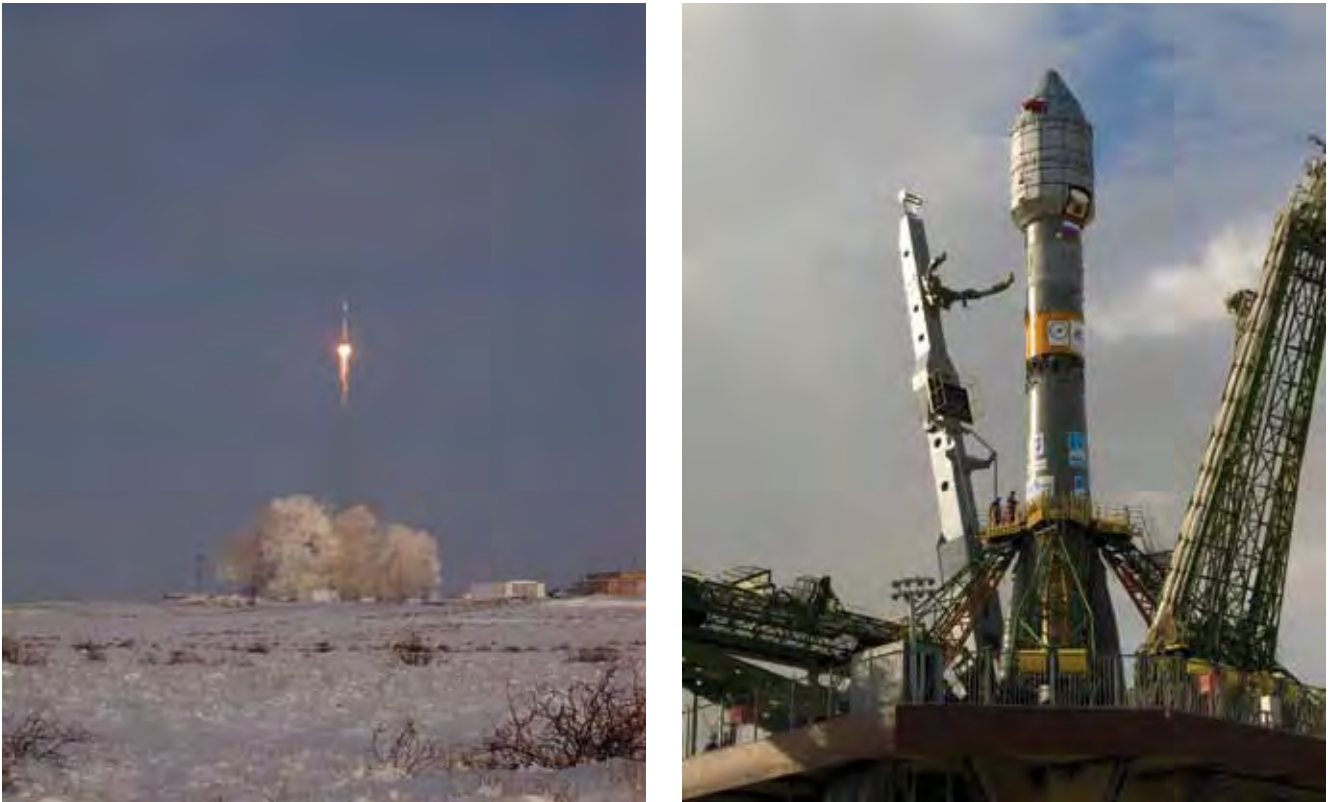


Figure 1.3. The launches of GIOVE-A (*left*) and GIOVE-B (*right*).

## 1.2 GIOVE-B

GIOVE-B was built by a consortium led by Astrium GmbH. When stowed, the 3-axis-stabilised satellite has dimensions  $0.95 \times 0.95 \times 2.4$  m, and a launch mass of 530 kg. Its two solar wings, each 4.34 m long, supply up to 1100 W. The propulsion system has a single tank carrying 28 kg of hydrazine (Figure 1.2, right).

The doubly redundant payload transmits a Galileo signal on two separate frequency channels. The main elements of the GIOVE-B payload are:

- the antenna (different from that on GIOVE-A): a phased array of individual L band elements, illuminating the whole visible Earth below;
- a signal generation unit (different from that on GIOVE-A) that is able to provide different types of signal, including the Multiplexed Binary Offset Carrier (BOC), the latest generation signal agreed between the European Union and the United States;
- the clocks, both the result of ESA developments: a PHM (stability 1 ns per day) that is the most accurate clock for navigation ever flown in space, and two compact RAFS clocks (stability 10 ns per day), one of which will be in hot redundancy with the PHM, and the other in cold redundancy; and
- a radiation monitor (different from that on GIOVE-A) to characterise the MEO environment.

The two satellites were successfully launched from Baikonur, Russian Federation, GIOVE-A on 28 December 2005 and GIOVE-B on 26 April 2008 (see Figure 1.3). For both satellites, the expected lifetime was 27 months, including the in-orbit test campaign. Due to the very good performance shown at the end of their lifetimes, both the GIOVE-A and GIOVE-B missions were extended.



**→ GIOVE-A: SATELLITE  
AND OPERATIONS**





## 2. GIOVE-A: Satellite and Operations

The GIOVE-A Signal-in-Space (SIS) system is almost fully representative of the Galileo system in terms of radio frequency and modulation, as well as chip rates and data rates. However, the spreading codes are different. Furthermore, the navigation message is not representative in terms of the structure and contents, and is used for demonstration purposes only.

Following a successful launch and early operations phase (LEOP) and platform commissioning phase, the payload units were commissioned in January 2006. The planned operations to commission the payload and perform the initial In-orbit Test (IOT) lasted almost two months. Subsequently, an Extended IOT (E IOT) measurement campaign lasted a further three to four months before the routine operations phase commenced. An overview of the initial GIOVE-A operations is presented in Figure 2.1.

### 2.1 Payload Operations

During the IOT campaign, a number of different signal modes were transmitted from GIOVE-A to confirm the correct functionality and performance of the payload in orbit, and also to gather sufficient data to allow ESA to claim that the Galileo frequency filings had been brought into use. GIOVE-A has three signal generation chains in the navigation payload. All initial activities were performed on the nominal payload A chain. Once the frequency filing activities were complete, the two redundant payload chains were then commissioned.

Figure 2.2 summarises the GIOVE-A payload operations. The operational time between 11 November 2010 and 30 April 2011 was 98.9%. In the period 22 February 2006 to 28 April 2009, the operational time on the payload was 93.9%. The availability between 28 April and 31 October 2009 was 55.0%, but if the repositioning period from 8 July to 24 August is excluded (as the payload was intentionally switched off during this period), this increases to 74.0%.

GIOVE-A transmits in two frequency bands at any one time as it can not broadcast in all three bands simultaneously. Thus, operations alternate between the E1–E5 and E1–E6 signals as required for each experimentation activity. Typically, E5–E1 signals are preferred for the clock characterisation experiments.

In the period from February 2006 to April 2011, GIOVE-A was transmitting mainly two nominal dual frequency signal modes: E5 ALTBOC – E1 Interplex (56.4% of the time) or E6 Interplex – E1 Interplex (31.2% of the time; see Table 2.2

Figure 2.1. GIOVE-A operations.

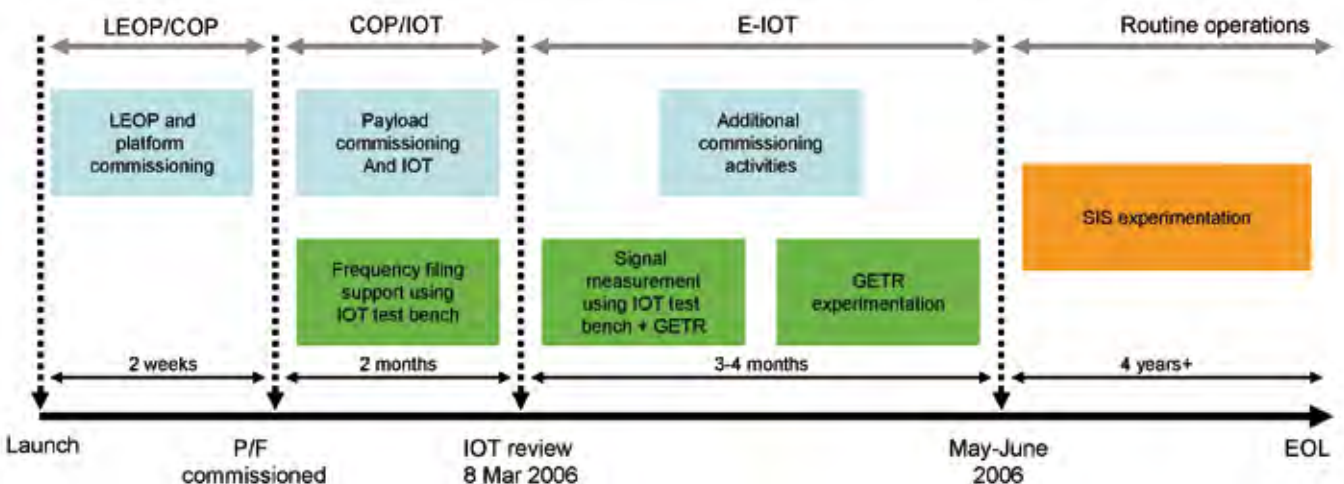
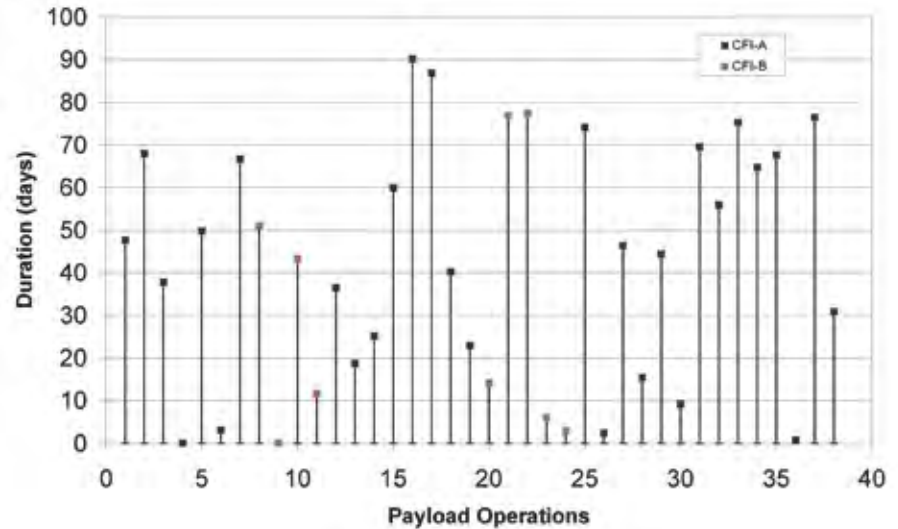


Figure 2.2. GIOVE-A payload operations.  
CFI A – nominal chain;  
CFI B – redundant chain.



for an overview). The rest of the time, GIOVE-A was either transmitting other signal modes (1.3%), or not transmitting (11.2%).

### Chilbolton Test Station

The GIOVE-A in-orbit test campaigns made use of the 25-m dish at the Chilbolton Observatory in the UK, which is owned and operated by the Science and Technology Facilities Council (STFC).

Based on the lessons learnt during the first GIOVE-A IOT campaign, a number of upgrades were performed at the station, including:

- the fabrication and installation of a new L-band feed, which led to an improved noise floor and provided better cross polar discrimination;
- a fast feed changer, in order to allow rapid switching from meteorological to Galileo measurements without having to repeat the full station calibration;
- the measuring equipment was moved from the control room to the radio cabin. This improved the reliability of the measurements by removing several hundred metres of cable and two amplifier units from the signal path through the receiver chain; and
- a better calibration procedure was used to derive  $T_{sys}$ ,  $G/T$ , and thus the antenna gain  $G$ .

The station calibration prior to the first IOT campaign followed a method that used the Artemis pilot signal as a reference at Artemis frequency, and inferred the gain across the band using  $G/T$  measurements from the Cassiopeia A radio source. In using this approach it was necessary to assume either a constant system temperature or a constant antenna efficiency across the band. For this initial calibration exercise, a constant system temperature was assumed.

Prior to the next campaign, however, when a constant temperature was assumed during the system calibration an unrealistically high efficiency was obtained. Alternatively, if the efficiency determined at the Artemis frequency was used across the band more realistic gains resulted. To resolve this issue an alternative method of determining the antenna gain was used.

Two Y-factors were extracted from the measurements. The first was the ratio between cold sky measurements and those obtained with a microwave absorber material placed in front of the feed. The second was the ratio between cold sky measurements and Cassiopeia measurements. These two Y factors were used to derive  $T_{sys}$  and  $G/T$ , respectively, and hence  $G$ . Figure 2.3 shows the tests using the absorber placed on the dish.

The performance of the Chilbolton station during the initial IOT campaign proved to be very good and generated high quality results to support both the frequency filing exercise and the initial commissioning and IOT measurements. The upgrades performed on the station for the subsequent campaigns were intended to refine the system to improve the reliability and quality of the results even further, and also to increase the efficiency of the operations and data capture.

## In-orbit Tests

A number of different signal modes were broadcast during the IOT campaigns, enabling a wide range of measurements to be taken. The key parameters measured for each of the modulated and continuous wave (CW) signals are listed in Table 2.1.

The nominal signals designated for investigation during the measurement campaigns are listed in Table 2.2. These signals consisted of the three primary signals broadcast during nominal operations. In addition, a CW signal was broadcast in each frequency band to confirm the Equivalent Isotropic Radiated Power (EIRP) of the payload transmissions.

Long duration passes were selected for the CW signals so that power measurements were taken over a large range of elevation angles. For all CW passes, alternate co- and cross polar measurements were taken. At least two IBUS measurements were interspersed with these power measurements to provide in band spectral plots.

During each pass dedicated to the modulated signal measurements, at least two IBUS plots were taken of each signal being broadcast, along with at least two full sweeps of the defined OBUS bands. Experience from the initial IOT campaign highlighted the benefit of having two independent measurements for each band of interest to help identify external sources of interference.

## EIRP and Received Power

The measurement of received power at Chilbolton was used to assess the EIRP of the GIOVE-A satellite. Within the measurement accuracy, the EIRP estimate agreed well with the results obtained during the initial IOT campaign. In general, more recent results are marginally lower than those obtained in 2006. The reason for this is considered to be an improved value of antenna gain rather than any degradation in output power from the payload.



Figure 2.3. Dish calibration measurements, Chilbolton station, UK.

Signal type	Measurements
Modulated signals	In-band spurious (IBUS) Out-of-band spurious (OBUS)
CW signals	EIRP In-band spurious (IBUS) Polarisation purity

Table 2.1. Key measurements during the IOT campaigns.

Signal type	Modulation
Modulated signals	E5 ALTBOC E6 Interplex E1 Interplex
CW signals	E5a CW E6 CW E1 BOC (15,0) CW

Table 2.2. Nominal signals.

Frequency	Minimum received power (dBW)
E1	-156.6
E5a	-154.4
E6	-154.1

Table 2.3. Minimum received power.

From the users’ perspective, the received power is a more important parameter than the EIRP, and the minimum received power in each frequency band is presented in Table 2.3. The results are within 1 dB of the requirements set out in the Signal-in-Space Interface Control Document (SIS ICD). It should be noted, however, that the transmitted power requirements on the GIOVE satellites are lower than those for the IOV satellites.

### CW Frequency

The frequency of each of the CW signals was measured, and the results were used to generate the Doppler shift at each point (Figure 2.4). Since the E1 CW signal is a BOC(15,0), there are two CW like signals offset either side of the E1 centre frequency by  $15 \times 1.023$  MHz. The frequency of each lobe was measured separately. The Doppler results for the E5 and E6 signals were continuous smooth curves, as the station was able to track the signals throughout the pass. The elevation of the E1 pass was  $84^\circ$ , however, which is above the limit of the dish. The discontinuity in the E1 lobes was caused by this break in the tracking of the signal.

### IBUS and OBUS

IBUS measurements were performed for both CW and modulated signals. The IBUS was assessed by performing a spectral sweep of the frequency band while a signal was being broadcast. The IBUS for each of the CW signals was analysed and no anomalies were present. The results from the repeat campaigns were very similar to those obtained in the initial IOT campaign. Similarly, the spectral plots obtained for the modulated signals were consistent with the measurements from the initial IOT campaign, indicating that there was no degradation in payload performance.

The OBUS bands investigated during the IOT were limited by the receiving bandwidth of the Chilbolton station, which covers the band from 1100 MHz to 1700 MHz. The OBUS bands contained within this frequency span are listed in Table 2.4. The noise floor of the Chilbolton measurements prohibited an in depth investigation of spurious signals down to the level of the specifications. Therefore, these in orbit tests were limited to looking for gross errors in the

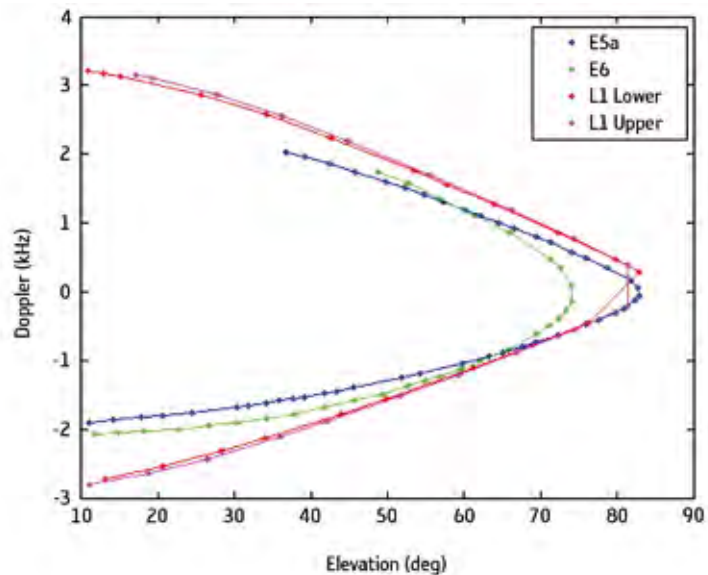


Figure 2.4. Measured Doppler on the CW signals.

Designation	Frequency band (MHz)
GPS L2	1215.60-1239.60
Glonass L2	1237.8275-1252.2220
Glonass L1	1592.9575-1610.0000
SAR	1544.2-1544.8
RA9	1330.00-1427.00
RA10	1610.60-1613.80
RA11	1660.00-1670.00

Table 2.4. OBUS bands investigated during the IOT.

transmissions and confirming that the performance was comparable with the results obtained in 2006.

None of the OBUS results indicated any unexpected anomalies and all of the plots were in good agreement with the initial IOT results. So, again, there was no evidence of any degradation in payload performance or functionality.

## 2.2 Current Status of GIOVE-A

Following the initial IOT campaign, four repeat IOT campaigns took place, in July 2007, February and August 2008, and February 2009.

In August 2009 the altitude of GIOVE-A was increased to 113 km above the nominal Galileo orbit, in order not to interfere with the upcoming Galileo IOV satellites. This was the first manoeuvre of its kind in MEO, and provided an important lesson in the Galileo constellation maintenance operations.

The transmission of navigation signals has since restarted, and a reduced measurement campaign was conducted by Chilbolton on the modulated signals. Measurement results indicated that the SIS was still as expected, and transmission continued, enabling the collection of additional experimental data.

As of August 2011, despite the loss of some redundancies including the TT&C transmitter TX-1 and the redundant side of the CMCU, GIOVE-A has been operating for 68 months, 41 months beyond its nominal lifetime, and performing pretty well. (The status of the GIOVE-A signal transmission can be checked online at [www.giove.esa.int](http://www.giove.esa.int))



**→ GIOVE-B: SATELLITE  
AND OPERATIONS**





### 3. GIOVE-B: Satellite and Operations

GIOVE-B continues to pursue the GIOVE Mission objectives, in particular:

- maintaining frequency filing;
- providing in orbit validation of the Galileo payload units, specifically the passive hydrogen maser and solid state power amplifiers (SSPAs) that were not flown on GIOVE-A;
- measuring the MEO radiation environment; and
- continuing the Signal-in-Space experimentation.

GIOVE-B's Signals-in-Space are fully representative of the operational Galileo system in terms of radio frequency and modulation, as well as chip rates and data rates. Before the launch, GIOVE-B's signal generator was upgraded to accommodate the Modified Binary Offset Carrier (MBOC) modulation on the E1 signal. In fact, the first signal successfully transmitted by GIOVE-B was the composite BOC (CBOC) version of the MBOC signal. However, the navigation message currently being transmitted is not representative of the fully operational version in terms of structure and contents, and is being used for demonstration purposes only.

In addition to the main IOT station in Redu, Belgium, ESA commissioned the Chilbolton IOT station in the UK – which is also used for GIOVE-A commissioning and experimentation – to provide complementary measurements for GIOVE-B as well.

This section presents the key results from the IOT campaign for GIOVE-B, which are based primarily on observations made at the Chilbolton station during May and June 2008.

#### 3.1 Payload Operations

As with the first Galileo satellite, GIOVE-B first underwent platform commissioning activities. In this phase, all the onboard systems underwent functional checks followed by the satellite's placement in its nominal Earth-pointing attitude and orbit control mode. Following the successful commissioning of the platform, the nominal payload units were switched on for the first time on 5 May 2008, and the first navigation signals were transmitted early on 7 May, as shown in Figure 3.1. The aim of the IOT campaign was to confirm that the payload functioned in orbit and that the operation of GIOVE-B's navigation signals was in line with the performance seen in ground tests completed before the launch of the satellite.

During the May–June campaign, GIOVE-B transmitted a variety of signals with which controllers could check out various performance parameters over all three frequency bands: E1, E5 and E6.

GIOVE-B has dual redundant payload chains. The first stage of the campaign involved testing and fully characterising the nominal payload chain, followed by a reduced set of tests performed on the redundant payload to verify the key parameters. This section presents the results for the nominal payload.

The default signals broadcast by GIOVE-B are E1 CBOC Interplex and E5 ALTBOC. These signals have been broadcast from the satellite since the end of the IOT campaign.

Figure 3.1. The first GIOVE-B Signal-in-Space.



## 3.2 The IOT Campaign

The IOT campaign consisted of preliminary checks on the station and verification of different characteristics of the payload.

### IOT Station Checks

Prior to commencing the IOT measurement campaign, a number of system checks were carried out on the Chilbolton IOT station. These checks were designed to confirm that the station was operating nominally and that its performance was in line with the most recent full calibration test results. Another important part of the system check procedure involved carrying out an interference scan to identify any terrestrial sources of interference. These results were referenced during the campaign if any unexpected spurious signals were discovered in the GIOVE-B measurements.

Previous Galileo test campaigns have used a precision spectrum analyser as the main measurement device. For the GIOVE-B campaign, a second similar device was installed to support the logging of large raw digitised data sets. An Offline Analysis of Signal-In-Space (OASIS) analysis tool set then used these digital samples to gain detailed insight into the signal spectrum envelope, modulation quality, time domain waveforms, code synchronism and accuracy at the chip level, and correlation loss. Figure 3.2 shows the Chilbolton signal acquisition and analysis system.

Telespazio controllers at the Fucino ground station in Italy commanded GIOVE-B to broadcast a number of different signal modes during the IOT campaign, which enabled a wide range of measurements to be taken. Table 3.1 shows the modulated and CW signals transmitted and characterised during the IOT campaign and the corresponding key parameters measured. These in-orbit results were then compared with those from ground tests, enabling ESA to confirm that the performance of the payload had not been affected during the satellite's launch and insertion into orbit.

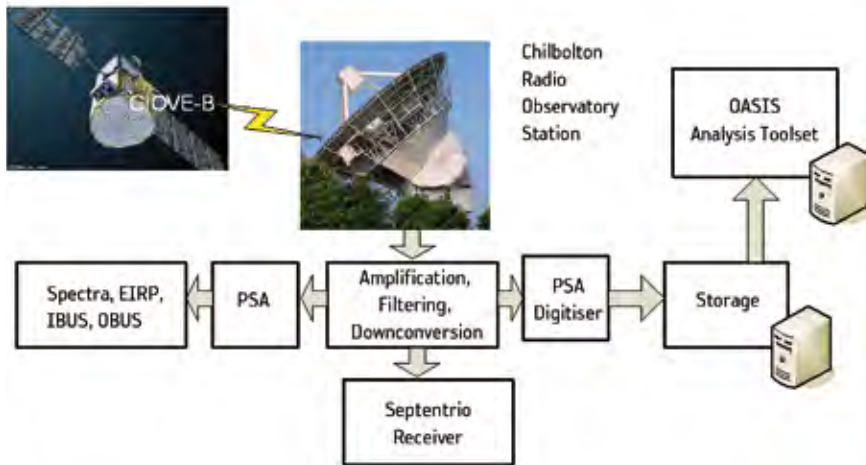


Figure 3.2. System for acquisition and analysis of GIOVE-B navigation signals at the Chilbolton test station.

Modulation	Modulation	Measurements
Modulation signals	E5 ALTBOC [15,10]	Spectral plots
	E6 Interplex {BOC[10,5],QPSK[5],QPSK[5]}	Occupied bandwidth
	E1 Interplex {BOC[15,2.5],BOC[1,1],BOC[1,1]}	Out-of-band spurious (OBUS)
	E1 CBOC {BOC[15,2.5],BOC[6,1],BOC[1,1],BOC[1,1]}	GIOVE receiver tracking
CW signals	E5a CW	Digitised data
	E5b CW	EIRP
	E6 CW	In-band spurious (IBUS)
	E1 BOC[15,0] CW	Polarisation purity
		Digitised data

Table 3.1. Modulation and key parameter measurements.

The GIOVE-B payload is capable of transmitting on two frequency bands simultaneously. Therefore, the modulated signals were always transmitted as part of a dual frequency signal mode, either E1–E5 or E1–E6. In addition, a CW signal was broadcast in each frequency band to confirm the Effective Isotropic Radiated Power of the payload transmissions.

During each satellite pass dedicated to measuring the modulated signals, at least two spectral plots were taken of each signal being broadcast, along with at least two full sweeps of the defined out-of-band spurious (OBUS) bands. Experience from previous IOT campaigns had highlighted the benefit of having two repeat measurements for each band of interest to help identify external sources of interference.

## EIRP and Received Power

Ideally, lengthier satellite transit paths should be assigned to the CW signals in order to enable the EIRP to be measured across a long cut through the antenna pattern. For all signals on the nominal payload, except E6 CW, two passes were dedicated to each CW signal to provide two different slices through the antenna pattern.

For users, probably the most relevant parameter of interest is the signal power they receive on the ground. This can be evaluated from the EIRP by subtracting the free space path loss experienced by the signals as they travel from the satellite to the user. Table 3.2 presents the minimum received power levels measured for each CW signal transmitted by GIOVE-B. These results were very much in line with those obtained during ground reference tests.

Table 3.2. Minimum received power levels.

Frequency	Minimum received power (dBW)
E1	-156.5
E5a	-152.1
E5b	-152.5
E6	-152.3

Table 3.3. Centre frequency measurements recorded at ESA's Redu station.

Date	PL A	Expected (MHz)	Measured (MHz)	$\Delta$ (Hz)
14 May 2008	E1 lower	1560.075000	1560.075044	44
14 May 2008	E1 upper	1590.765000	1590.765044	44
19 May 2008	E5a	1176.450000	1176.450032	32
20 May 2008	E5b	1207.140000	1207.140032	32
26 May 2008	E6	1278.750000	1278.750036	36

### CW Frequency

The centre frequencies of the CW signals were measured by ESA at the Redu station. The relative motion of the satellite was estimated to remove the Doppler shift from the measurements. ESA's Redu results are summarised in Table 3.3. The measured results are in good agreement with the expected centre frequency values, from a frequency filing point of view. The differences ( $\Delta$ ) are due mainly to uncertainties in the measurement system.

### Spectral Plots, IBUS and OBUS

Spectral plots were taken for every modulated signal to verify that the signals were being generated correctly. Figure 3.3 shows the E1 CBOC Interplex signal recorded at the Chilbolton station. As can be clearly seen, an asymmetry of around 1 dB appears in the BOC[15,2.5] major sidelobes. Note that in Figure 3.3, the spur at 1600 MHz is from a known terrestrial source of interference, and was not transmitted by the GIOVE-B payload.

Figure 3.4 presents similar spectral plots for the default modulated signals on the E5 and E6 frequency bands. The two spurs at 1250 MHz and 1300 MHz on the E6 plot are from known terrestrial sources of interference. The noisy spurs at the lower end of the E5 band represent interference from distance-measuring equipment (DME) transmitters at several airports in the vicinity of the Chilbolton station.

All spectral plots obtained during the IOT campaign compare well with the spectra measured during the reference ground tests. Similarly, an analysis of the IBUS for each of the CW signals detected no anomalies.

The OBUS bands investigated during the IOT campaign were limited by the receiving bandwidth of the Chilbolton station, which covers the RF spectrum from 1100 MHz to 1700 MHz. The noise floor of the Chilbolton measurements prevented an in depth investigation of spurious signals down to the level of the

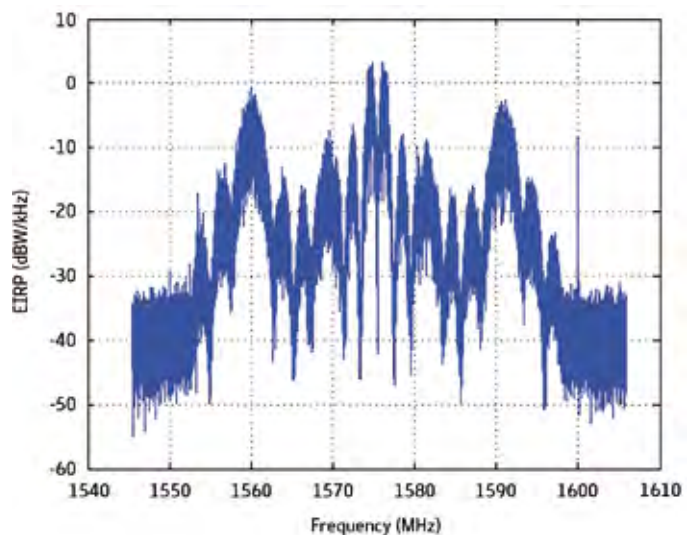


Figure 3.3. E1 CBOC Interplex spectrum.

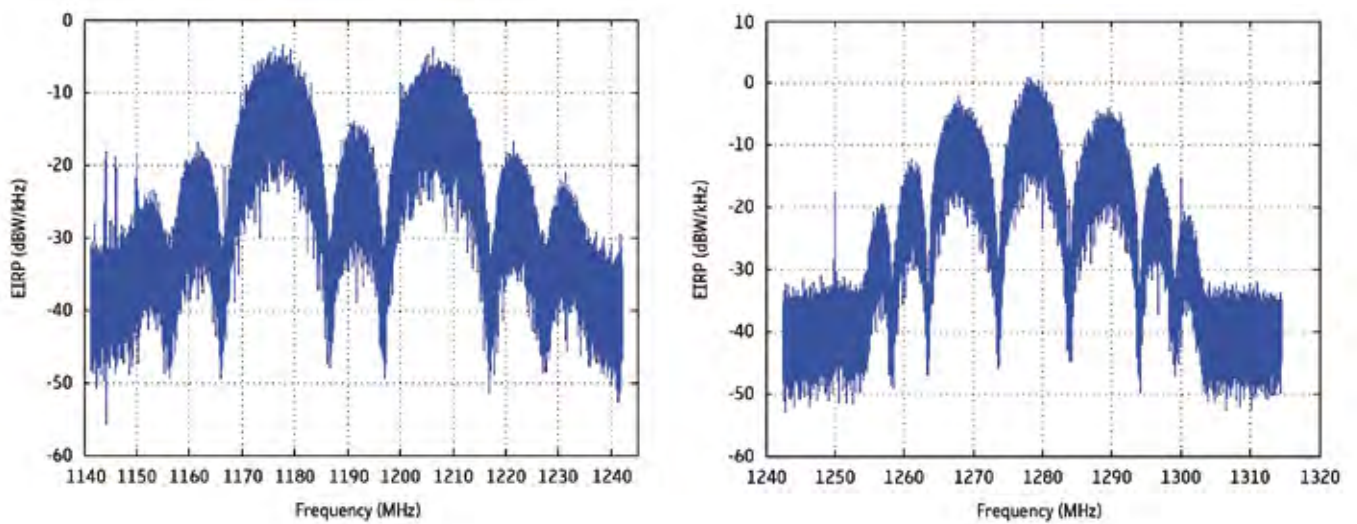


Figure 3.4. E5 ALTBOC and E6 Interplex spectra.

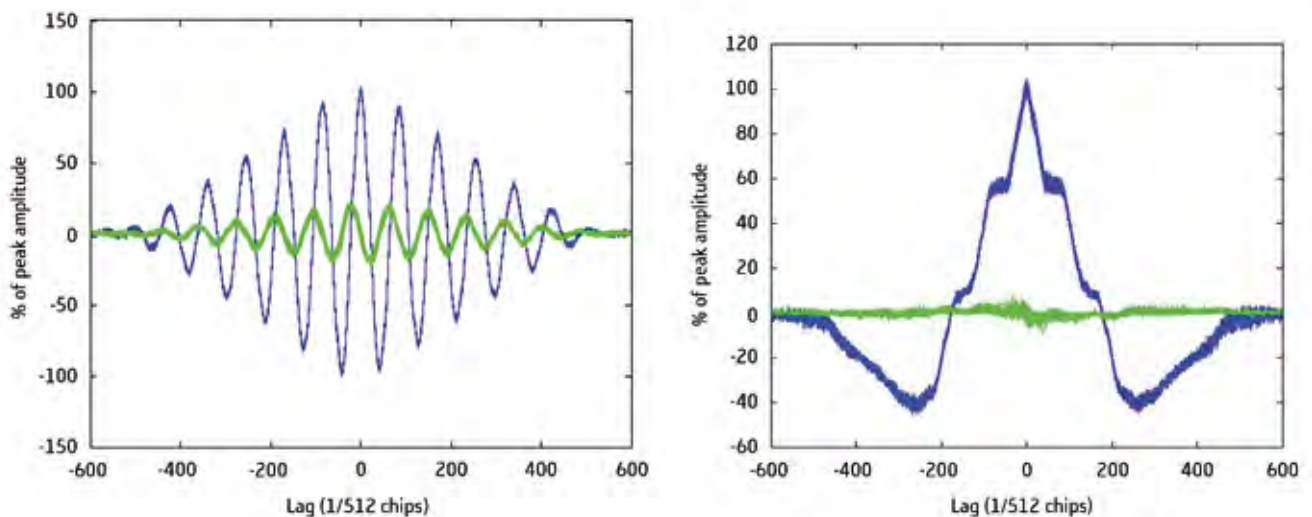
GIOVE-B specifications. These in-orbit tests were therefore limited to looking for gross errors in the transmissions. None of the OBUS results indicated any unexpected anomalies that could be attributed to the GIOVE-B payload.

## Receiver Tracking

A GIOVE experimental receiver has been installed at the Chilbolton station in a dual mode configuration that enables it to be connected either to the 25-m dish or to an omni-directional antenna. During the IOT campaign the receiver was connected to the 25-m dish to enable ESA to track the navigation signals with an excellent signal-to-noise ratio.

For each modulated signal, including the new MBOC signals, the receiver was used to log both navigation and measurement data. In addition, the receiver can measure and record the auto correlation functions (ACFs) of the signals. Figure 3.5 presents the auto-correlation functions measured for the E1-A BOC(15,2.5)-C and E1-BC CBOC(6,1,1/11)-S signal components. Figure 3.6 presents similar results for the E5 ALTBOC and E6-A BOC(10,5)-C signal components.

Figure 3.5. Auto-correlation functions for the E1-A and E1-BC CBOC signal components.



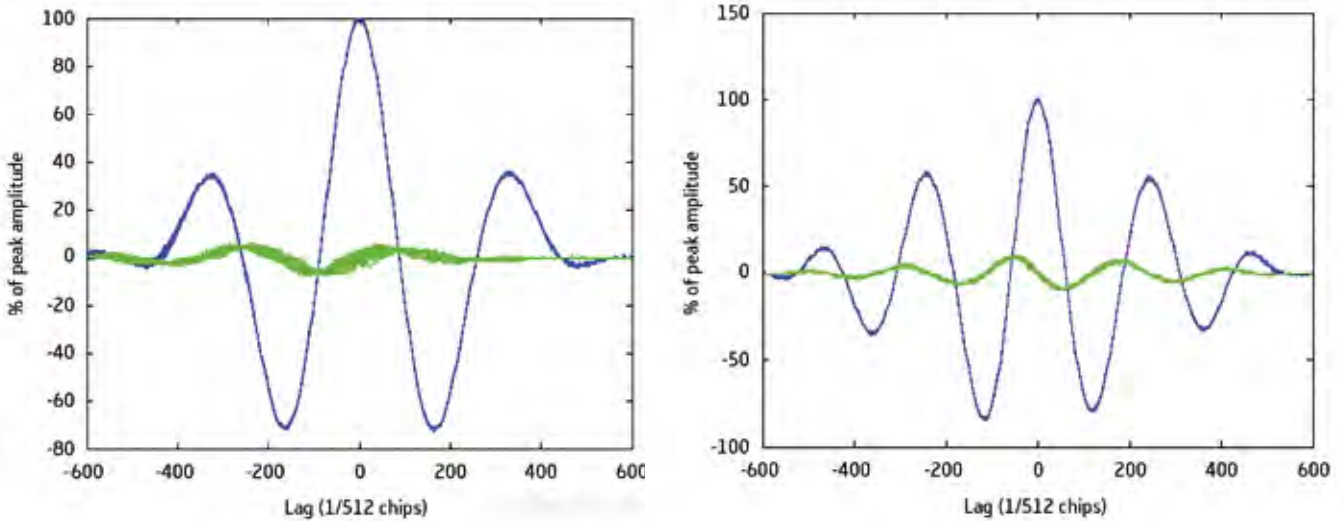


Figure 3.6. Auto-correlation functions for the E5 ALTBOC and E6-A BOC signal components.

All ACFs measured on the signals transmitted in orbit were in line with the reference ground results. Please note that the E1-A BOC [15,2.5] ACF is symmetrical and therefore easily tracked by the receiver.

### OASIS Results

Offline analyses were performed on digitally sampled segments of the GIOVE-B navigation Signal-in-Space received by Chilbolton station’s high-gain antenna and compared with the ‘ideal’ waveforms of such signals.

These analyses were used to gain detailed insight into the signal spectrum envelope, modulation quality, time domain waveforms, code synchronism and accuracy at the chip level, and correlation properties such as correlation loss and deviations from the ‘ideal’ shape. Figure 3.7 shows the E1 CBOC Interplex observed spectrum (red) against the ideal spectrum with equivalent power (blue).

The default GIOVE-B configuration for E1 consists of E1-A using a BOCc(15,2.5) signal on the quadrature component, and E1-B/C using CBOC modulation with power sharing 1/11 for BOC(6,1) and 10/11 for BOC(1,1) on the in-phase component of the carrier.

A slight imbalance, with decreasing amplitude towards higher frequencies, appeared in the observations at Chilbolton. After removing the estimated contributions from the measurement station, the average imbalance was estimated to be of the order of 1 dB.

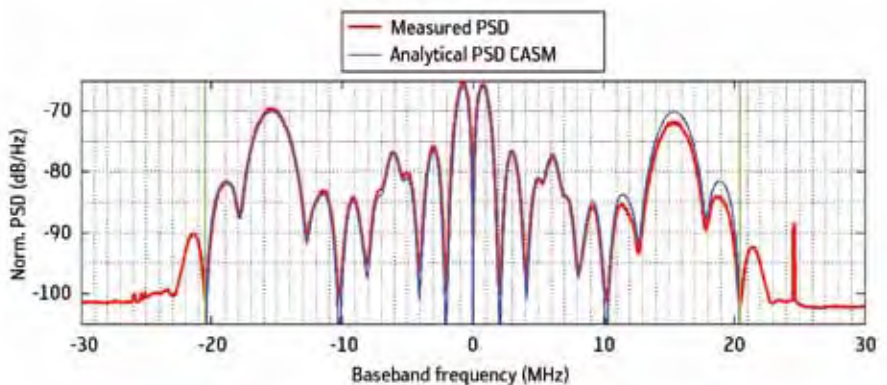
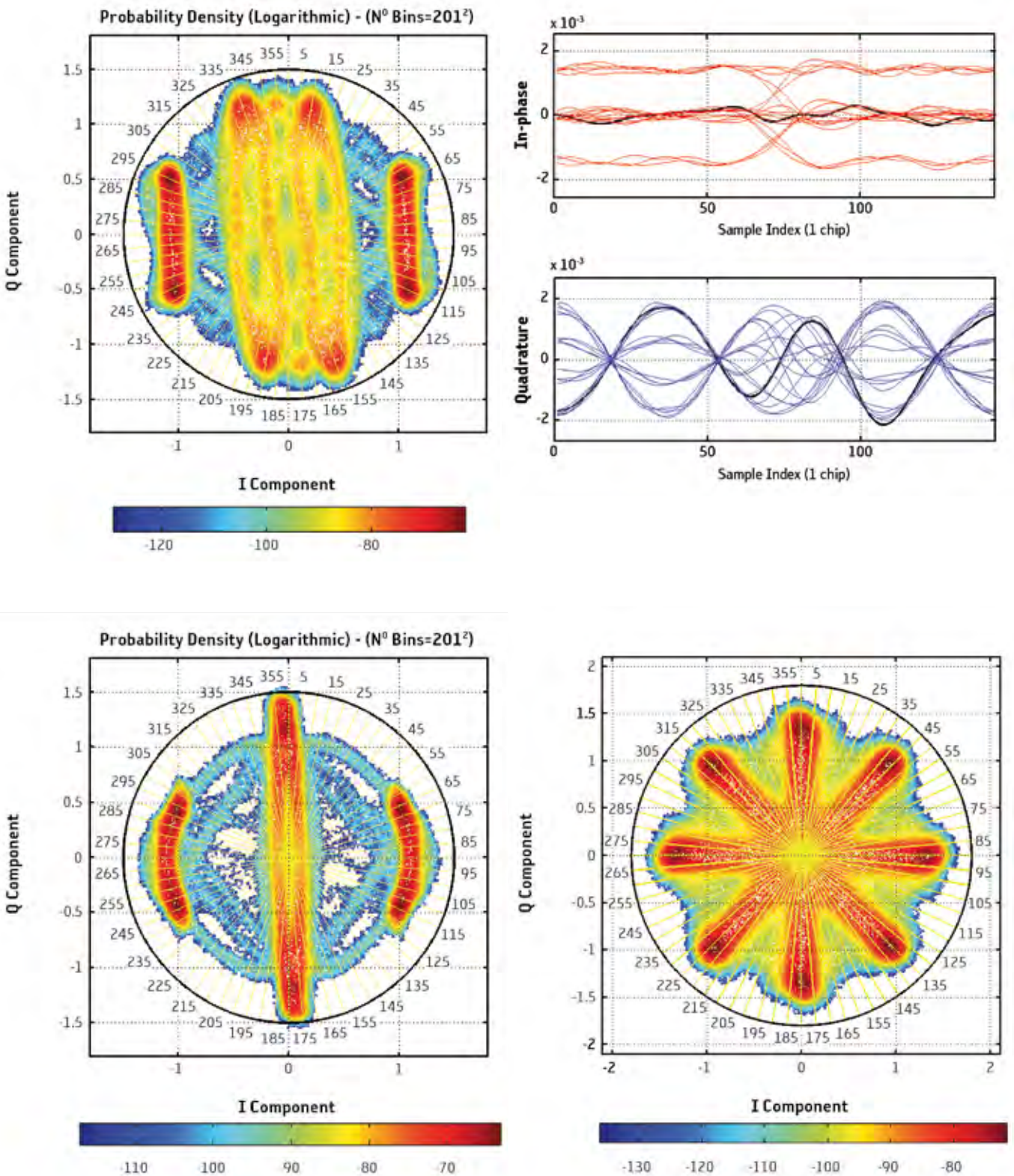


Figure 3.7. OASIS E1 CBOC Interplex spectrum.

After baseband conversion, the modulation quality can be analysed from scatter plots in the form of histograms, as shown in Figure 3.8.

The OASIS results for all the signal samples were encouraging, and confirmed that GIOVE-B was transmitting the expected navigation signals.

Figure 3.8. E1 CBOC (top left), E6 Interplex (bottom left), and E5 ALTBOC (bottom right) phase states and E1 CBOC time domain plots (top right).



### 3.3 Current Status of GIOVE-B

Following the initial IOT campaign, five repeat IOT campaigns took place in February and September 2009, February and September 2010, and February 2011, which included taking the following measurements:

- EIRP, polarisation purity, centre frequency and IBUS on the E5a, E5b, E6 and E2E1E1 BOC(15,0) CW signals; and
- spectral plots, OBUS and Galileo Experimental Test Receiver (GETR) auto-correlation functions for the E5 ALTBOC, E6 Interplex and the E1 Interplex CBOC and time-multiplexed BOC (TMBOC) modulated signals.

In addition, multiple sets of digitised raw data samples were recorded for ESA to post-process using its offline analysis tools.

The report on the February 2011 repeat campaign concluded that all of the results showed good agreement with those from the previous IOT campaign and indicated that there had been no significant changes in the performance of the navigation payload since the previous campaign. GIOVE-B was maintaining consistent performance in the navigation signals being transmitted and there were no signs of degradation.

Over the period from May 2008 to June 2011, the GIOVE-B signal availability has been 96.9%. For 79.9% of the time GIOVE-B broadcast the signal couple E1–E5, and for 11.2% it broadcast the couple E1–E6. For the rest of the time it broadcast other signal modes or it was not broadcasting.

As of August 2011, GIOVE-B has been operating for 40 months, 13 months beyond its nominal 27-month lifetime. GIOVE-B has not suffered the loss of or damage to any unit. (The status of the GIOVE-B signal transmission can be checked online at [www.giove.esa.int](http://www.giove.esa.int))



**→ GIOVE MISSION SEGMENT**



## 4. GIOVE Mission Segment

The GIOVE Mission Segment infrastructure consists of two main elements: the worldwide network of Galileo Experimental Sensor Stations (GESSs), and the GIOVE Processing Centre (GPC) laboratory located at ESA/ESTEC (see Figure 4.1).

### 4.1 GPC Operations

The GPC generates several core products of interest to external registered users in the fields of satellite clock characterisation, precise orbit estimation, navigation message generation, Galileo sensor station error budget characterisation, broadcast group delay modelling, and satellite telemetry data. The GPC is based on a standard computing centre whose hub is a Data Server Facility (DSF) consisting of several Sun servers with a total data storage capacity of 3 TB.

The main objective of the GPC operations is to support experimentation activities by ensuring the collection of data required by the Experimental Orbitography and Synchronization Processing Facility (E-OSPF) and for the offline experiments, as well as by processing and distributing Orbit Determination and Time Synchronisation (ODTS) data, including the navigation messages for GIOVE-A and GIOVE-B. Besides handling the system monitoring and control, an important role of the GPC is to provide quality assessments of station characteristics, transmitted signals, collected data and overall processing. The global objective is for the GPC to act as an early prototype for the Galileo Mission Segment by providing feedback to the Galileo programme on issues related to the design and exploitation of the final system.

Figure 4.1. GIOVE sensor stations.



The GPC operations can be grouped into three functional chains:

- the *data collection chain* consists of the collection of data from the GESS stations and their storage in the central Data Server Facility at the GPC;
- the *payload interface chain* involves interfacing with the GIOVE Satellite Control Centres (GSC-A/B) for telemetry, flight dynamics, operations and navigation data exchange;
- the *processing chain* (navigation message loop) involves ensuring the routine generation of near-real-time orbit and clock information based on data collected by the GESSs, and the generation and uplink of the computed GIOVE-A navigation messages through the relevant GIOVE Satellite Control Centre.

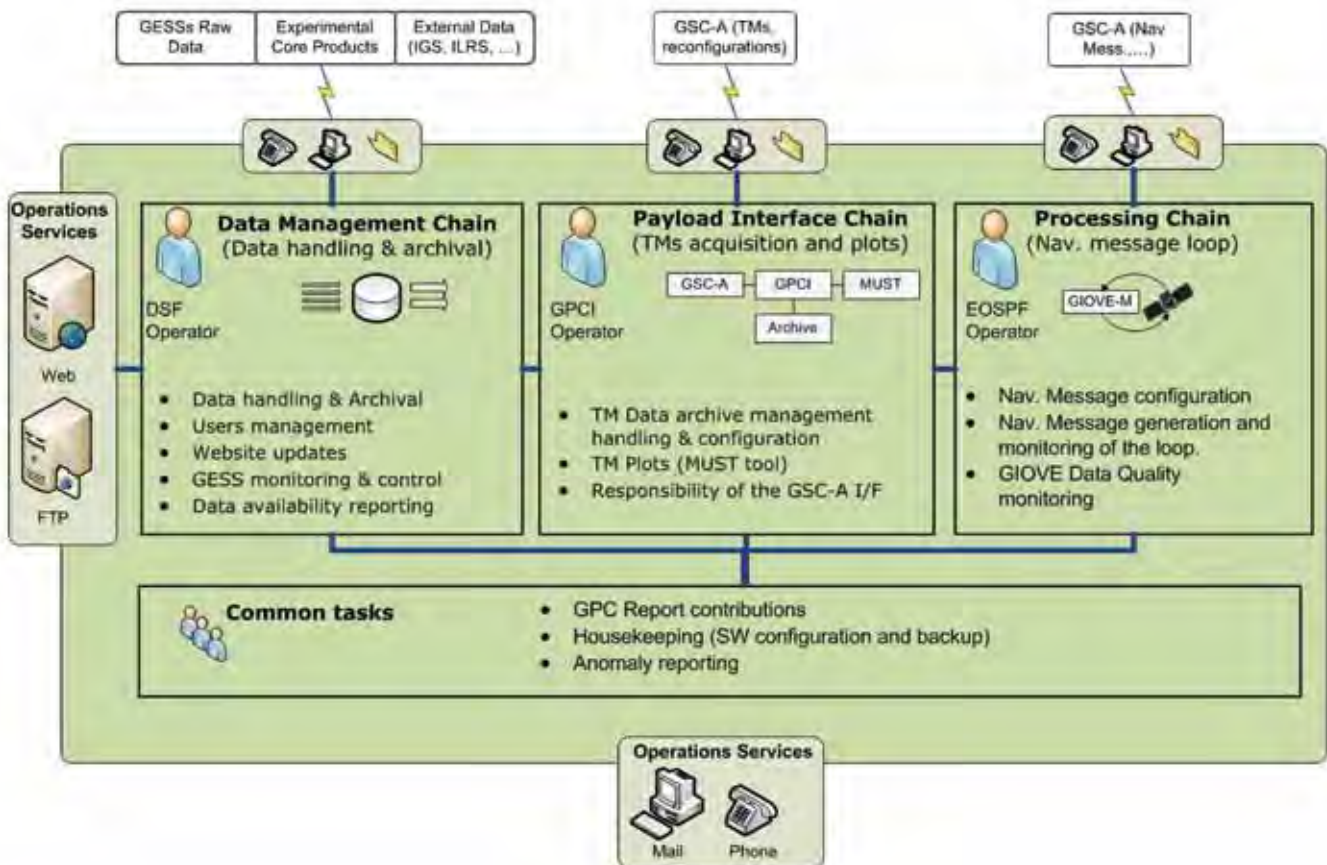
In addition to these three functional chains, the operators share a number of common tasks. These mainly involve housekeeping activities, anomaly management and provision of services to external users supporting the GIOVE Mission experimentation.

The three GPC functional chains and common tasks are reflected in the organisation of the GPC team, as depicted in Figure 4.2. The nominal GPC operations started in April 2007.

### Data Collection Chain

A high level of automation is built into the GPC system in order to ensure the uninterrupted collection of signal data, and to minimise the need for manual intervention and control.

Figure 4.2. GPC operational chains.



The first chain of the GPC operations involves near-real-time systems for monitoring data collection processes and for assessing the quality of the collected data.

The near-real-time monitoring and control of data collection processes of the GPC facility is, to a large extent, a manual operator-driven task involving direct operative, preventive and intervention actions. Various tools have been developed on a needs-driven basis to facilitate and improve the operations. The GIOVE Mission system for monitoring data collection processes is provided by the monitoring and control console of the DSF. The outcomes of the data collection attempts initiated by the DSF are displayed on the console.

The near-realtime monitoring of the collected data is carried out by means of a data availability tool dedicated to the continuous visualisation and reporting on collected GIOVE observables and by a data quality tool (see Figure 4.3). The GPC operations room hosts two large monitors driven by near-real-time visual aids, flags and alarm systems that enable the operators to take rapid action when needed. The large screens can also be driven by the data availability tool (Figure 4.4).

The complexity of the overall system requires the GPC to interpret monitoring plots for the early detection of problems at the system, processing network and GESS site levels. This requires the GPC to perform a number of checks to verify the origin of any data unavailability.

The GESSs are unmanned and operated remotely from the GPC. The GPC also verifies the data unavailability against the planned/known remote and local maintenance and operations. The maintenance and remote operations shown in Figure 4.5 explain most of the missing observations

The GPC is also required to keep in contact with experimenters to ensure they are aware of station characteristics that could impact on data availability. Missing observations may be linked to high multipath and/or masking angle problems and interference at the GESS sites.

The data received from the GESS network is processed by a dedicated facility, and its quality is monitored using a specific data quality tool (DQT), which generates daily and weekly quality indicators that are published on the GIOVE website. Data quality reports are generated for both GIOVE-A and GIOVE-B, as well as GPS signals covering multipath and cycle slip detection. Figure 4.6 shows examples of the weekly multipath plots computed by the data quality facility published on the GIOVE website.

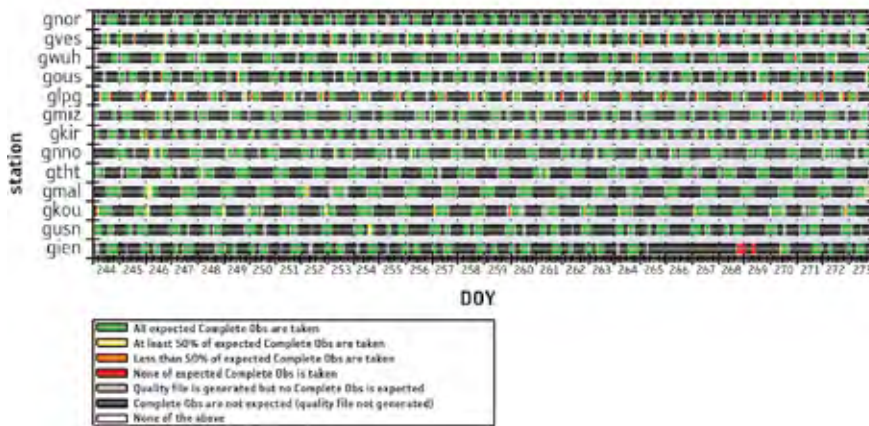
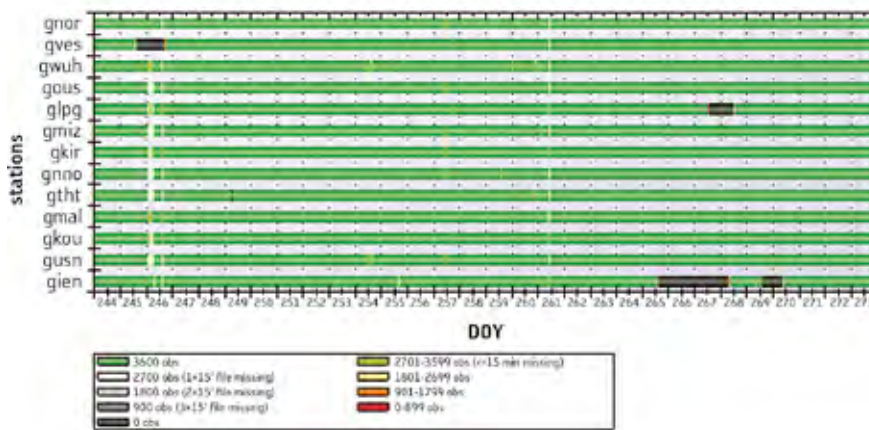


Figure 4.3. GIOVE pass prediction and GIOVE/GPS complete observation data availability.  
 Middle: GPS observable availability in hourly quality files (from all GPS satellites).  
 Bottom: Available complete observations (L1 + E6) in hourly quality files (above masking angle).

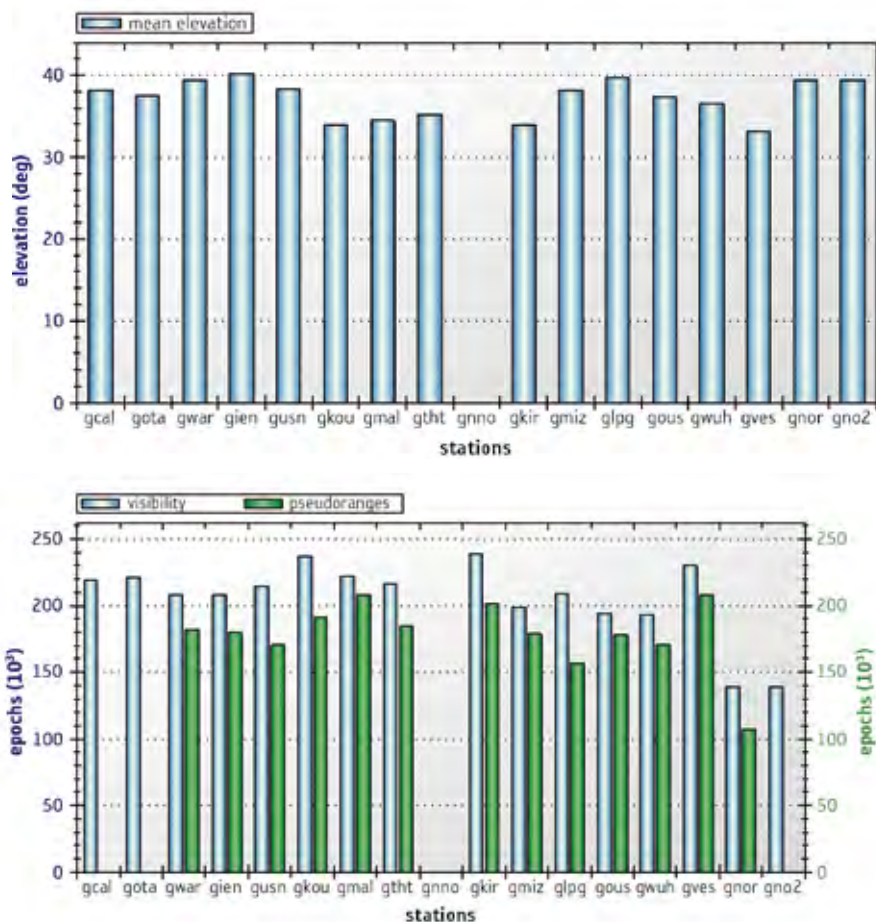


Figure 4.4. GIOVE availability per signal component and quality indicator.  
 Top: Average mean elevation  
 Bottom: Complete observations (L1 + E6)

month	JULY																																
day	1	2	3	4	5	6	7	8	9	10	11	12	13	14	15	16	17	18	19	20	21	22	23	24	25	26	27	28	29	30	31		
dow	S	M	T	W	T	F	S	S	M	T	W	T	F	S	S	M	T	W	T	F	S	S	M	T	W	T	F	S	S	M	T		
GNOR											1																						
GVES																																	
GWUH																																	
GOUS																																	
GLPG																																	
GMIZ																																	
GKIR																																	
GNNO																																	
GTHT																																	
GMAL																																	
GKOU																																	
GUSN																																	
GIEN																																	

Figure 4.5. GESS network maintenance and operations, July 2007.

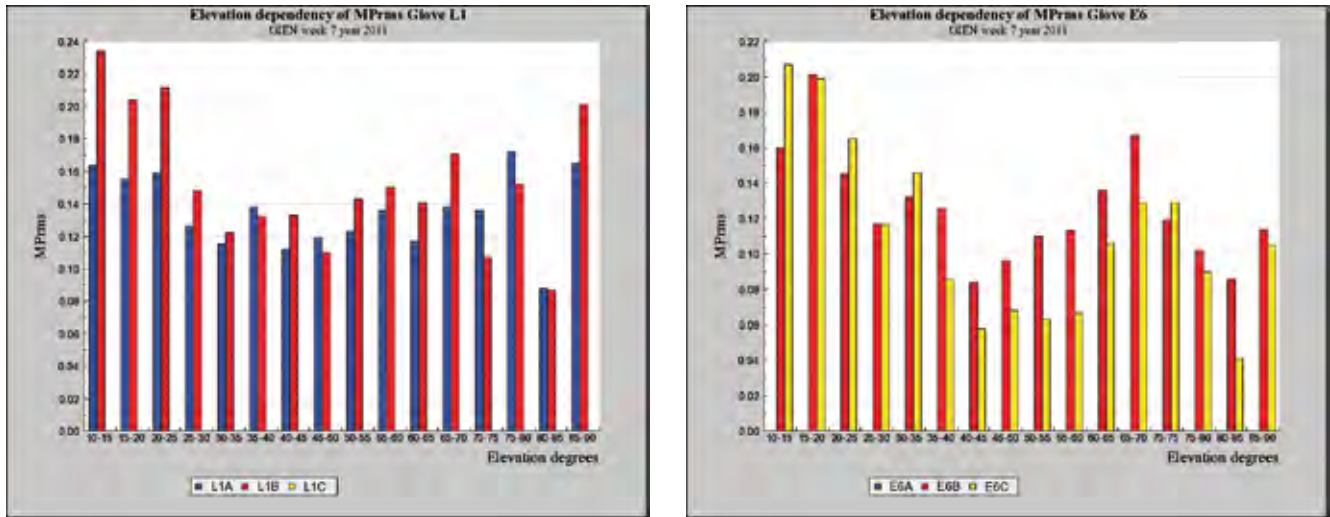


Figure 4.6. GIOVE-A multipath versus elevation (GIEN).

### Payload Interface Chain

Built around the ESA SCOS2000 control system architecture, the GIOVE Payload Control Interface (GPCI) reuses the same databases as those employed by the GSCs, allowing rapid updates during development.

While continuously archiving telemetry from both satellites, the GPCI also stores telecommand history and event history records from GSC-B. This enables the GPC to monitor and trace all satellite and control centre events in near real time.

The GPCI operations are not limited to the collection of telemetry data from the satellites. The GPCI is also responsible for:

- extracting useful telemetry data and making them available to external users;
- collecting and acquiring MEO radiation post-processed data from GSC-A; and
- submitting payload operation requests (PORs) to GSC-B. The PORs are inputs in the form of spacecraft telecommand schedules that are sent to the GSC’s Mission Planning Facility for processing. The PORs are preplanned and sent to the GSC for detailed planning. Once each POR is processed, a receipt is returned prior to uplink, which may include necessary command time-tag shifts. The GPC has developed procedures for dealing with three kinds of POR: onboard clock frequency adjustments; Navigation Signal Generation Unit (NSGU) time resynchronisation; and space radiation environment monitoring data sampling rate requests (see Figure 4.7).

The GPCI’s SCOS2000 environment is designed for spacecraft control in real time and is less suitable for telemetry data analysis. This is why another PC-based analysis system has been added, which is dedicated to statistical analysis and plotting of telemetry data. This system, called the Mission Utility and Support Tool (MUST), automatically retrieves data from the GPCI, and provides users with a flexible and intuitive way of displaying telemetry parameters for post-processing analysis.

The MUST software development and other support for the GIOVE Mission are provided by ESOC.



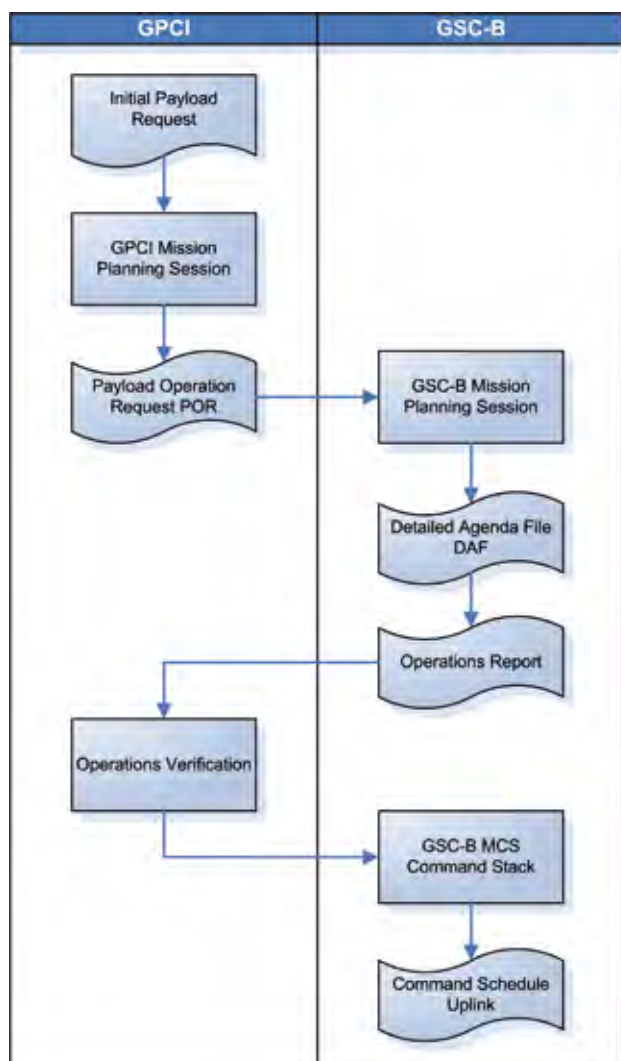


Figure 4.7. Payload operations request (POR) – data flow diagram.

### Processing Chain (Navigation Message Loop)

Every hour, the GPC automatically prepares and launches a new session of the E-OSPF to generate fresh orbit and clock information. The GIOVE navigation messages are forwarded to the Satellite Control Centre for uploading to the satellite. The data availability tool developed by the operation can be used to display the ongoing navigation message generation process on the GPC’s large monitors (Figures 4.8 and 4.9).

Figure 4.8. Navigation message availability, November 2007 (typical availability figures). OSPF routine core products.

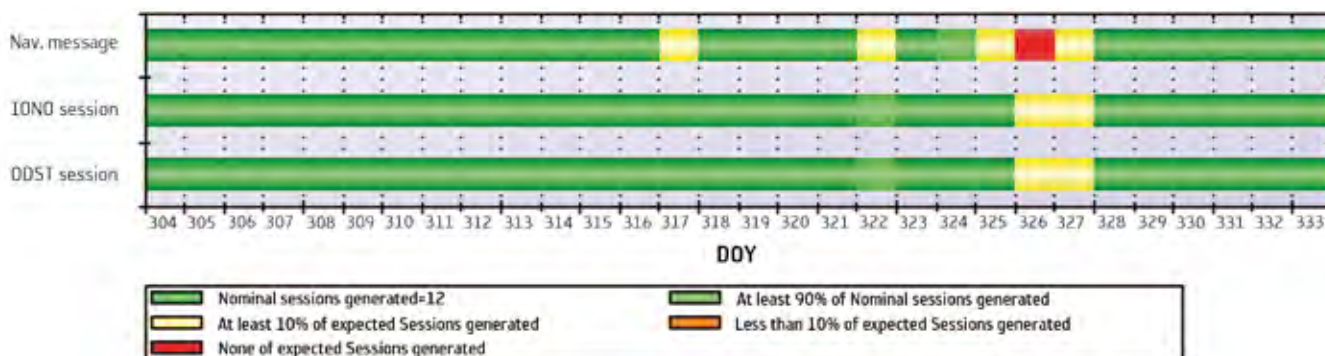


Figure 4.9. The GIOVE Processing Centre.



## Common Tasks

Common tasks include housekeeping and maintenance, reporting and operations services to external users.

The housekeeping and maintenance of the system involves both hardware and software aspects. Within the core infrastructure, operational downtimes were due mainly to platform obsolescence and software maintenance activities. In particular, the failures impacted the hard disk array and corrupted the Sun Solaris file system.

On the other hand, the internal power supply of the Galileo Experimental Test Receiver showed some limitations that led to an inability to acquire from all receiver channels. The problem may have been the result of environmental conditions, and was solved with an upgraded version of the GETR power supply.

The antennas are in the process of being corrected in order to improve the multipath performance of the GIOVE signals.

The reporting task involves providing the mission experimenters with reports on the data collected, focusing on the following areas:

- data availability;
- data from the GESS network;
- generated GIOVE-A and GIOVE-B navigation messages;
- data from GSC-A and GSC-B (TMs and MEO radiation);
- data from external servers; and
- data quality.

The operations services to external users follow the needs of experimenters and external users, providing information from operations and maintenance logs, planned activities and outages, and transmission logs in the most convenient way.

Full access to data and reports via the website/ftp server is granted only to certain external users. As of June 2011, the GIOVE Mission has received more than 280 requests for external user accounts, of which more than 70 have been granted. The accounts provide access to various online services, depending on the specific rights of the type of account granted.

## 4.2 Evolution of the GIOVE Mission

During the experimentation period, the availability of the system was good, except for some short outage periods related to hardware failures at the GESS stations and storage/processing servers. Figure 4.10 shows the data availability at GESS stations on a typical day.

However, there were several reasons to start the modernisation of the GPC infrastructure, in areas such as the GESS network, the GPC platform, monitoring tools, and the GIOVE website.

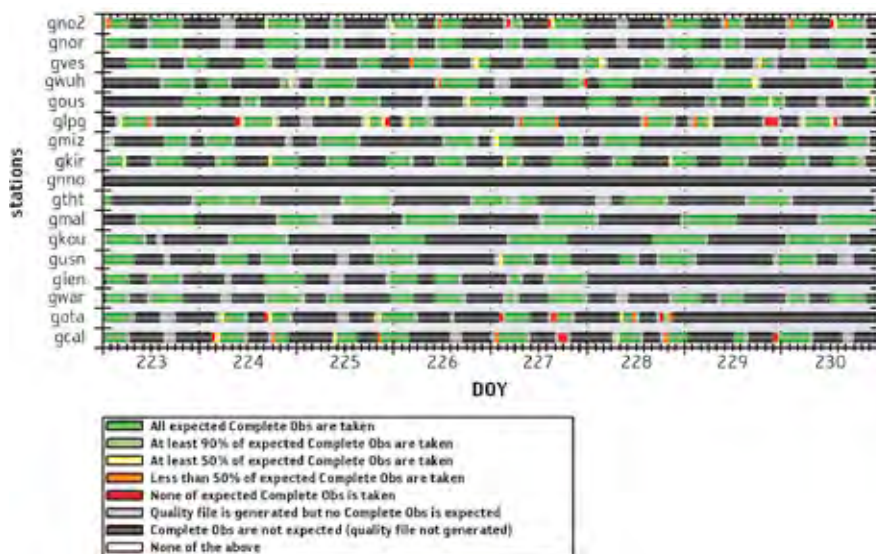


Figure 4.10. GESS station data availability for DOY 320–326, 2007. Complete observations (L1 + E5) in hourly quality files (above masking angle).

## The GESS Network

This section presents details of the following four upgrades to the GESS network:

- developing an improved version of the GESS stations capable of hosting up to three receivers and two antennas (GESS+);
- upgrading the GESS network to enable the reception of the MBOC signals transmitted by GIOVE-B;
- upgrading the antennas of the GESS network to improve the multipath characteristics; and
- deploying two additional GESS stations in Canada equipped with Novatel Galileo Test Receivers (GTRs), procured by the Canadian Space Agency, in 2008.

Additional stations will be deployed through arrangements with other space agencies.

## Development of GESS+

The current stations, operated by Indra Espacio, include a Septentrio Satellite Navigation (SSN) GETR, and upgrades to the system will make it possible to work not only with an SSN GETR receiver but also with a Novatel GTR in either a single-receiver (any one of them) or dual-receiver configuration. To achieve this, important station hardware changes were necessary, starting with increasing the size of the station cabinet itself to host two receivers and allow for addition of a third one in the future. The modified station, called GESS+, will have two antenna inputs to feed the receivers separately if needed.

From the point of view of the GIOVE network, each physical station will become two virtual stations, with different identifiers, and the two raw datasets will be available for collection and performance analysis from the GPC. With this objective, new data flow interfaces from the DSF to all sites will be put in place, and the specific GTR raw data to RINEX converter will be implemented.

The main components of GESS+ are:

- the GETR receiver subsystem, including a space engineering antenna;
- the GTR receiver subsystem, including a Novatel Galileo antenna;
- the core computer subsystem;
- a frequency reference subsystem based on a high-quality RAFS and frequency distributor; and

- an uninterruptible power supply (UPS), to maintain the station in the event of brief interruptions in the local power supply.

At the software level, a data acquisition and formatting chain, and a monitoring and command (M&C) chain will be developed specifically to deal with the GTR receiver. In this way, the changes to the existing chains that are already interfacing with the Septentrio receiver will be minimised, thus reducing the development time. The underlying philosophy is that each virtual station will have dedicated raw data collection and M&C modules, while the station's local M&C module will manage the equipment that is shared by the virtual stations, such as RAFS and the UPS.

As mentioned previously, GESS+ has been conceived to allow the easy integration of a third receiver whose only requirements are to provide raw data in RINEX 3.0 format, PPS synchronisation through up to two serial ports, and to be up to five 19" rack-mountable units in height.

The strategy for the deployment of GESS+ and for retrofitting existing stations has been designed to reduce the need for equipment changes, and it allowed a reduced deployment schedule. The solution consists in reusing equipment that will not change from GESS to GESS+ design, thus assuring a high degree of technical confidence since elements have already been tested and qualified in the project.

The first retrofit was carried out at the GPC co-located sensor station at ESTEC in October 2008.

### Support to MBOC signals

The GIOVE-B satellite is capable of transmitting all Galileo signals, including multiplexed BOC (MBOC) signals. The GESS network needed to be upgraded to allow signal support for the time-multiplexed BOC (TMBOC) and composite BOC (CBOC) modulations.

In particular, it was necessary to upgrade both the receiver software and the FPGA firmware of the Septentrio receivers. The upgrade of the FPGA was performed by GESS local support while the software upgrade was performed remotely from the GPC.

### Antenna upgrade

Figure 4.11. A GESS antenna.



During the GIOVE experimentation phase a code carrier signal divergence dependent on the satellite elevation was detected on the antennas from Space Engineering installed at GESS sites (see Figure 4.11). Further investigations were made by Space Engineering to find a solution. It was concluded that the observed behaviour was due to out-of-band internal resonance. The Group Delay Variation (GDV) characteristics were observed in the operational bands as a function of the azimuth and elevation. A slight modification of the antenna was required to reduce this effect.

The results obtained with the reworked antennas have been satisfactory (see Figure 4.12). GIEN and GNOR are already equipped with the improved antenna. The process of installing this new antenna at all sites across the GESS network has now begun.

### Additional stations

In the frame of a bilateral agreement between ESA and the Canadian Space Agency, two GESS stations have been deployed in Ottawa and Calgary, and connected to the current ground network in order to increase the satellite

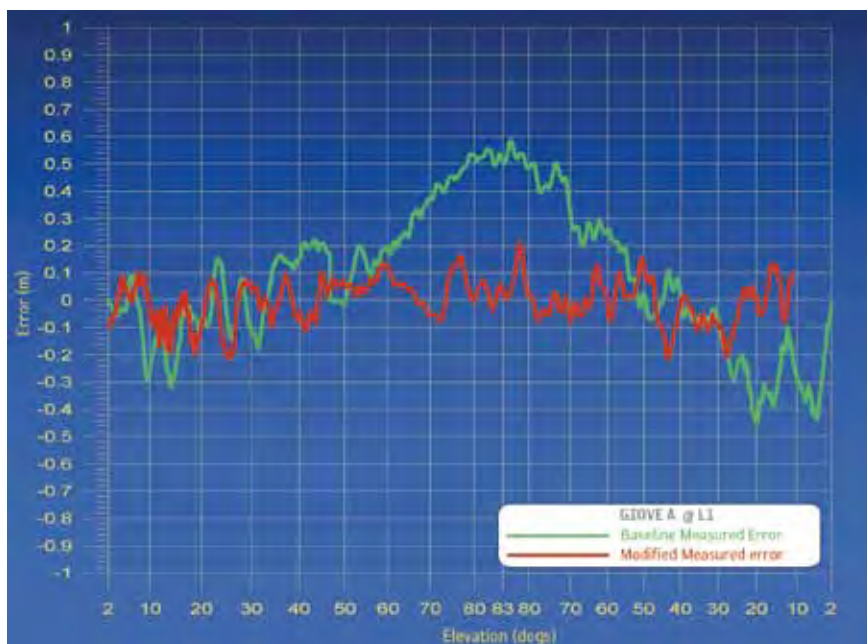


Figure 4.12. Code carrier coherence of the baseline and the modified antenna.

coverage. Three additional stations have been established in Warsaw (Poland), Oberpfaffenhofen (Germany) and Milan (Italy) through arrangements with the Polish, German and Italian space agencies.

## GPC Platform Migration

Part of the GIOVE Processing Centre infrastructure had become obsolete and needed to be renewed in order to reduce outages and maintenance efforts. Furthermore, the GIOVE Mission was requested to be capable of supporting the collection of data from up to 20 GESS stations in view of the potential extension of the network, and to store and process data from those stations for at least two years.

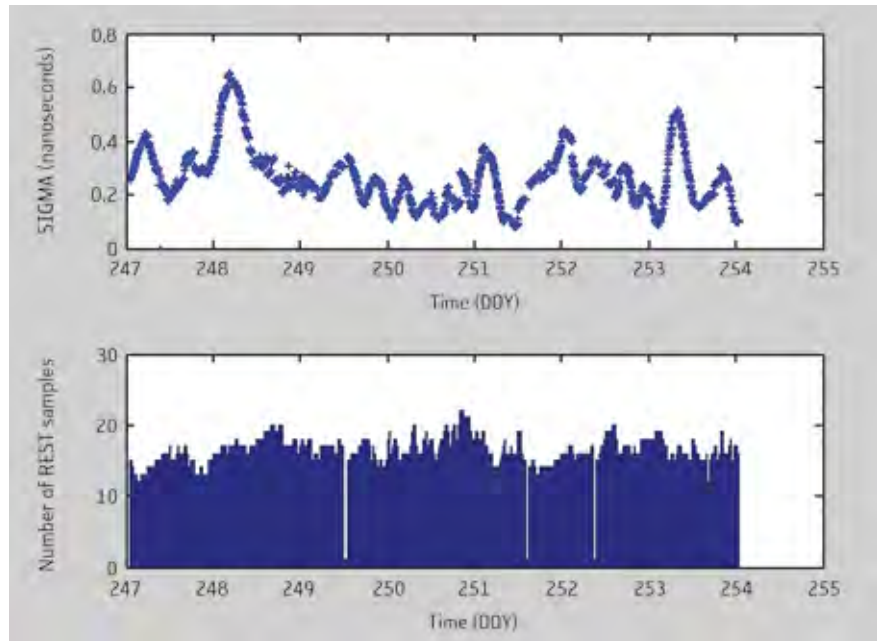
The main objectives of the GPC platform migration were to:

- renew all DSF servers, the disk array unit, the E-OSPF workstations and the M&C workstation;
- rack-mount all upgraded servers and workstation to a new rack to ease maintenance and operations;
- install operator terminals equipped with 20" flat screens;
- set up the external (DMZ) web/ftp server as proxy to provide capability for external users to access all the archived data through the DMZ;
- add a configuration & reporting workstation acting as a centralised operations configuration backup & restore facility;
- ensure warranty coverage extension;
- increase the disk array space to 3 TB to ensure the capability to store at least 2 years of data;
- double the memory and CPU power of all servers and workstations to provide the capability to process data from 20 stations without introducing processing delays (see Figure 4.13 );
- increase the size of the tape unit to 400 GB;
- migrate from Sun OS 9 to Sun OS 10, and from Sun SPARC V9 to Sun AMD Opteron workstations.

Figure 4.13. A new GPC storage server.



Figure 4.14. Standard deviation of the averaged restituted clock.



### Evolution of GPC Monitoring Tools

One of the basic functions of the GPC is to monitor its system and processing functions as well as the quality of the data collected from the GESS network, in order to ensure uninterrupted operations and quality of the services provided to GIOVE Mission experimenters.

### Key performance indicators

The GPC has been upgraded to provide new capabilities to generate a set of key performance indicators (KPIs) to measure continuously the quality of the GPC processing. The KPIs cover the following areas:

- orbit determination and time synchronisation processing performance;
- orbit and clock estimation and prediction accuracy;
- the Experimental GPS to Galileo Time Offset (EGGTO) estimation and prediction accuracy;
- the Broadcast Group Delay (BGD) stability; and
- the input data latency and completeness for processing.

The KPIs will also cover the stability of the Experimental GIOVE System Time (EGST), the intersystem bias and the delay and validity of the generated and received navigation messages.

The KPI tool provides statistical analyses of performance, as shown for the clock estimation error in Figure 4.14. A threshold value can be configured in order to inform and alert users in the event of anomalies or significant errors.

### The GIOVE Website

Since the publication of the GIOVE SIS Interface Control Document on 13 October 2008, a general update of the website has been carried out. In particular, new products are accessible, new forms are available to request user accounts and general information. Moreover, a mechanism to distribute standardised notifications to users on the status of the spacecraft and ground segment, the



Figure 4.15. NAGU page on the GIOVE website.

Notice Advisories to GIOVE Users (NAGUs), has been implemented. Figure 4.15 shows the NAGU page on the GIOVE website ([www.giove.esa.int](http://www.giove.esa.int)).

### 4.3 GIOVE Mission in the IOV/FOC context

The GIOVE Mission Segment is planned to evolve and be integrated in the validation tools in support of the IOV and FOC activities, especially because of its capability to make raw measurements available from a set of stations deployed worldwide.





**→ GIOVE-A: FIVE YEARS  
OF EXPERIMENTATION  
RESULTS**



## 5. GIOVE-A: Five Years of Experimentation Results

The GIOVE Signal-in-Space is acquired by the GESS network together with GPS signals. The DSF periodically acquires the data files and converts them to standard RINEX 3.0 format. In addition, the GIOVE flight dynamics data and the telemetry and telecommand processed by GSC-A and GSC-B are also archived in the data server, through the GPCI. These data are the basis for the offline experimentation process.

The reference clock for the GIOVE experimentation is normally a free-running Active Hydrogen Maser (AHM) connected to the GIEN station, a GESS at the Italian National Metrological Laboratory (INRiM) in Turin. All clocks in the GIOVE segment are synchronised to the INRiM master clock. The AHM output signal, both 10 MHz and 1 pulse per second (PPS), is fed to the GIEN station as an external reference time scale. The clock is continuously monitored and compared with the ensemble of atomic clocks at INRiM, and with external reference time scales such as the Coordinated Universal Time (UTC) maintained by the BIPM.

In Figure 5.1, the colours indicate the Depth of Coverage (DOC), which is the number of GESS sites in view of GIOVE-A as it passes over a particular location. In order to reduce the estimation uncertainty, the GIOVE-A clock is calculated when at least DOC-2 is available.

The GESS network has been designed to minimise the extent of DOC-1 areas (shown in red in Figure 5.1). The stations within the network are listed in Table 5.1.

### 5.1 The Observation System

The technique used for clock characterisation is called Orbit Determination & Time Synchronisation (ODTS), a batch least-squares algorithm that processes undifferentiated iono-free GIOVE-A and GPS code and phase combinations, together with GIOVE-A Satellite Laser Ranging (SLR) measurements. The 1-s code measurements are smoothed with phase using a Hatch filter.

Figure 5.1. Depth of coverage of the 13-GESS nominal network (number of stations in view of GIOVE-A).

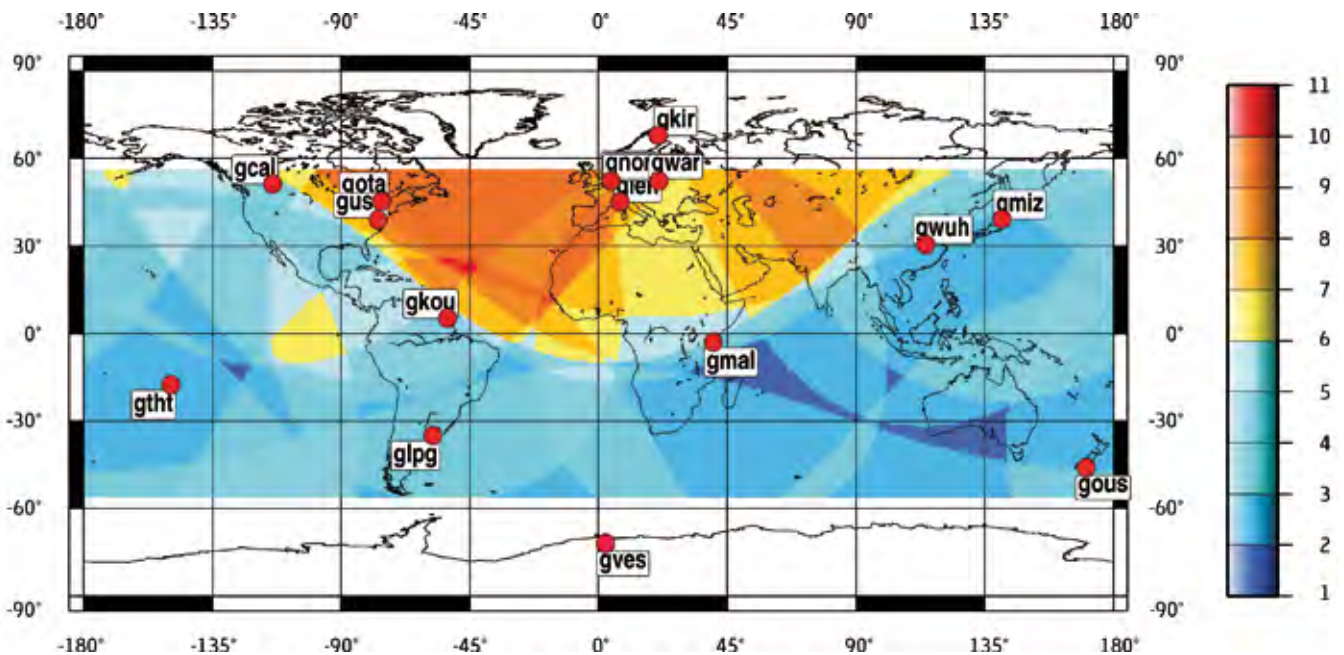
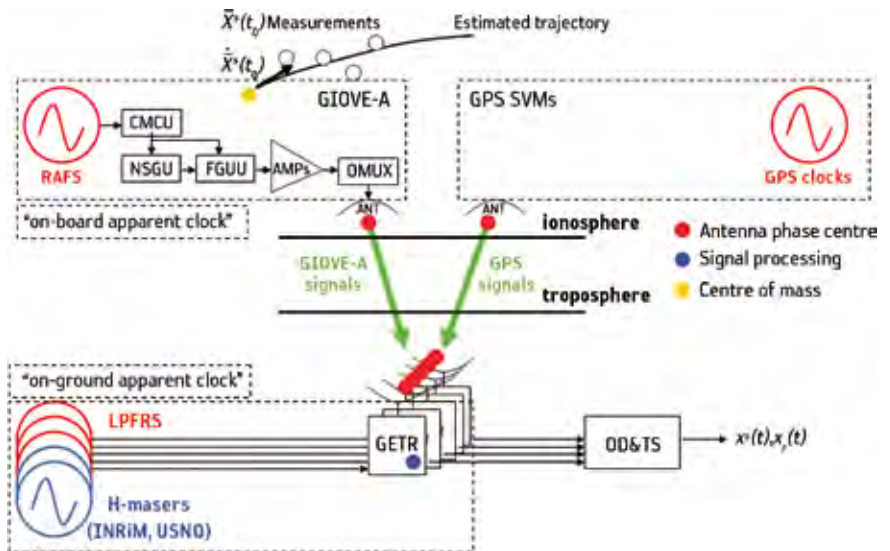


Table 5.1. List of GESS stations.

Station	Acronym	Authority	Station type	Latitude (deg N)	Longitude (deg E)
Kourou	GKOU	ESOC	GESS GETR	5.3	-52.8
Torino	GIEN	IEN	GESS GETR	45.1	7.7
La Plata	GLPG	GFZ	GESS GETR	-45.1	-58.0
Mizusawa	GMIZ	GFZ	GESS GETR	39.1	141.1
New Norcia	GNNO	ESOC	GESS GETR	-31.0	116.2
Noordwijk	GNOR	ESA	GESS+	52.2	4.4
Dunedin	GOUS	GFZ	GESS GETR	-45.9	170.5
Wuhan	GWUH	GFZ	GESS GETR	30.6	114.3
Tahiti	GTHT	ESOC	GESS GETR	-17.6	-149.6
Kiruna	GKIR	ESOC	GESS GETR	67.9	21.0
Malindi	GMAL	ESOC	GESS GETR	-3.0	40.2
Washington	GUSN	USNO	GESS GETR	38.9	-77.1
Troll	GVES	ESOC	GESS GETR	-71.7	-2.8

Figure 5.2. Schematic overview of the measurement system.



The ODTS solves for orbits (dynamic parameters), clocks, troposphere, and the so-called station inter-system bias (ISB), following a dedicated strategy in order to deal with different effects, such as the ionosphere, troposphere, relativity, phase centre offsets, phase wind-up, tides, site displacements and ocean-atmosphere loading.

One particular aspect of the ODTS process is the use of a simplified Solar Radiation Pressure (SRP) model for GIOVE-A and all GPS satellites, adapted from the GPS and Glonass literature on the subject. Based on estimates of five coefficients that best fit the orbit, the model requires no a priori information about the satellite geometric and reflectivity properties. No other empirical accelerations are estimated in ODTS. In total, only 11 dynamic parameters are estimated per satellite (position, velocity and five SRP coefficients).

Figure 5.2 summarises the main clocks, reference points and components of the measurement system.

Together with the dynamic parameters, the main product of ODTS is the estimated clocks (for all satellites and all stations). The clocks are generated in clock-RINEX (CLK) format as phase offsets relative to the reference clock, at a nominal output rate of 5 min.

## System Validation

A first indicator of the quality of ODTS results is the measurement residuals, i.e. the difference between real data and the measurements as modelled by the processing algorithms. Optimally, the residuals should be small and randomly distributed, showing only the un-modelled error contained in the data (for example, code multipath). In the case of the GIOVE Mission, a systematic elevation-dependent pattern can be observed on code residuals (an example is shown in Figure 5.3) that is believed to be due to a code/phase incoherence generated at the station antenna. Typical ODTS residuals are 40 cm RMS for code measurements, 1 cm for phase and 3 cm (one-way) for SLR.

A successful determination of the GIOVE-A clock depends to a large extent on the correct determination of the station inter-system bias. This is essential, in particular to avoid satellite clock jumps when GIOVE-A passes over different ground stations. Since the ISBs and the GIOVE-A clock are clearly correlated, it is not so obvious that the ODTS software should be able to separate correctly the clock and ISB contributions from the GIOVE-A measurements. In spite of this, the ISBs calculated by ODTS over the data analysis period show good stability. In addition, no phase jumps are observed on the GIOVE-A clock, which is also a good sign of correct ISB estimation.

An alternative method based on a dedicated algorithm called IONO has been used to calculate station ISBs using geometry-free GIOVE-A and GPS code and phase. Geometry-free measurements contain ionospheric Total Electron Content (TEC) information and satellite and station inter-frequency bias (IFB). The IFB is the difference between the P1 and P2 code delays (for GPS), and between the E1 and E5 (or E6) code delays (for GIOVE-A), at both satellite and station levels.

The station ISB is calculated as the difference between the station E1–E5 or E1–E6 IFB (GIOVE-A chain) and the P1–P2 IFB (GPS chain), assuming that the delay on E1 codes (E1 and P1) is approximately the same for both systems. In order to calibrate the whole IFB system in the IONO software, the average satellite P1–P2 IFB (GPS) has been fixed at 5.4 ns (from the navigation message BGD values) and the satellite E1–E5 and E1–E6 IFBs (GIOVE-A) has been fixed to the values calibrated by the satellite manufacturer.

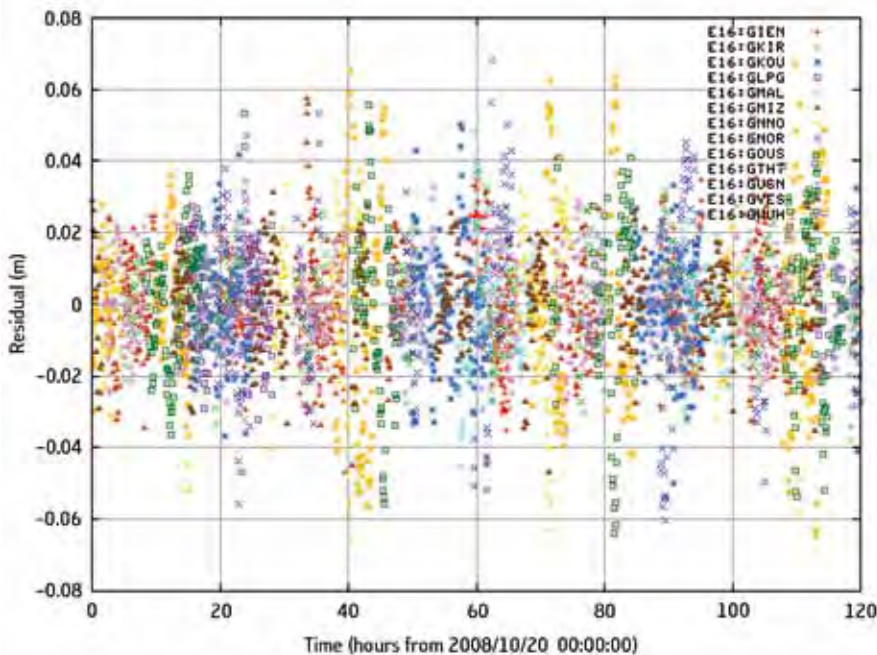


Figure 5.3. Elevation-dependent pattern observed on pseudorange residuals. Carrier phase residuals (PRN: E16, GSS: All).

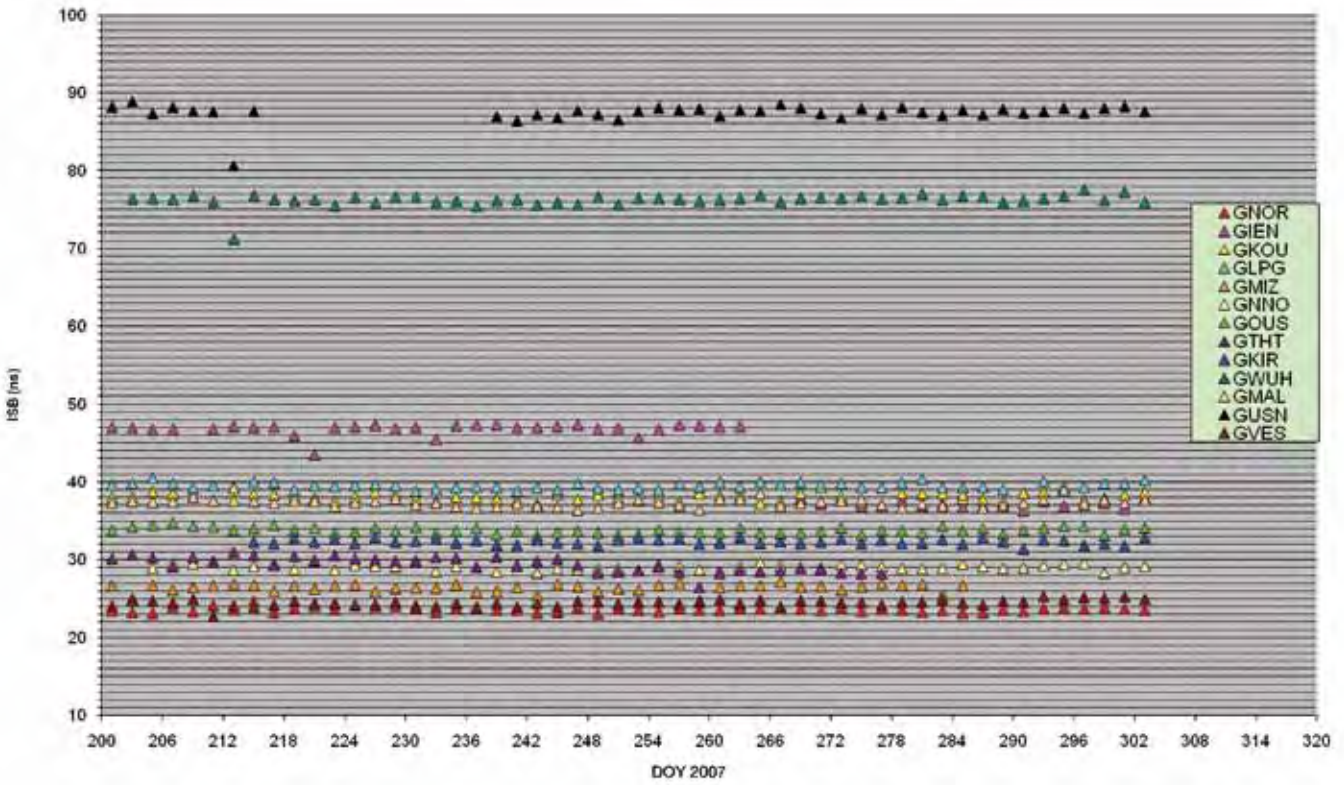
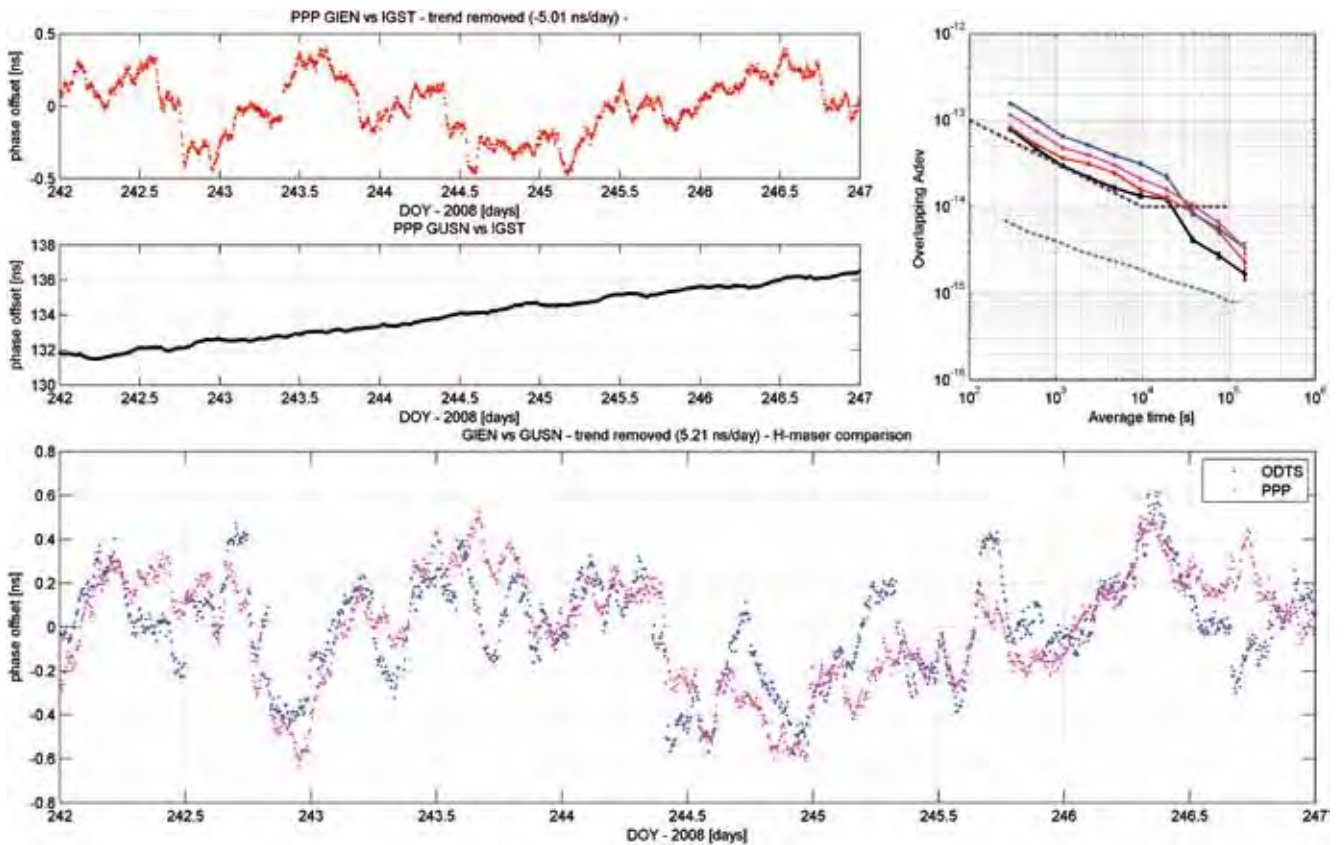


Figure 5.4. GESS station absolute inter-system biases (ISBs).

Figure 5.5. Stability of the hydrogen masers at INRiM (GIEN) and USNO (GUSN).



The station ISB values calculated by IONO (every two days), depicted in Figure 5.4, show good stability and are in agreement with those calculated by ODTS (at the ns level). The jump in the GIEN ISB around DOY 265 is due to an intentional hardware configuration change at the station.

An additional validation exercise consists in evaluating the behaviour of the INRiM free-running hydrogen maser, to check that its levels of noise and drift are well below the analogous quantities that are under evaluation for the onboard clock. This is done using two almost independent techniques.

First, since three AHMs are included in the GIOVE mission network at INRiM, Turin, Italy (GIEN station), at the US Naval Observatory (USNO), Washington, DC (GUSN station), and at the GPC at ESTEC, the ODTS also allows the estimation of their phase offset. In addition, the NRCan Precise Point Positioning (PPP) algorithm is used to process the GPS observables extracted from the two station data files and also to estimate the clock phase difference. An example of the results is reported in Figure 5.5 for the period 14–18 May 2007 (DOY 134–38).

## Experimentation with GIOVE-A

Data from the GESS network, together with GIOVE-A SLR measurements from the International Laser Ranging Service (ILRS), have been processed since the beginning of the GIOVE mission (around May 2007). During some periods, the payload was configured to transmit the E1 and E5 signals using the nominal payload chain (driven by RAFS FM4) and, during other periods, the redundant payload chain (driven by RAFS FM5). At other times, the payload was configured to transmit the E1 and E6 signals using the nominal payload chain. The Galileo Experimental Test Receivers (GETRs) within the GESS stations were configured according to the payload configuration during each period.

The characterisation of the onboard clock is significantly enhanced by the use of Satellite Laser Ranging, a high-precision technique for orbit determination that is independent of the navigation signal generation. Given the high altitude of GIOVE-A and the reduced size of the laser retro-reflector on board, the satellite is regularly tracked by a limited number of stations (around 12).

The GSTB-V2 mission experimentation activities have been grouped into seven areas, each containing a number of test cases (TCs). The most relevant results of these experimentation areas and test cases are summarised in the following sections.

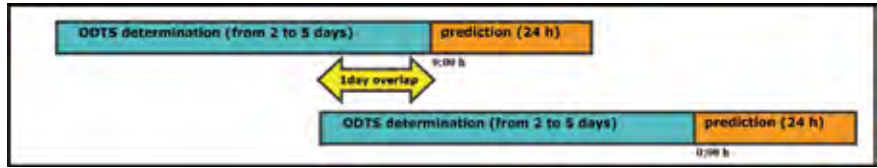
## 5.2 Navigation Assessment and Orbit Models

The experimentation in this field has several objectives:

- to confirm the adequacy of the routine process to generate reliable navigation messages;
- to confirm the use in the ODTS of the best orbit models available (and to assess whether these models provide the required accuracy on orbit and clock results); and
- to assess the GESS coordinates on a regular basis, verify the GIOVE-A reference points, and process and analyse the SLR data.

The main experimentation activity has been the execution of consecutive and overlapping ODTS arcs. After the end of each arc, the orbits and clocks are also predicted in order to compare them with the estimation of the following arc. The scheme is depicted in Figure 5.6.

Figure 5.6. Consecutive ODTS arcs.



In summary, the experimentation is based mainly on the following comparisons:

- GPS: orbit and clock estimations and predictions are compared with IGS products; this gives a general idea of the ODTS quality, independent of the Galileo performance;
- GIOVE estimations: for each new ODTS arc, estimated orbits and clocks are compared with those of the overlapping period in the previous arc (typically a 12-h comparison);
- GIOVE predictions: for each new ODTS arc, estimated orbits and clocks are compared with the predicted orbits and clocks of the previous arc (typically a 12-hour comparison); and
- GIOVE near-realtime estimated orbits and clocks: the orbits and clocks calculated routinely in area 1 (navigation assessment) for the online navigation message generation are compared with the best available estimations computed offline (reference orbit).

The results of the most relevant test cases are presented in the following paragraphs.

### Navigation Algorithm Performance Assessment

The routine E-OSPF (ODTS + IONO) has been executed in the operational machine at the GPC for navigation message generation. It is executed every hour, in order to update the navigation message as frequently as possible. The duration of the ODTS arc is 2 days and that of the IONO arc is 1 day.

### ODTS stability, robustness and tuning

The execution of ODTS sessions has shown to be quite robust and stable. Results achieved with the routine configuration are in good agreement with the offline ones, so it is believed that any conclusion from the offline arcs is directly applicable to the routine ones.

### GESS network latency evaluation and impact on ODTS

The GESS latency has been defined as the difference between the last valid epoch in the arc and the time at which all the input files were downloaded by the E-OSPF. The latency has been shown to be below 75 min 84% of the time, and below 2 h 92% of the time. The impact of latency on the orbit and clock accuracy is presented in Figure 5.7.

### Near-realtime satellite clock characterisation (from ODTS)

The proposed method to assess the clock prediction error from ODTS has been the analysis of the clock model fit residuals.



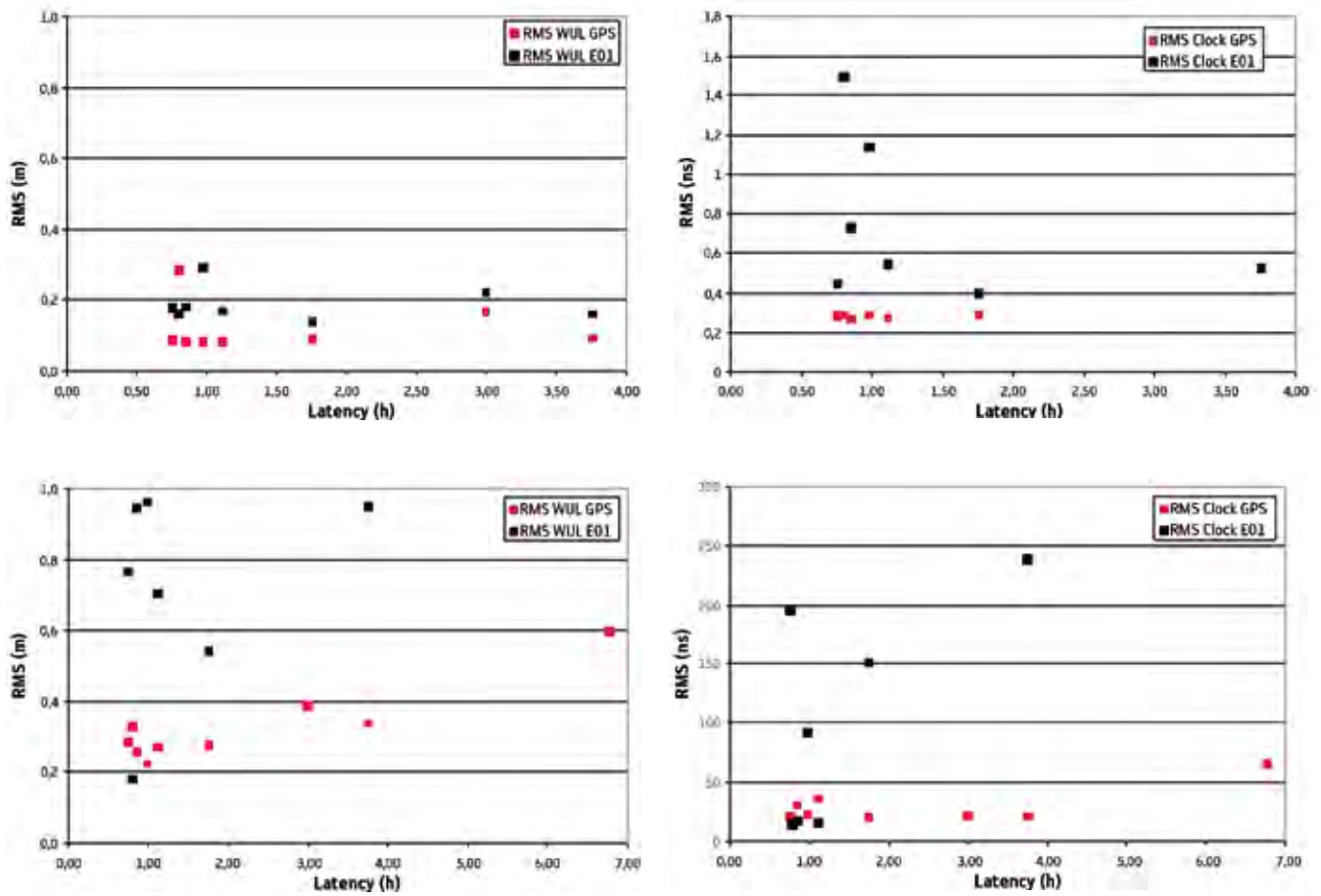


Figure 5.7. Impact of latency on the orbit and clock accuracy.

These analyses have not provided a reliable indication of the prediction error as there is no correlation between clock prediction error and clock model fit residuals. It has been proven that the main sources of GIOVE-A clock prediction error are events occurring during the prediction interval, and not problems during clock model estimation.

### Navigation message generation and uplink assessment

A closed-loop test of GIOVE-A navigation message generation has been successfully performed. The results verified that the broadcast message fully matches the original binary message. Some issues were identified and corrected in early 2009.

### Orbit Models

The results of this experimentation area were obtained from the processing of GPS + GIOVE RINEX data using the ODTS module of the offline E-OSPF software installed at the GPC. GIOVE-A SLR data were processed together with the RINEX data in ODTS, typically in a de-weighted mode. The nominal length of the estimation arc was 5 days, while the prediction period considered for statistics was 1 day. Some typical results are shown here, from 2007–2009.

### Galileo observation pre-processing assessment

The typical level of GIOVE code residuals is 40 cm (RMS) for the E1 + E5 ionosphere-free combination and 50 cm for E1 + E6. These code residuals showed a linear elevation-dependent pattern that originated at the GESS antenna. The typical level of GIOVE phase residuals is 1.1–1.3 cm (RMS), while that for GPS data is 0.9 cm. It has been verified that the use of antenna correction files (ANTEX) improved the phase residuals by 30%.

### Offline ODTs orbit and clock determination and predictions

The overall difference between the GIOVE-A overlapping restituted orbits is 14.3 cm in RMS at the Worst User Location (WUL), i.e. the point on Earth’s surface where the projection of the orbital error is maximum. This is considered a good value, despite the high variability in the overlap performance between arcs, as shown in Figure 5.8.

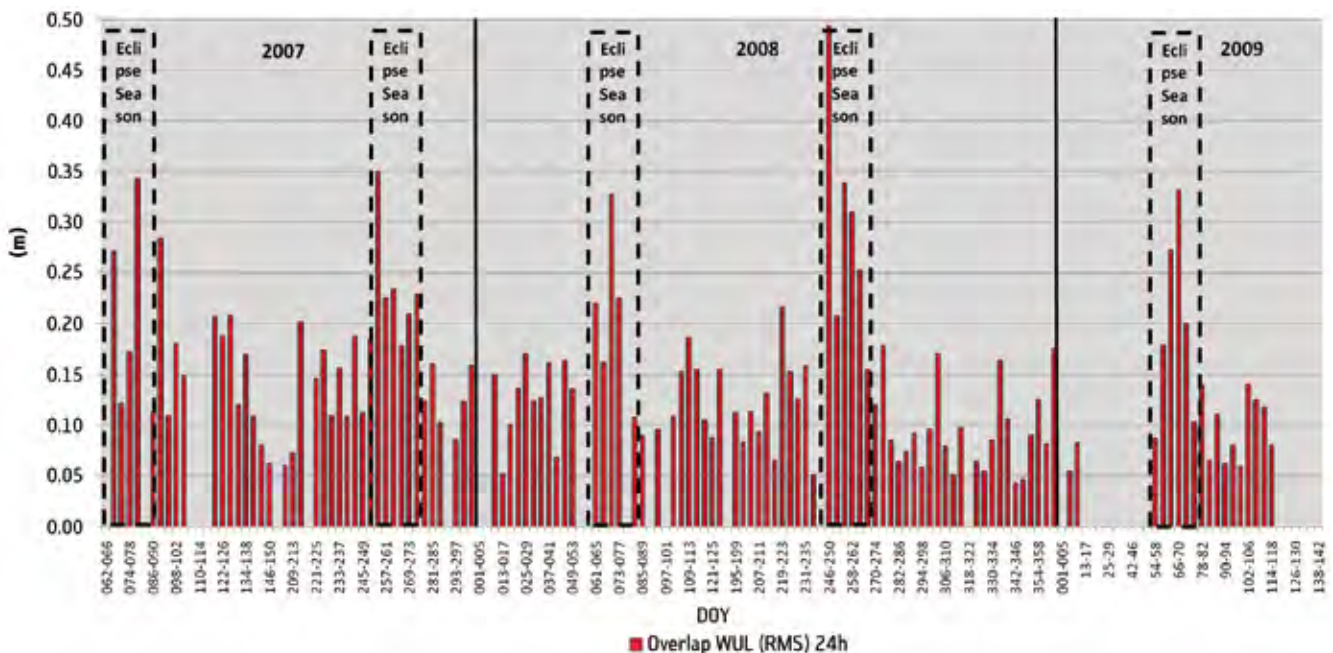
The variations are associated with the eclipse condition, and the characteristics and performance of the tracking network (given the reduced number of stations). The RMS value for eclipse arcs is 22.4 cm.

With regard to the comparison of predicted orbits (1-day predictions) and restituted orbits (considered to be the true orbits), the overall difference is 19.4 cm RMS at the WUL (25.6 cm during and 16.7 cm outside the eclipse period; see Figure 5.9).

The overall restituted clock difference is 0.56 ns (RMS), after the removal of outliers (see Figure 5.10), whereas the clock prediction error at 100 min is close to 0.8 ns (95%) (see Figure 5.11).

Results from the years 2010 and 2011 have been consistent with those shown in Figures 5.8–5.10.

Figure 5.8. GIOVE-A orbit overlap consistency.



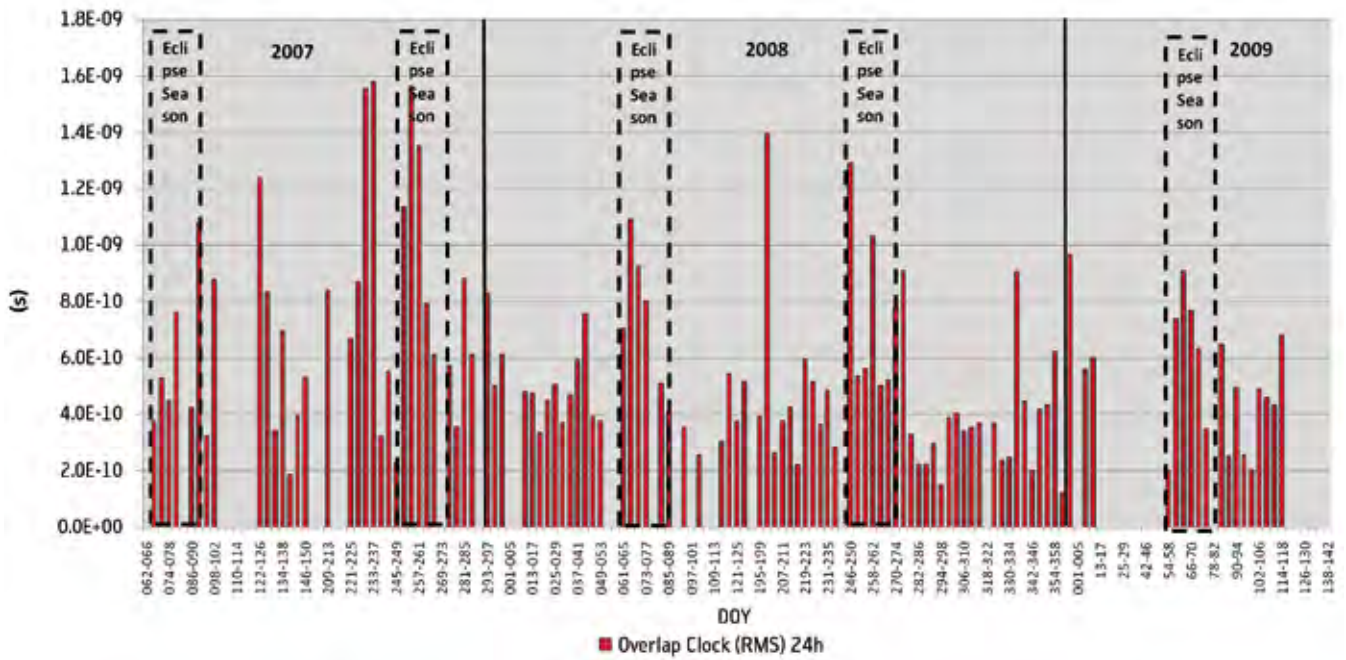


Figure 5.9. GIOVE-A orbit prediction error statistics.

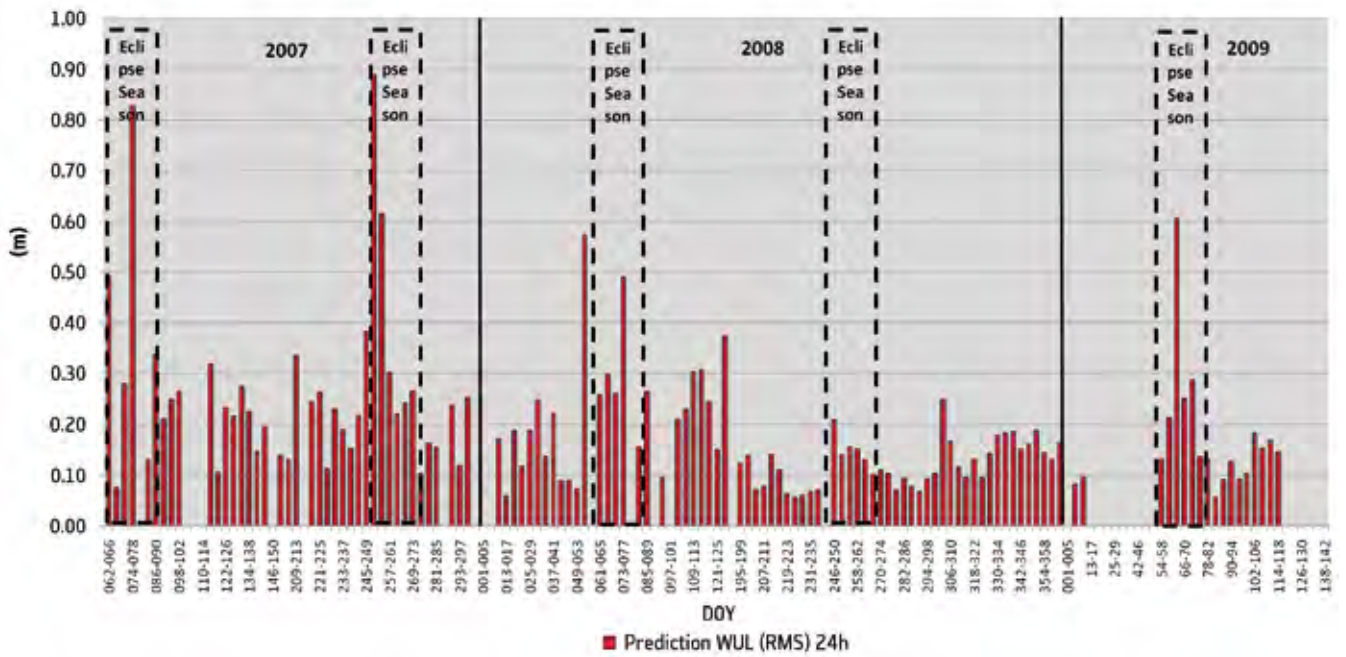
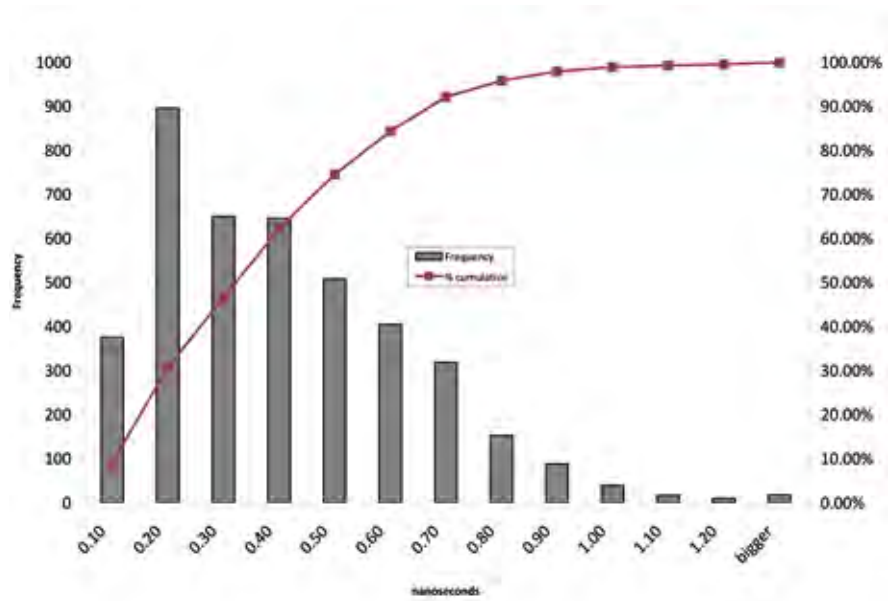


Figure 5.10. GIOVE-A clock overlap consistency.

Figure 5.11. GIOVE-A clock prediction error at 100 min.



### Accuracy of a posteriori routine ODTS orbit and clock determination and predictions

The results for these test cases were obtained considering the offline ODTS orbits and clocks as the true ones. The agreement between the routine and offline estimates were considered good, with an orbit difference of around 15 cm RMS at the WUL, and a clock difference of around 0.5 ns RMS. The difference between the routine predicted and offline restituted orbits was typically below 50 cm RMS at the WUL.

### GPS orbit and clock determination accuracy versus IGS products

To assess the quality of the ODTS orbits and clocks, the results were compared with those obtained using IGS products. The results were quite good (orbit differences of 0.08 m RMS at the WUL and clock differences of 0.3 ns RMS) and showed good consistency among the experimentation arcs. No systematic error between ODTS and IGS GPS orbits and clocks was identified.

Figure 5.12 shows the statistics of the GPS orbit and clock comparisons against IGS products. This suggests the adequacy of the models implemented using the ODTS software, most of which are common to GPS and GIOVE.

### Solar radiation modelling

The acceleration due to Solar Radiation Pressure (SRP) was first modelled in the GSTB-V2 experimentation through five coefficients that are to be estimated in the ODTS process. The evolution of these coefficients for GIOVE-A showed reasonable stability over the different ODTS arcs outside the eclipse period, whereas under eclipse conditions the stability of the SRP coefficients showed anomalous behaviour. Experiments with additional models have shown marginal improvements.

### Attitude modelling

The evolution of the satellite yaw angle was monitored during GIOVE eclipse periods. During those periods when the satellite is eclipsed, a deviation from the theoretical attitude law is expected.

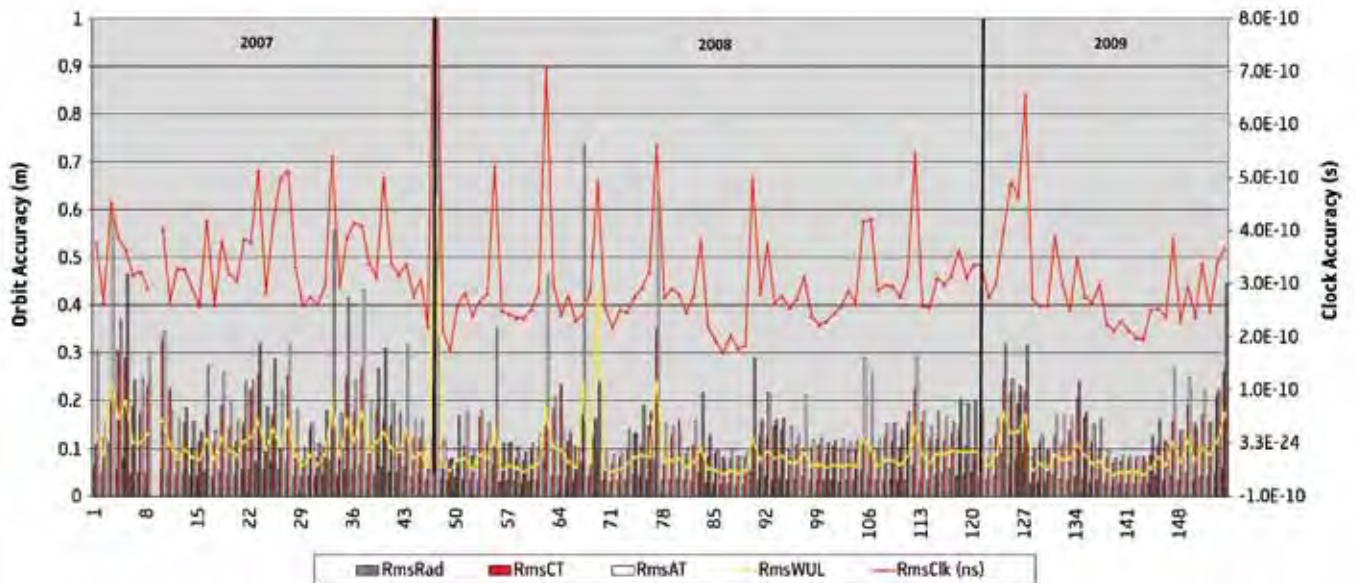


Figure 5.12. Comparison of IGS estimates for GPS satellites.

Three attitude laws are available in the ODTs software: theoretical, implemented and reconstructed (from an external source, e.g. satellite telemetry). The ODTs results have been shown to be nearly identical for all attitude laws, so there is no particular advantage in using the reconstructed law rather than the coded attitude laws (theoretical and implemented).

### Eclipse analysis

The processing of ODTs arcs during eclipse periods has shown that in many eclipse arcs there is a noticeable degradation compared with the usual results outside the eclipse. Further analysis of the eclipse period, such as the reduction of the estimation arc length to 2 days, showed no improvement in the orbit prediction error.

### Calibration and Validation

#### GESS coordinate estimation

The coordinates of the GESS antenna phase centres are needed as input values for the ODTs process. To assess the capability of ODTs to estimate the sensor station coordinates, a comparison with the estimated GESS coordinates through external sources – online precise point positioning and Galileo Terrestrial Reference Frame (GTRF) data – was performed. The level of agreement between corresponding PPP and ODTs estimated coordinates was better than 3 cm in the horizontal directions (east and north), and 5–6 cm in the vertical direction (up), while the agreement between GTRF and ODTs station coordinates was better than 2 cm in the horizontal directions in RMS.

#### Verification of the position of satellite reference points

The results of this test case were computed by configuring the E-OSPF process to use RINEX observation files and Satellite Laser Ranging normal points (NPTs). However, the laser measurements were de-weighted in order to provide

a quality check of the L-band orbit estimated by the ODTS process. This procedure allowed the assessment of systematic offsets of the different satellite reference points that might have been introduced in the estimation process.

An overall offset of 24.5 mm was observed when considering all ODTS arcs with the satellite transmitting E5, whereas the offset between the SLR measurements and the L-band GIOVE-A E1/E6 orbit was 1 mm. Therefore, no systematic offset between the coordinates of laser retro reflector and antenna phase centre can be pointed out, as the largest offset found (when considering the phase centre of the E5 signal) was within the expected noise of the SLR measurements.

### GIOVE SLR data processing

The processing of SLR data is considered valuable in order to have an independent means to validate the estimated orbits obtained using L-band measurements from the GESS.

Typical values of the standard deviation of the SLR residuals depend upon how laser measurements are considered in the ODTS process. In this way, a standard deviation of 4 cm two-way (2 cm one-way) is the accuracy of the estimated orbit with respect to the SLR points when these measurements are considered weighted in the ODTS estimation, while a standard deviation of 8 cm two-way is a normal value when SLR is de-weighted. Therefore, the validation of the GESS-only orbits has been considered successful, due to the good agreement between the SLR residuals and the L-band orbit.

## 5.3 GIOVE-A Clock Characterisation

The GIOVE-A onboard clocks are two Rubidium Atomic Frequency Standard (RAFS), FM4 and FM5, operating in cold redundancy. They were developed by SpectraTime and represent the first models of the Galileo onboard clocks.

During the design of the GIOVE-A satellite, it was identified that the baseplate design temperature limits of the RAFS (−5°C to +10°C) could not be guaranteed by the platform. It was recognised that this limitation would have affected neither the integrity nor the functionality of the RAFS, but it may affect its performance slightly. On the basis that this would not affect the achievement of the GIOVE-A Mission objectives, this limitation was accepted.

### Operation of GIOVE-A Clocks

The first switch-on of FM4 in orbit took place on 10 January 2006 at 08:30 UTC. Due to various payload operations, FM4 underwent more than 20 switch-on/off sequences; all of them were fully nominal. FM5 was first successfully switched on during payload commissioning on 16 February 2006 at 18:00 UTC, and underwent a second successful switch-on sequence on 26 February 2007 at 09:24 UTC.

As of 15 June 2011, the two RAFS clocks on GIOVE-A had accumulated 41 000 h of successful operation (see Table 5.2). During these operating periods, the RAFS telemetries were fully nominal, showing variations in full agreement with expectations.

Table 5.2. Summary of the operation of the RAFS clocks on GIOVE-A as of 31 October 2010.

	FM4 (RAFS-A)	FM5 (RAFS-B)
No. of on-off sequences	20	3
Accumulated operation (days)	1449	286
Longest uninterrupted operating period (days)	428	179

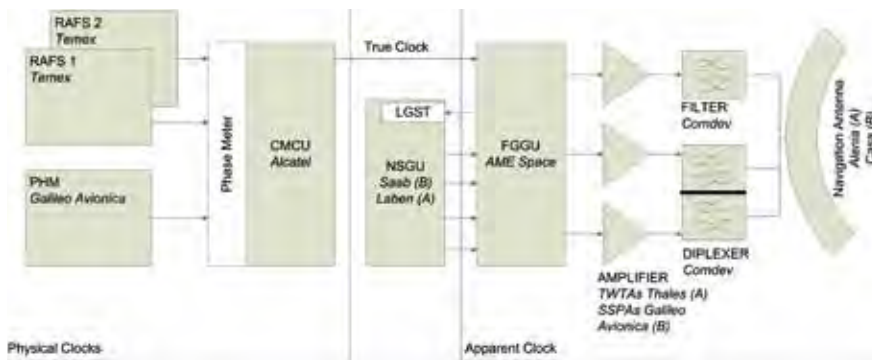


Figure 5.13. Payload equipment on GIOVE-A and GIOVE-B (A and B, respectively). Note that the PHM is present only on GIOVE-B.

The GIOVE-A clock characterisation was performed by INRiM and based on the ODTS clock estimates. Since the ODTS clock estimate is the output of a complex process of GESS observation measures, the ‘clock’ estimate is actually an ‘apparent clock’ estimate, defined as the clock as seen by the measurement system. It therefore consists of the ‘true’ or ‘physical’ clock that may be affected by both the onboard transmission chain (up-conversion, amplification, filtering and emission) and the measurement system noise (see Figure 5.13).

The onboard clocks are estimated with reference to a ground GIOVE Mission reference clock, which may be the INRiM active hydrogen maser, a similar hydrogen maser maintained at USNO, or a third hydrogen maser that was added to the GIOVE network at the GNOR station in February 2009. The INRiM free-running reference clock is monitored continuously to ensure its high performance in relation to Universal Time.

The clock characterisation test cases involved determination of the following:

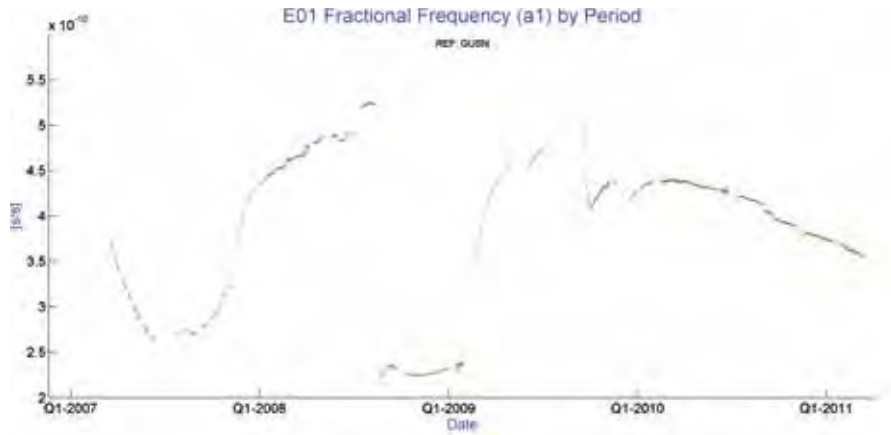
- *Clock deterministic behaviour.* This involved evaluating the frequency offset  $y$  and the frequency drift  $d$ . RAFS typically provide a signal whose frequency offset changes linearly with time; hence, the frequency offset is said to have a linear frequency drift. Typically, the linear frequency drift, after stabilisation, is constant. A constant frequency variation (drift) is fundamental if a good clock prediction is to be uploaded in the navigation message.
- *Clock stochastic noise.* The clock signal is affected by random noise, the type and level of which can be estimated by means of the Allan variance. The type and amount of random noise gives an indication of the clock prediction error, and therefore of the contribution to the User Equivalent Ranging Error (UERE) due to clock prediction.
- *Clock sensitivity to environmental parameters.* In the space environment, a clock may be influenced by environmental variations, and their effects, if any, need to be evaluated since they can degrade clock performance and hence predictability. In particular, the sensitivity of the clocks to variations in temperature and radiation dose have been estimated.

## Overview of the Performance of the RAFS Clocks on GIOVE-A

Figure 5.14 gives an overview of the operation and estimated fractional frequency offsets of the two RAFS clocks on GIOVE-A throughout the mission until mid-March 2011. Although RAFS-A was in continuous operation most of that time, the estimated fractional frequency offset shows data gaps that are due mainly to missing observation data or the effects of spacecraft operations (e.g. switch-off of signal transmission), as shown in Figure 5.14.

RAFS-B was first operated and estimated over about three months in 2007, and then over six months from the end of 2008 to the beginning of 2009.

Figure 5.14. Estimated fractional frequency offsets of the two RAFS clocks on GIOVE-A.



**Performance of RAFS-A**

Figure 5.15 shows the estimated fractional frequency offset of RAFS-A on GIOVE-A during its longest period of operation, from 12 June 2007 to 13 August 2008. During that period, the long-term drift stabilised at around 2 ns per day. From this figure it can be pointed out that over shorter time frames, the variation of the drift does not always follow a smooth and monotonic trend and is affected by sudden frequency changes.

This rather unexpected behaviour is currently explained as being the result of a combination of various factors, including some design limitations, the high-temperature operation, the large number of on-off sequences both onboard and on the ground during satellite integration tests. However, a review of the GPS literature has shown that this kind of behaviour, although at a lower level, seems to be related to rubidium clock technology.

A further examination of the fractional frequency offset behaviour shows a periodic variation with a period equal to the orbital period, as depicted in the upper plot of Figure 5.16.

The lower plot in Figure 5.16 shows the variation in temperature as measured on GIOVE-A at the location of the RAFS-A. The fractional frequency offset behaviour is clearly explained by the fact that the clock is operating outside its nominal operating temperature range (but within its design temperature range), and also that the temperature variation over one orbit is larger than expected. Tests on the ground of similar units have confirmed that the temperature sensitivity outside the nominal operating temperature range is in line with the results observed onboard. The observed oscillations are therefore predominantly explained by temperature effects. As indicated earlier, this high operating temperature was a known and identified limitation of the GIOVE-A platform.

Figure 5.17 shows a typical Allan deviation for the RAFS-A ‘apparent’ clock on drift-removed ODTS data (evaluated over the period from DOY 60 to DOY 64

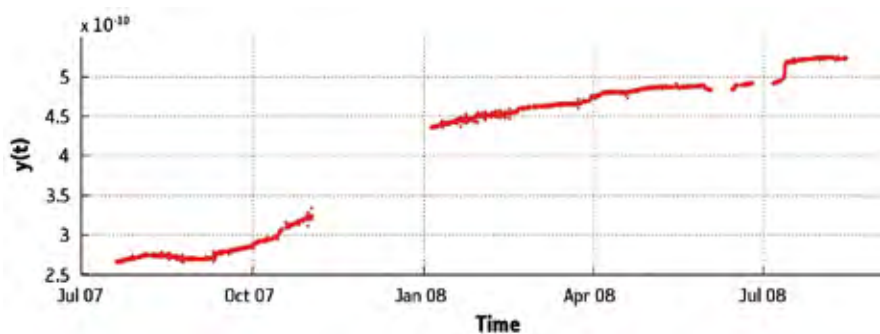


Figure 5.15. Estimated fractional frequency offset of RAFS-A on GIOVE-A during its longest operating period.



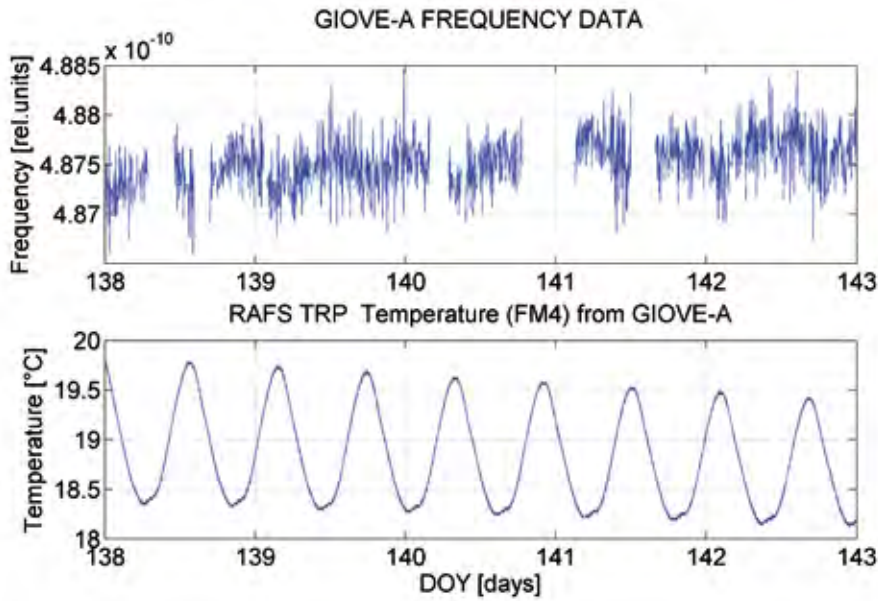


Figure 5.16. Estimated fractional frequency offset of RAFS-A on GIOVE-A, and the associated temperature variation, 18–23 May 2008.

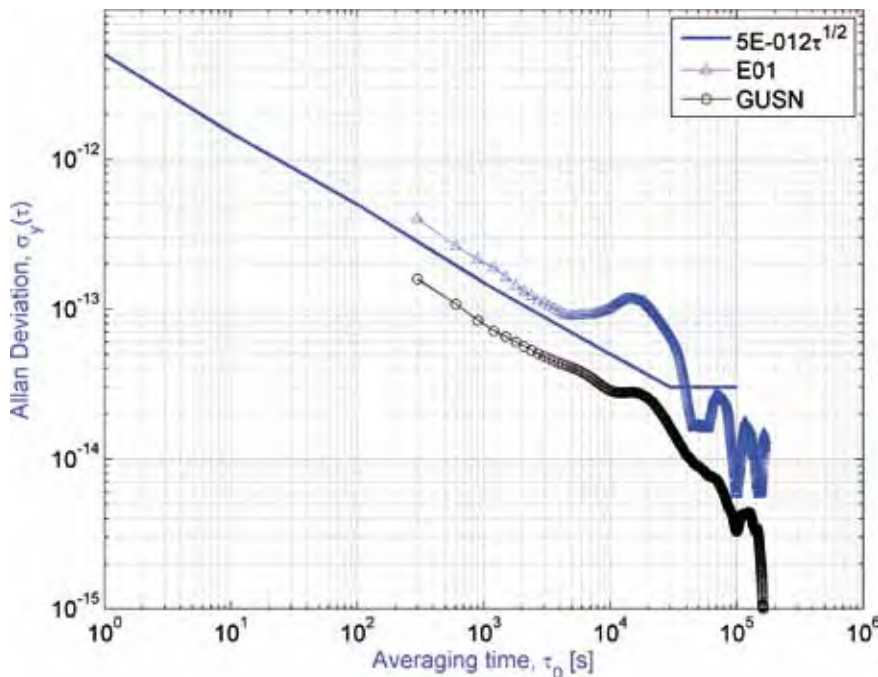


Figure 5.17. Typical Allan deviation of the estimated RAFS-A on GIOVE-A, 29 February to 4 March 2008.

in 2008). It shows that the short-term frequency stability is at the expected level, while at longer integration intervals, the oscillation in the Allan deviation reflects the oscillation at the orbital period due to temperature sensitivity, showing a bump at around  $\tau = 20\,000$  s of about  $2 \times 10^{-13}$  of amplitude, which is in line with the amplitude of the frequency fluctuation shown in Figure 5.16.

Also reported on this plot is the level of system noise estimated over this particular period, which is well below the estimated clock performance.

### Performance of RAFS-B

Figure 5.18 presents the estimated fractional frequency offset of RAFS-B on GIOVE-A over its longest operating period. It is noticeable that the unit demonstrates a switch-on period characteristic of space rubidium clocks before

Figure 5.18. Estimated fractional frequency offset of RAFS-B on GIOVE-A during its longest operating period.

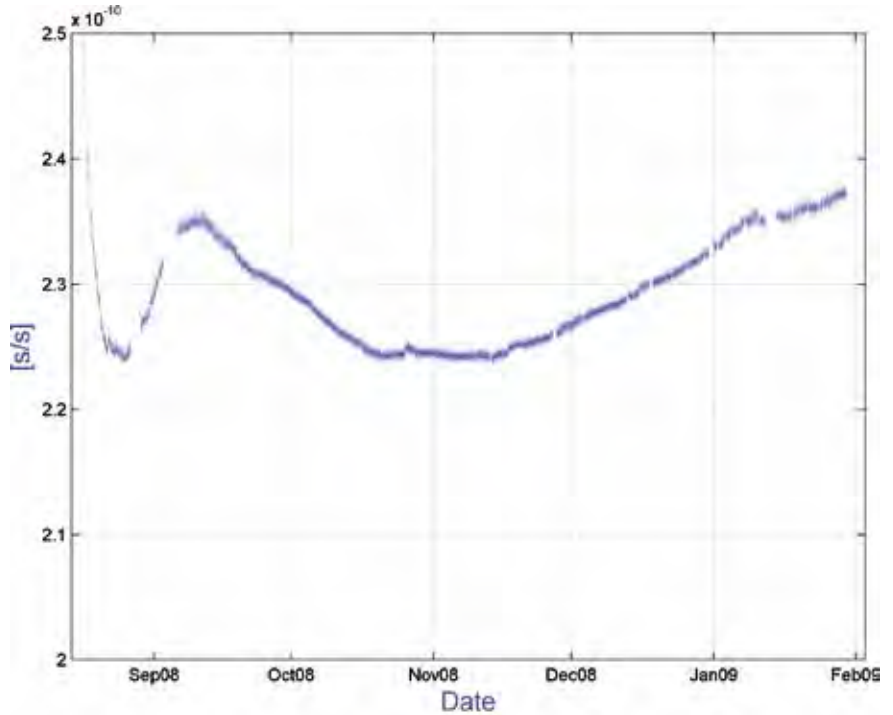
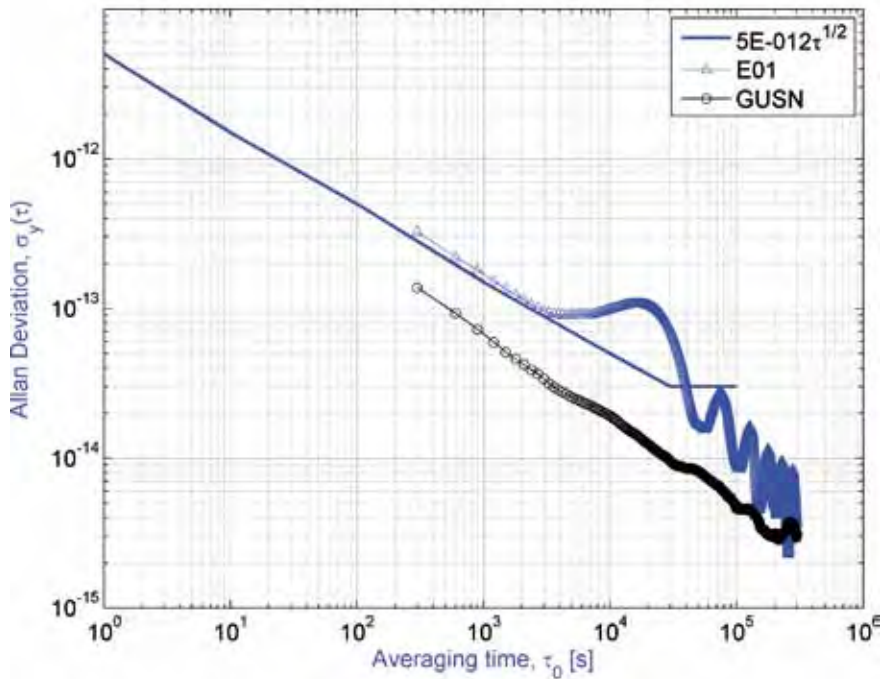


Figure 5.19. Typical Allan deviation of estimated RAFS-B on GIOVE-A, 25 October to 1 November 2008.



assuming nominal operation, with a frequency drift stabilising at around  $2 \times 10^{-13}$  per day about one month after switch-on.

Figure 5.18 also shows that the estimated fractional frequency offset is affected by an oscillation in the orbital period, with an amplitude similar to that obtained with RAFS-A. This behaviour is also explained by high-frequency sensitivity to temperature due to operation outside the nominal operating temperature range. The long-term behaviour of RAFS-B is clearly smoother and more monotonic than that of RAFS-A, for various reasons, in particular the fact that this specific unit has undergone a much shorter operating period, and fewer on-off cycles at atmospheric pressure during ground tests at satellite level.

Finally, Figure 5.19 presents a typical Allan deviation for RAFS-B on drift-removed data. Here, the above comments on RAFS-A results are also applicable to RAFS-B.

## 5.4 IONO and BGD Experimentation

The IONO and BGD experimentation consisted in running the E-OSPF IONO and BGD module every 48 h (starting from 00:00 UTC) in order to generate the estimated GESS vertical total electron content ( $\nu$ TEC) at each epoch, the satellite and station BGDs, Az coefficients and the ionospheric disturbance flags. The tests designed for the IONO part of the experiment focused on analysing the stability of the GIOVE and GESS BGDs, checking the accuracy of the GPS BGDs and the GESS  $\nu$ TEC determination, and checking the accuracy of the NeQuick  $\nu$ TEC values when Az is estimated from the IONO + BGD module Az ionospheric coefficients.

The experimentation involved six test cases:

- GIOVE and GESS group delay stability;
- GPS group delay determination accuracy versus IONEX;
- IONO TEC determination accuracy versus IONEX;
- single-frequency IONO performance;
- IONO disturbance flag analysis; and
- IONO + BGD algorithm performance.

With 48 h batches, only 24 out of the 48 h can be assessed using the SF IONO algorithm. In future experiments, the 48 h could be considered at least as a moving window with a period of 24 h.

The main results for the IONO + BGD test cases are summarised in the following sections.

### GIOVE and GESS Group Delay Stability

It is important to point out the stability of the GIOVE E–E5 and E1–E6 inter-frequency bias over time, with a peak-to-peak maximum deviation of less than 0.81 ns and a standard deviation of 0.15 ns. Figure 5.20 shows the variability of the GIOVE-A and GIOVE-B E1–E5 IFB.

As for the Inter-System Bias, all GIOVE-A E1–E5 and GPS satellite P1–P2 ISBs are relatively small (except for GUSN), but not negligible. The GIOVE-A E1–E6 and GPS satellite P1–P2 ISBs are higher than +20 ns for all stations. This is due to the fact that the mean values of the GIOVE-A E1–E6 IFBs are considerably higher than the corresponding GPS satellite P1–P2 IFBs. Figure 5.21 shows the mean values of the GESS IFBs and ISBs for the E1–E6 frequency signal combination over the period analysed.

Figure 5.22 shows the standard deviation values of the GESS IFBs and ISBs for the E1–E5 frequency signal combination over the period analysed. The stability of the P1–P2 and E1–E5 IFBs is remarkably good, with the GIEN and GNOR stations showing the worst stability. The stability of the P1–P2 and E1–E6 IFBs is also remarkably good, with the GIEN station showing the worst stability.

### GPS Group Delay Determination Accuracy versus IONEX

The agreement between the IONO module and the IONEX IFB values was remarkably good over the whole period analysed. Figure 5.23 shows the IONEX–IONO GPS IFB RMS values against the day of the year for the E1–E5 frequency signal combination.

Figure 5.20. Temporal evolution of the GIOVE-A and GIOVE-B E1-E5 IFB (DOY 191-360, 2008).



Figure 5.21. Mean values of the GESS IFBs and absolute GIOVE-A E1-E5 and GPS satellite P1-P2 ISBs (DOY 70-151, 2007).

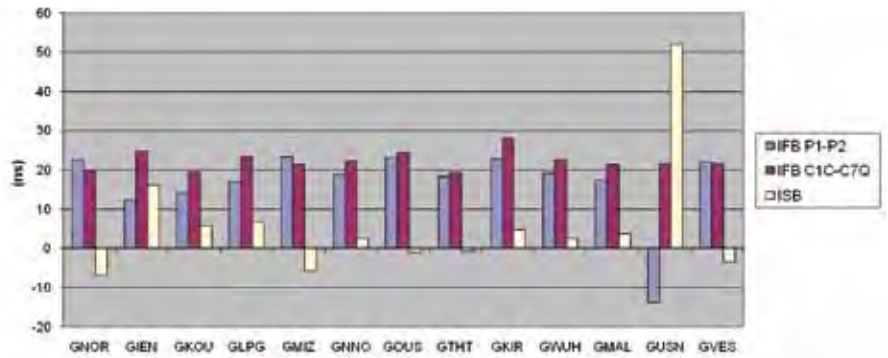
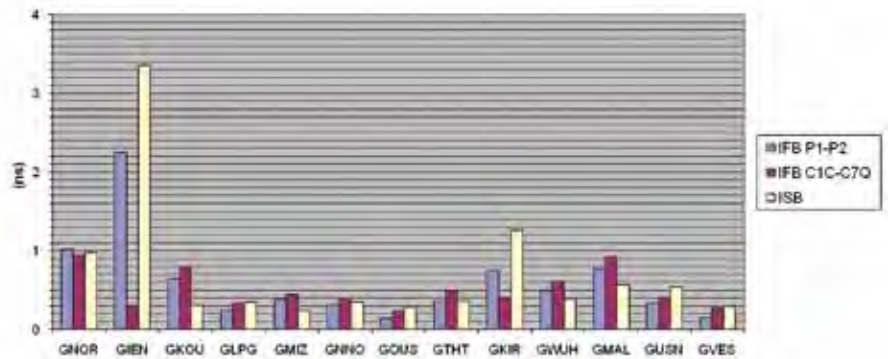


Figure 5.22. Variability of station differential group delay (IFB) (DOY 70-151, 2007).



Despite the good stability and high level of agreement between the satellite IFBs with IONEX, the accuracy of the STEC estimation is not fully guaranteed. In fact, a bias may be introduced if part of the STEC is assumed into the GESS IFBs or vice versa. In future experiments, some methods could be designed to minimise this effect.

### IONO TEC Determination Accuracy versus IONEX

The IONO module estimates the  $\nu$ TEC values at each GESS location by means of its Kalman filter, which also estimates the satellite and GESS inter-frequency biases. Both results (IFBs + IONO  $\nu$ TEC values) are outputs of the IONO algorithm, but they differ in importance: whereas the IFBs are broadcast in the navigation

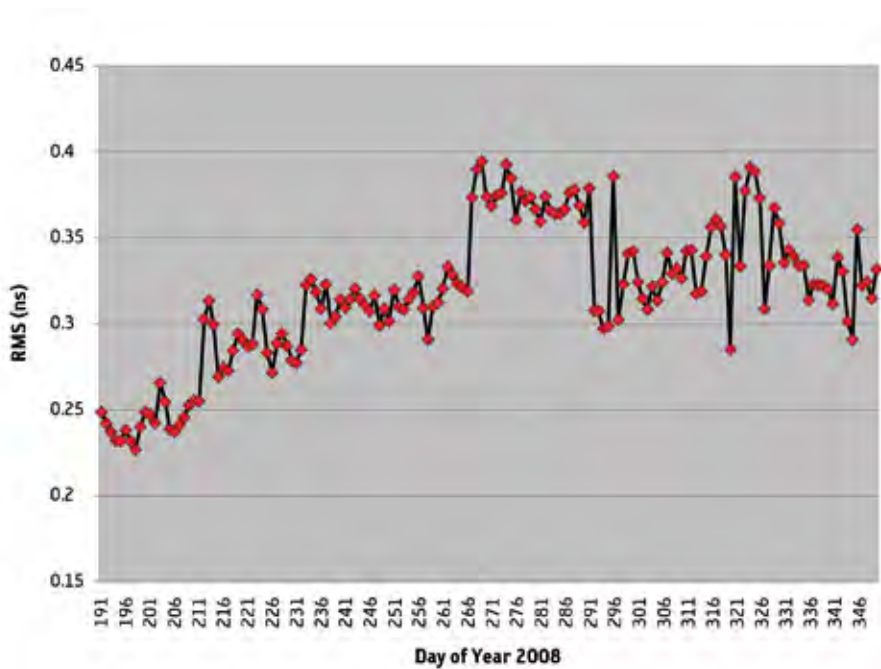


Figure 5.23. IONEX-IONO GPS satellite IFB RMS values, 9 July to 15 December 2008.

message and are necessary for users to estimate their location, the IONO  $v$ TEC values constitute a secondary IONO output, since users do not need them (they need only the Az coefficients to compute the NeQuick TEC values and the ionospheric delay for their approximate location). This is the main reason why the IONO  $v$ TEC values are analysed only during a precise campaign.

In order to analyse the IONO  $v$ TEC values at each GESS location computed using the IONO IFB module, a brief analysis was developed. IONO and IONEX  $v$ TEC values for each GESS location were computed for several selected days. Table 5.3 shows the days selected for this campaign and the corresponding maximum Dst index, which represents the axially symmetric disturbance magnetic field at the dipole equator on Earth's surface. They all correspond to magnetically quiet days.

The RMS values of the IONEX-IONO  $v$ TEC values have been computed for each day analysed (see Figure 5.24). The equatorial stations Kourou (GKOU) and Malindi (GMAL) show the largest differences between the IONO and IONEX  $v$ TEC values. As a consequence of these results, the NeQuick  $v$ TEC daily variation using the local Az value for the GKOU station will generally show the maximum difference from the IONEX  $v$ TEC values.

The average relative errors in the IONEX-IONO  $v$ TEC values have also been computed for each day analysed (see Figure 5.25). For each day, the average relative error is calculated by dividing the daily RMS IONEX-IONO  $v$ TEC values (shown in Figure 5.24) by the average IONEX  $v$ TEC value for each location. In this case, as observed, the GOUS station shows the maximum values over the last three IONO arcs.

Calendar date	DOY	Dst index
15 March 2007	74	-12
25 March 2007	84	-33
04 April 2007	94	-23
20 April 2007	110	-42
30 April 2007	120	-9
10 April 2007	130	-9
20 May 2007	140	-9
30 May 2007	150	-13

Table 5.3. IONO  $v$ TEC determination accuracy versus IONEX on selected days.

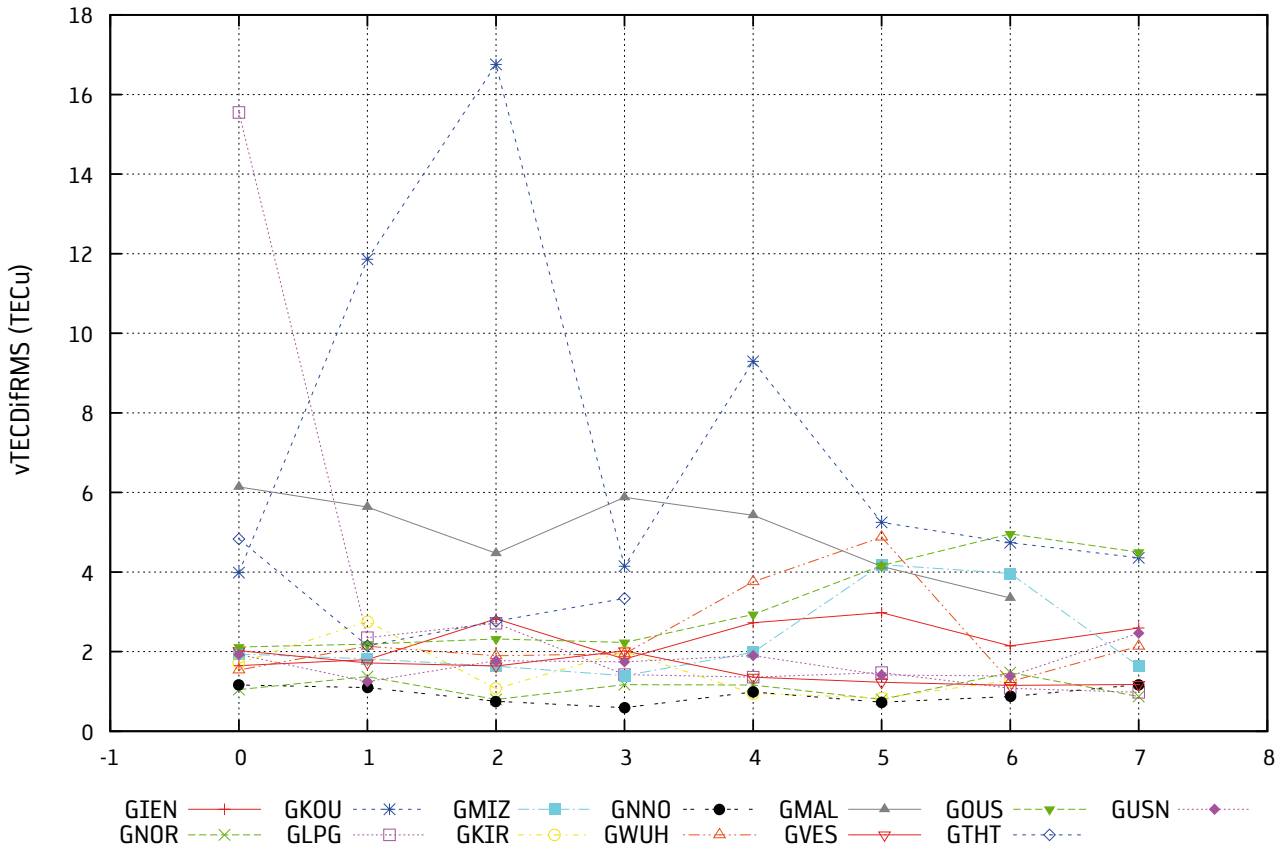


Figure 5.24. Daily RMS values of the IONEX-IONO vTEC differences for eight selected days (shown on the x-axis).

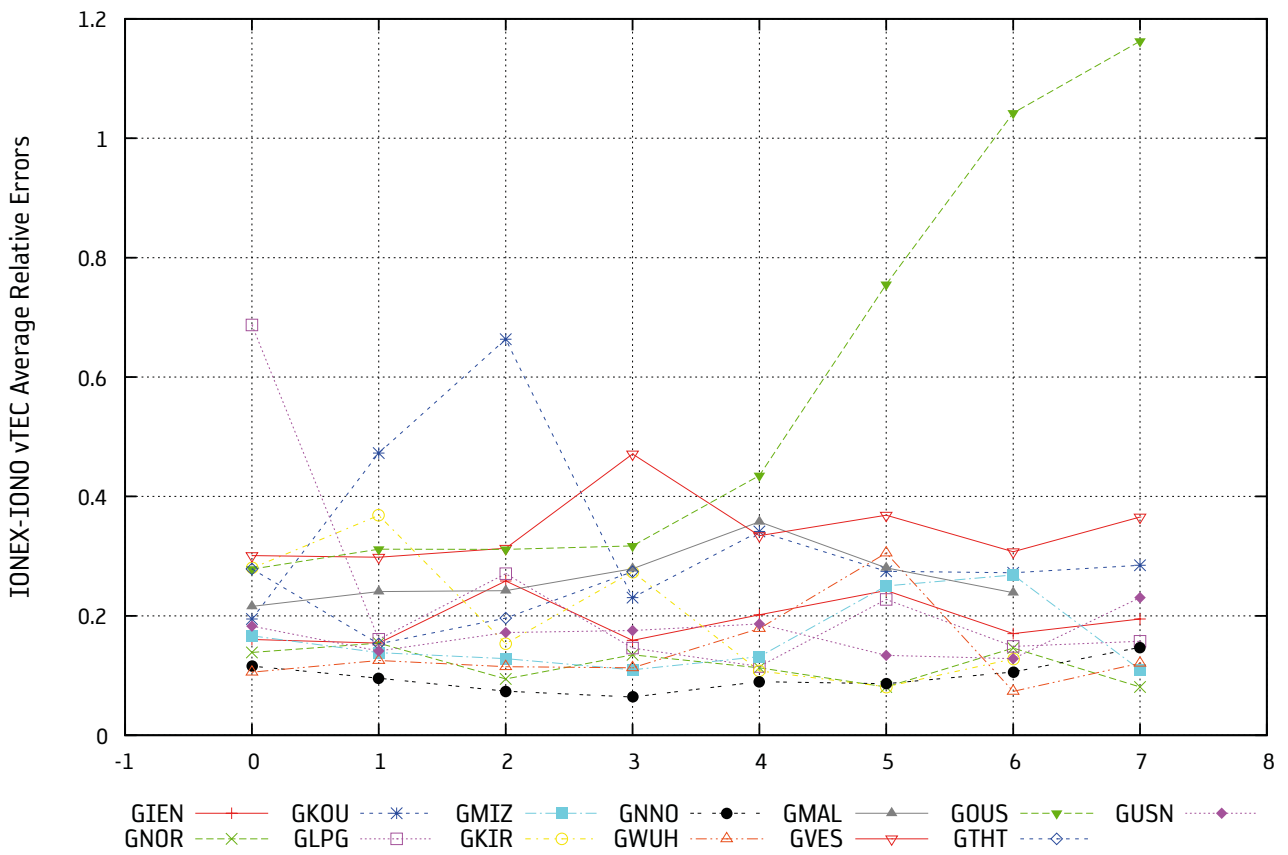


Figure 5.25. Daily average relative error values of the IONEX-IONO vTEC differences for eight selected days (shown on the x-axis).

### Single-frequency IONO Performance

It has been observed that the local Az mean value increases as the absolute Modified Dip Latitude (MODIP) angle increases, whereas the standard deviation does not show a clear dependence on the MODIP angle and shows very low values for the analysed period (see Figure 5.26). Note that the MODIP is a latitude modified with the magnetic inclination.

Two methods have been used to determine the accuracy of the single-frequency IONO algorithm. With the first method, the GESS sTEC estimation using NeQuick and Az coefficients with respect to the sTEC value given by the IONO algorithm for each GESS are compared. In this method, both global and MODIP region statistics are computed.

The five predefined regions in the navigation message (see Figure 5.27) are:

- zone A: northern region ( $60^\circ < \text{MODIP} < 90^\circ$ )
- zone B: northern middle region ( $30^\circ < \text{MODIP} < 60^\circ$ )
- zone C: equatorial region ( $-30^\circ < \text{MODIP} < 30^\circ$ )
- zone D: southern middle region ( $-60^\circ < \text{MODIP} < -30^\circ$ )
- zone E: southern region ( $-90^\circ < \text{MODIP} < -60^\circ$ ).

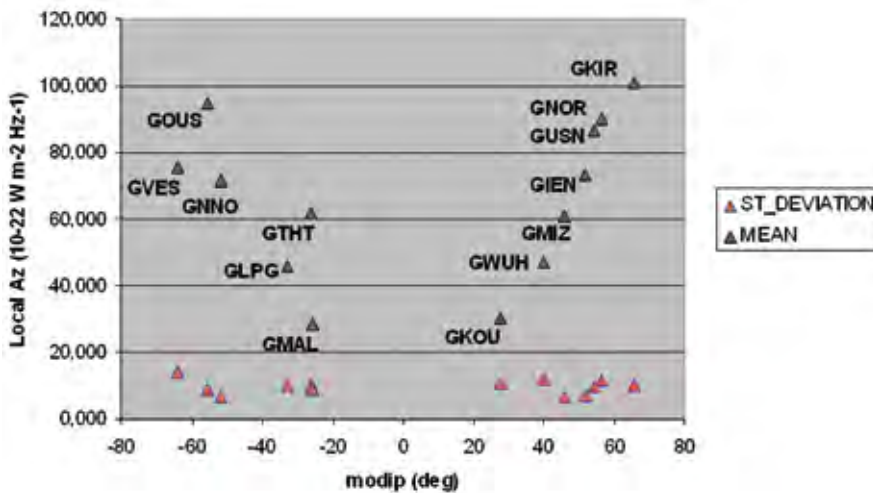


Figure 5.26. IONO local Az mean and standard deviation values against MODIP angle, from 11 March to 31 May 2007.

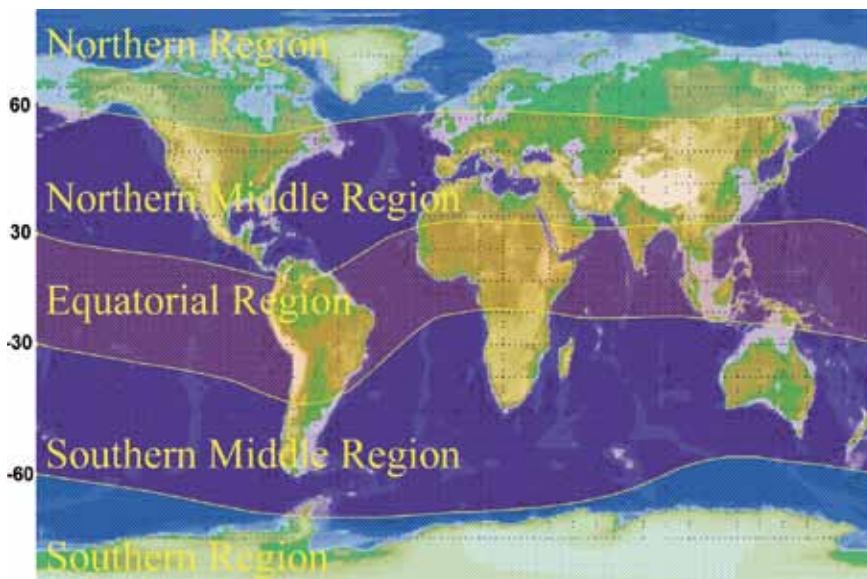


Figure 5.27. MODIP regions.

The following compliance targets are defined (the same as for the Galileo mission):

- for regions B and D, accuracy >95% within specification,
- for regions A, C and E, accuracy >85% within specification, and
- global combined accuracy >90% within specification,

where the required level of accuracy is achieved if the residual error is less than 20 TECUs or less than 30% RMS.

The experimentation results can be summarised as follows:

- compliance targets are largely met for all the regions, which demonstrates the good internal consistency of the NeQuick algorithm (i.e. how the model fits to its input values);
- as expected, errors are the largest in region C, which is reflected in the percentage of compliance for this region (around 3–4 % less than the other regions);
- it must be noted that 2009 was a year of low solar activity and so the errors are small, which explains the large relative errors observed; and
- whether using the IONO Disturbance Flag (IDF) or not, no significant differences were observed as the percentage of time it was raised during this period was very small.

With the second method, for each grid point on the global ionospheric map, the sTEC value at a range of elevations and azimuths is derived and compared with the sTEC value at the same range of elevations using NeQuick and Az coefficients. Using these differences, sTEC absolute errors are computed by weighting them by elevation and geographical position.

In this case, the results can be summarised as follows (see Figure 5.28):

- compliance targets were achieved for all regions, even if the margin for region C was narrow (86%, while the target was 85%);
- as for method 1, whether the IDF flags were used or not, the differences were insignificant;
- again, errors in region C were the largest, since in the equatorial region absolute sTEC values and gradients are higher, and it is known that for these latitudes, the performance of the NeQuick model is poor; and
- the RMS error decreases as the MODIP angle increases.

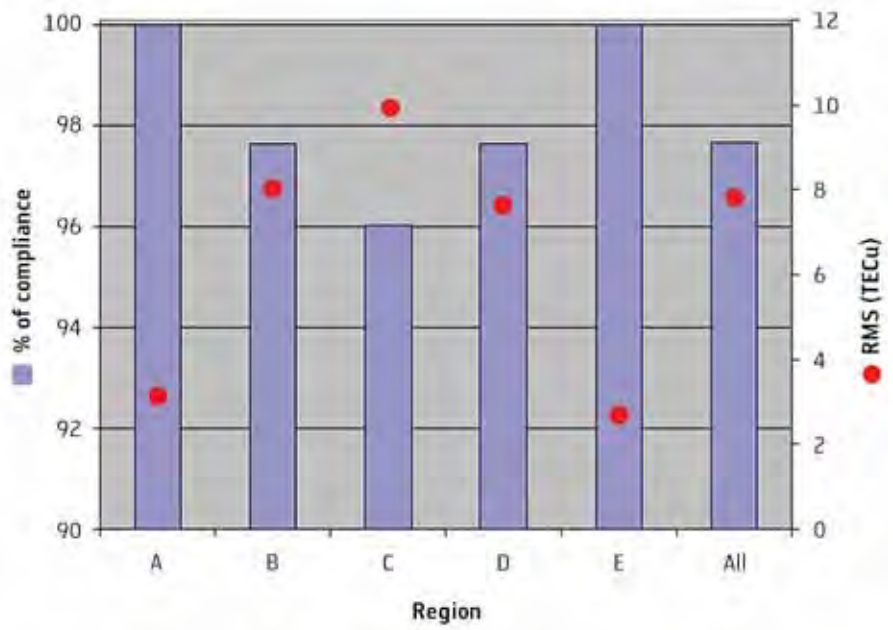


Figure 5.28. Single-frequency IONO algorithm (method 2).



Finally, two versions of NeQuick have been tested: the Galileo baseline and a variant. The variant performed slightly better, but as the impact on the final Galileo performance is minor, this variant was not included in the Galileo baseline.

## IONO Disturbance Flag Analysis

The IDF flags are generally valid for all regions and days during the experimentation period. The equatorial region shows the highest probability of occurrence of an invalid flag, due to the largest sTEC RMS errors computed for the equatorial stations, while the southern middle region usually presents the lowest percentages.

Even if the percentage of time when the flag is raised is low, it has been observed that IDF flags do not behave as an effective barrier. To overcome these problems, modifications could be envisaged, such as combining all error observations for each region, rather than taking into account the disturbance conditions for each station individually.

## 5.5 Sensor Station Characterisation

Part of the GIOVE Mission experimentation was dedicated to the ‘characterisation’ of the GESS stations. These activities consisted of two main streams. The first was based on the survey of the RF environment of the site, with the aim of characterising the GESS RF input, while the second was based on Rx output analysis, with the aim of characterising the Rx performance, and establishing a link between the two. Several samples of 20 days for GIOVE-A and of 5 days for GPS observables were analysed.

The sensor station experimentation had multiple objectives:

- to assess the completeness and quality of the observables collected by the network and to identify possible anomalies that can have an impact on the execution or on the validity of the results of the orbit and clock experiments, and try to implement possible corrective actions;
- to perform a preliminary evaluation of the Galileo signal and receiver performance in a real environment representative of the final Galileo sites based on the GIOVE signal; and to review and compare the measured performance with the specification and assumptions of the Integrity and ODTS algorithm performances;
- in connection with the survey activities performed at the sites, to review/ assess/consolidate the procedure/criteria for Galileo site acceptance; and
- to consolidate the tools and parameters to be monitored during the IOV phase.

The various experimental activities were organised according to the following test cases:

- code phase error analysis (COPE);
- carrier phase error analysis (CAPE);
- C/N analysis (CNAA);
- cycle slip analysis (CYSA);
- station availability analysis (STAA);
- Galileo Sensor Station model update (GSMU);
- Galileo versus GPS analysis (GVGA);
- site installation sensitivity analysis (SESA); and
- antenna experiments.

### Sensor Station Measurement Quality Test Cases

The first achievement concerned the characterisation of the Galileo signals under real conditions: signals transmitted from a flying payload and received at reference stations deployed under real conditions. The opportunity was therefore taken to analyse the receiver measurement error budgets. As an example, the E5a pilot errors were analysed: code phase global error (Figure 5.29 left), multipath error (Figure 5.29 right), uncorrelated code phase error (Figure 5.30 left), and uncorrelated carrier phase error (Figure 5.30, right).

These results represent a key achievement since they are linked to the consolidation of GMS assumptions about the quality of observables. In particular, they allow an assessment of the error reduction through the Integrity Processing Facility (IPF) pre-processing (600-s Hatch filter, computed as the 600-s code residual error).

As for the cycle slip characterisation, two elements must be considered. First, the detection methods are to be assessed and tested, and second, the rate of occurrence of such an event properly assessed. Indeed, the detection of any cycle slip would lead to the re-initialisation of the integrity filter, leading to raw data being unavailable over the filter convergence time.

The detection algorithm is based on a phase prediction approach. A phase value is predicted from six consecutive measurements, with a least-squares process on a second-order polynomial, and compared with the actual phase

Figure 5.29. E5a pilot – global and multipath code phase error.

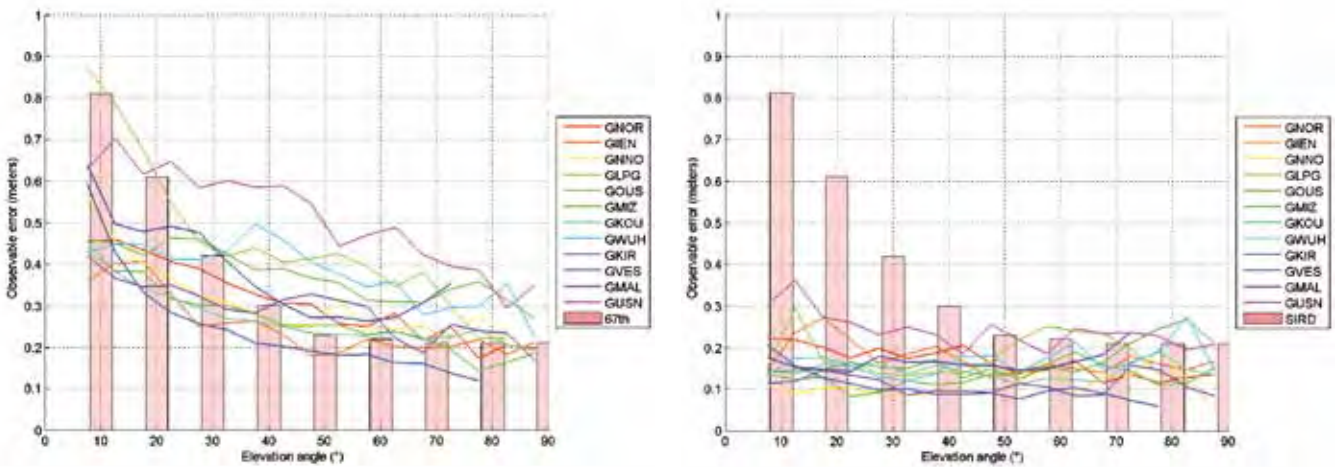
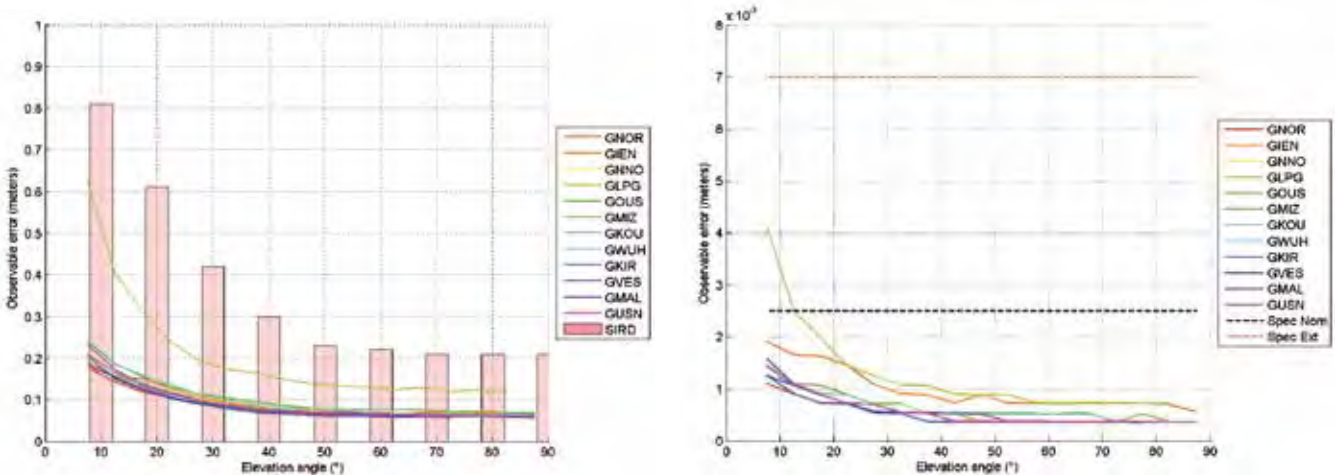


Figure 5.30. E5a pilot – uncorrelated code/carrier performance



measurement value. If the difference between the predicted and actual values exceeds a configurable threshold, it can be deduced that a cycle slip has occurred.

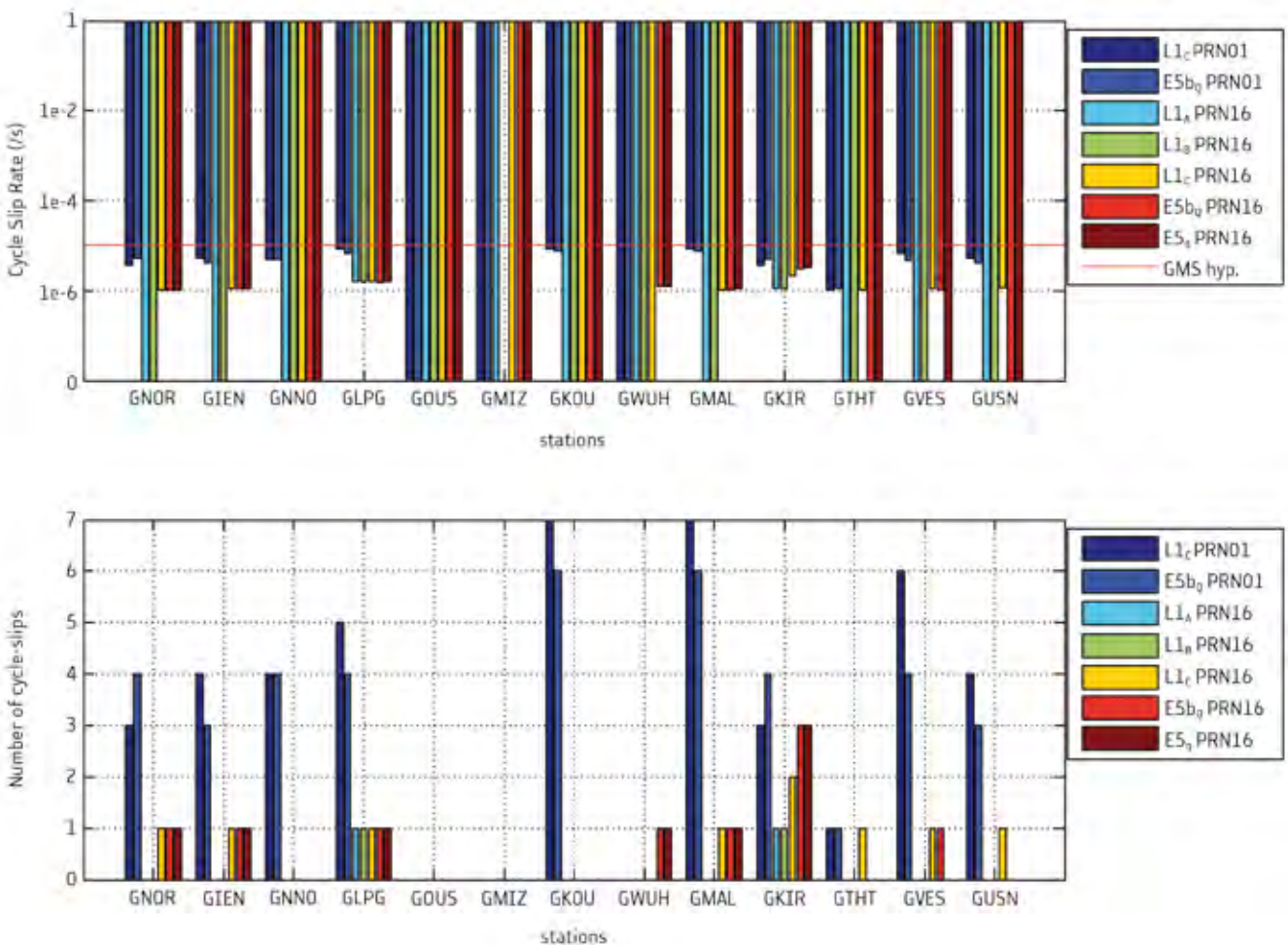
In the GIOVE sensor station analysis, the threshold was set to 0.7 cycles (around 13 cm at E1), which is above the level of phase noise observed (usually well below 1 cm RMS).

Figure 5.31 (lower plot) shows the number of cycle slips detected for GIOVE-A and GIOVE-B and the whole GESS network in August 2008. The upper plot shows the associated probability of occurrence. For information, the Ground Mission Segment (GMS) hypothesis is recalled ( $1e-5/s$ ), corresponding to the occurrence of one cycle slip every 4–6 satellite passes. No excessive cycle slip rate was detected with respect to the hypothesis, except for the Kourou (GKOU) and Malindi (GMAL) stations.

### Station Performance Sensitivity to the Environment Test Case

In addition, an intensive coordinated effort has been made to obtain station RF environment data. The RF survey procedure was designed with the support of RF experts at the TAS-F GMS sites. An exhaustive database concerning the GESS site environments was built (including site images, RF spectra, etc.). The GESS sites were then subjected to the IOV GMS GSS site acceptance criteria. This process demonstrated the relevance of the GMS site specifications, and their capability to determine, from complex measurements, ‘simple’ parameters to accept a site. Furthermore, it allowed the effective control of any site parameter that is likely to affect the receiver performance.

Figure 5.31. Cycle slip characterisation results, August 2008.



This is considered a key achievement, since being able to master the connection between the site RF specifications and GSS performance is one of the key elements in anticipating and controlling the GMS segment performance.

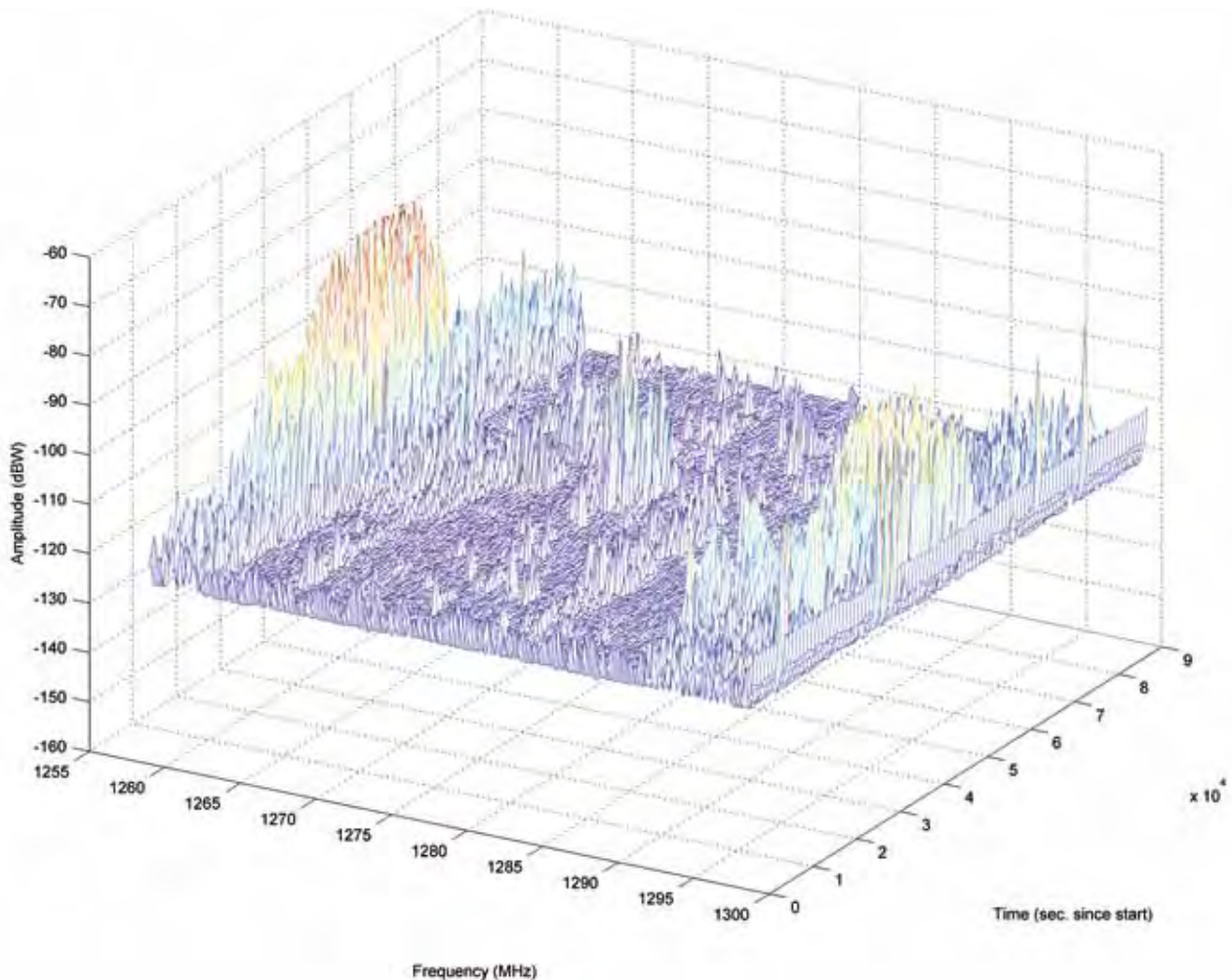
### Antenna Experimentation Test Case

An issue concerning antenna performance emerged during the first phase of the experimentation. The antenna was affected by a variation in the group delay (GD), which was correlated with the line-of-sight elevation angle for the E1 measurement. This group delay instability was also observed on E5 and E6 but without any specific dependence on elevation (see Figure 5.32).

A consequence was the introduction of an incoherence between code and carrier phase measurements. From the point of view of the Galileo algorithm (ODTS and integrity), this is actually similar to a very low-frequency multipath, and would have a considerable impact on its performance. Within the frame of the experiment, a retrofitted antenna unit was deployed at the GPC at ESTEC, and was used for operational data collection.

Since the phenomenon had a very clear signature on the E1 band. The results for this band signal are displayed in Figures 5.33 and 5.34, which show the E1C code carrier coherence for the original and retrofitted antenna. The blue noisy curves are the unfiltered ‘code minus phase’ outputs, while the red curves show the 600 s filtered code carrier coherence.

Figure 5.32. E6 band 3D spectrum, GNOR, 23 and 24 June 2005 (update rate 900 s).



From these figures, it can be noted that the modification to the antenna brought about significant improvements in the group delay stability. The filtered code carrier coherence has this typical elevation-like pattern for the original antenna, whereas no specific pattern appears on the modified antenna.

This is also confirmed by the residual code phase error statistics, plotted for both the original and retrofitted antenna as a function of SV elevation in Figure 5.35. The dashed line indicates the performance of the original antenna, and the solid line that of the retrofitted antenna ('SPENG model').

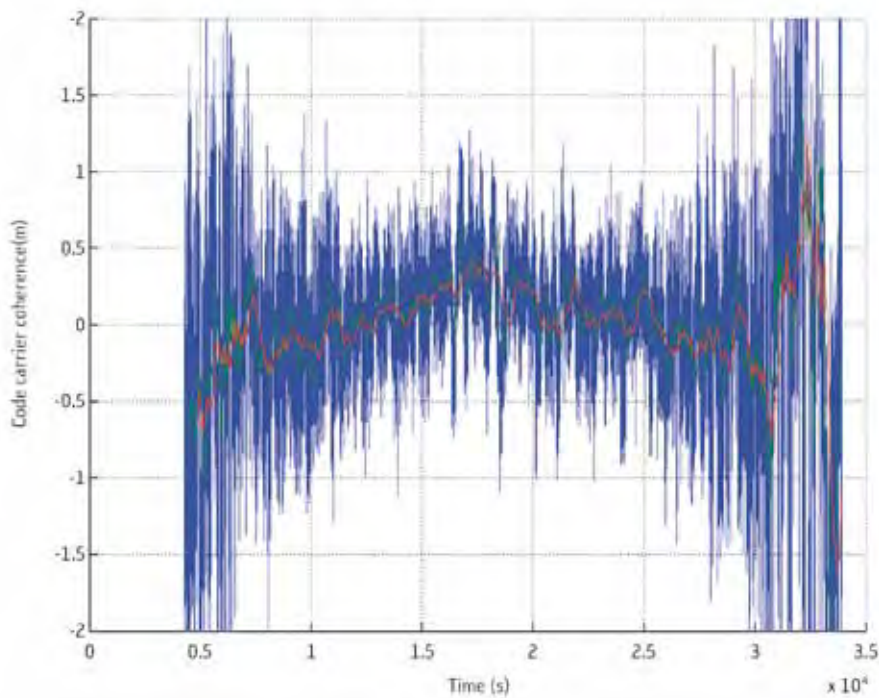


Figure 5.33. Original antenna code carrier coherence.  
CCC function of time - PRN 01 - signal  $L1_C$  - station GNOR.

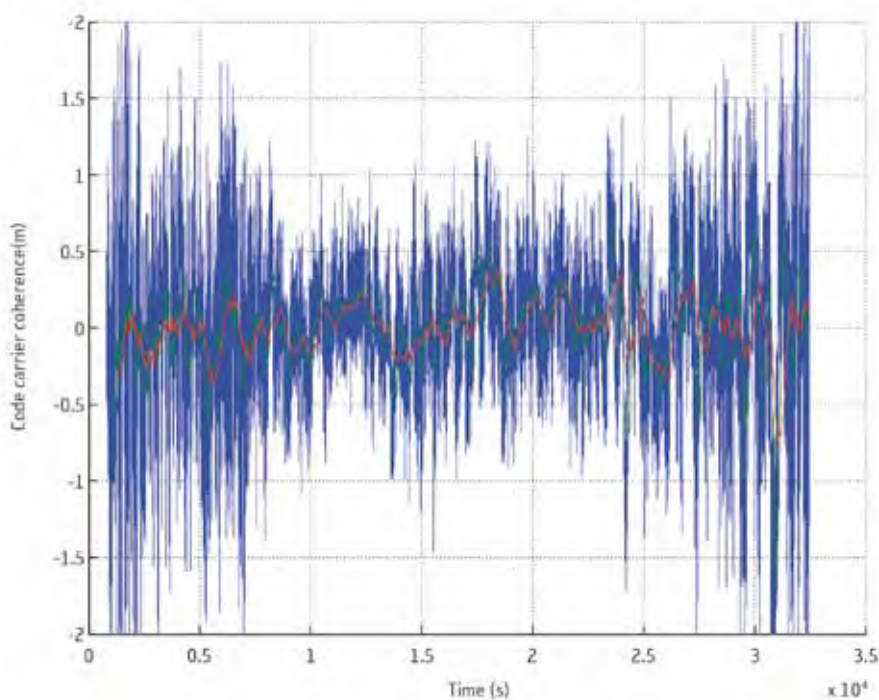
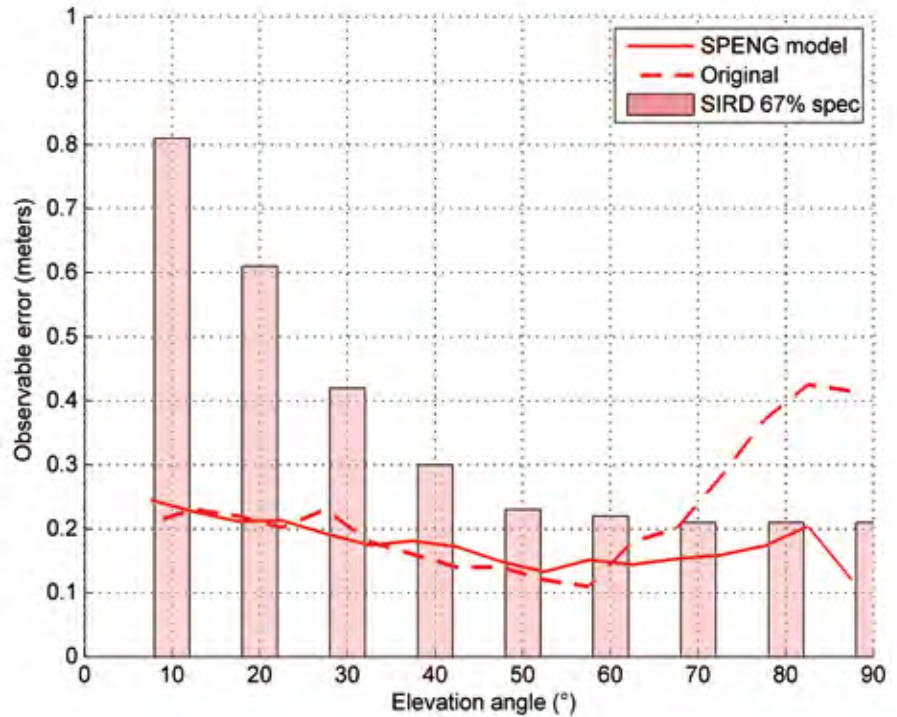


Figure 5.34. Modified antenna code carrier coherence.  
CCC function of time - PRN 01 - signal  $L1_C$  - station GNOR.

Figure 5.35. Residual code phase errors – EIC.



The filtering does not mitigate the error of the original antenna at high elevation, but it is clearly much more efficient on the retrofitted antenna. This tends to show that the Group Delay stability has been much improved.

### 5.6 GPS to Galileo Time Offset (GGTO) Experimentation

The aim of the GGTO experimentation was to study and compare different alternatives for the future operational computation of the GGTO, including its estimation and prediction by means of a linear model that will be included in the Galileo navigation message.

The reference point for this study was the GGTO Preliminary Interface Definition Document agreed between the GPS (represented by USNO) and the Galileo Project Office. This document defined the following key requirements:

- the GGTO has to be broadcast in both Galileo and GPS navigation messages as a linear model (parameters  $a_0$  and  $a_1$ ) with validity of 24 h; and
- the GGTO has to be determined during the Galileo IOV using the connected clock approach, i.e. by measuring the time offset between GST as produced at the Galileo Precise Timing Facility (PTF) and GPS time as reconstructed from the GPS SIS at USNO. In Full Operational Capability (FOC), as the primary method, the GGTO will be computed from the Galileo and GPS SIS received by a dedicated, combined GPS/Galileo receiver at the Galileo PTF.

In the GIOVE activities, the connected clock approach was tested by computing the offset between clocks at USNO (USN3 station) and INRiM (GIEN station) using GIOVE ODS products (method GGTO1), and in a measurement campaign based on two-way satellite time and frequency transfer between USNO and INRiM (method GGTO3). The combined receiver approach was tested by computing the GGTO as the difference between the satellite clock offsets in the GPS navigation messages and those estimated by GIOVE ODS.

The GGTO experimentation results – the GGTO estimation, GGTO prediction performance and GGTO stability comparison – are presented below.

## GGTO Estimation

The operational procedure to compute the experimental GGTO broadcast in the GIOVE navigation message is GGTO2. This estimation is based on the GIOVE ODTS results for GPS satellite clocks (referred to EGST) and the first-order polynomial clock correction broadcast in the GPS navigation message (referred to GPS time):

$$\begin{aligned} \text{GGTO2} &= \text{MEAN}([\text{SATCLK} - \text{GIEN}]_{\text{odts}} - [\text{SATCLK} - \text{GPSt}]_{\text{nav}}) \\ &= \text{MEAN}(\text{GPSt}_{\text{nav}} - \text{GIEN}_{\text{odts}}) \\ &= \text{GPS Time} - \text{GST} \\ &\equiv \text{MEAN}(\text{GGTO}) \end{aligned}$$

The estimated GGTO2 is used to derive the coefficient of the first-order polynomial broadcast in the Galileo navigation message. The broadcast GGTO can be used to correct pseudorange measurements, thus enabling GIOVE/GPS combined navigation solution. Therefore, the accuracy of the GGTO estimation is a driver for the combined GIOVE/GPS positioning performance.

Figure 5.36 shows an example of the GGTO2 mean RMS prediction error over 1 day, and its standard deviation.

The GGTO Preliminary Interface Definition Document specifies the requirements for the GGTO accuracy: 5 ns ( $2\sigma$ ), and the GGTO frequency stability:  $8 \times 10^{-14}$  over 1 day. The GIOVE mission has evaluated the feasibility of meeting these requirements.

Figure 5.37 illustrates that the frequency stability of GGTO2 over 1 day is around  $2 \times 10^{-14}$ , i.e. well below the required  $8 \times 10^{-14}$ .

An assessment of the GGTO accuracy requirement should account for the total GGTO error, i.e. not only the prediction error shown above, but also of the GGTO estimation uncertainty. For example, a systematic bias in the estimation would not show up in the prediction error.

Figure 5.37 also shows that the dispersion of GGTO estimates is around 2 ns –  $1\sigma$ . This is due to a combination of the uncertainty in the GPS clock parameters broadcast in the GPS navigation message and the GPS clocks estimated by the GIOVE ODTS. The two values obtained by comparing with IGS products are around 2 ns and 0.3 ns –  $1\sigma$ , respectively.

Assuming that both the estimation and prediction GGTO errors are uncorrelated, and taking into account the uncertainties in the prediction error (1.26 ns –  $1\sigma$ ) and the estimation error (2 ns –  $1\sigma$ ) over the experimentation period, the total uncertainty of GGTO2 (excluding the contribution of Galileo/GPS ISBs) is:

$$\sqrt{u_{\text{statistical}}^2 + u_{\text{prediction}}^2} = \sqrt{2^2 + 1.26^2} = 2.36 \text{ ns}$$

These results can be extrapolated to the Galileo FOC GGTO determination (making use of the combined GPS/Galileo receiver).

In addition to GGTO2, GGTO1 was computed by studying the consistency of GGTO2.

This estimation was performed by differencing the GIOVE ODTS clock estimates for the USN3 and GIEN stations. USN3 is an IGS station connected to UTC (USNO) and calibrated, located at the USNO centre in Washington, DC.

USN3 is not a GESS. There is also a GESS station (GUSN) installed at USNO and also connected to UTC (USNO), but it is not calibrated. The offset between USN3 and GUSN was studied in order to make the calculation of GGTO1 independent of non-GESS stations.

According to the experimentation results, this offset can be considered stable at around 104 ns with a small non-deterministic ripple. Assuming this experimental value as the offset between the two stations, GGTO1 can be calculated as (GUSN – 104 ns) – GIEN.

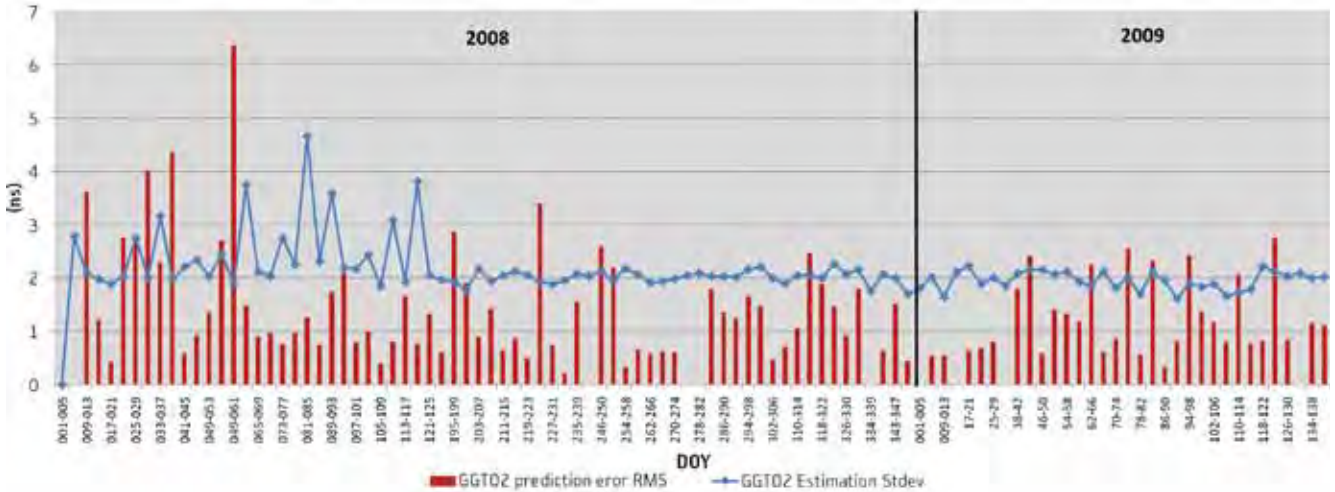


Figure 5.36. GGT02 prediction error and its estimation.

Finally, GGT03 was evaluated using the USNO and Two-way Satellite Time and Frequency Transfer (TWSTFT) measurements. Figure 5.38 shows the preliminary GGTO estimates obtained using all three methods. The drift in the GGTO values is due to the fact that EGST is a free-running maser. The difference between the methods is due to calibration biases. The comparison refers to 2007 since GGT03 was evaluated on a campaign basis at that time.

Table 5.4 presents an overview of the GGTO determination methods implemented during the GIOVE mission and their properties.

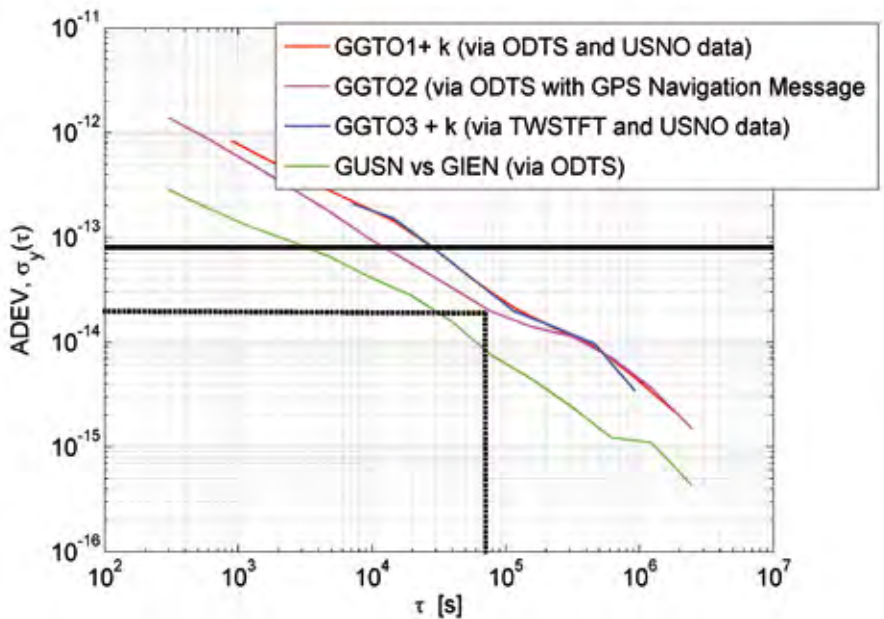


Figure 5.37. GGT02 frequency stability. Allan deviation (1 January to 31 March 2008).



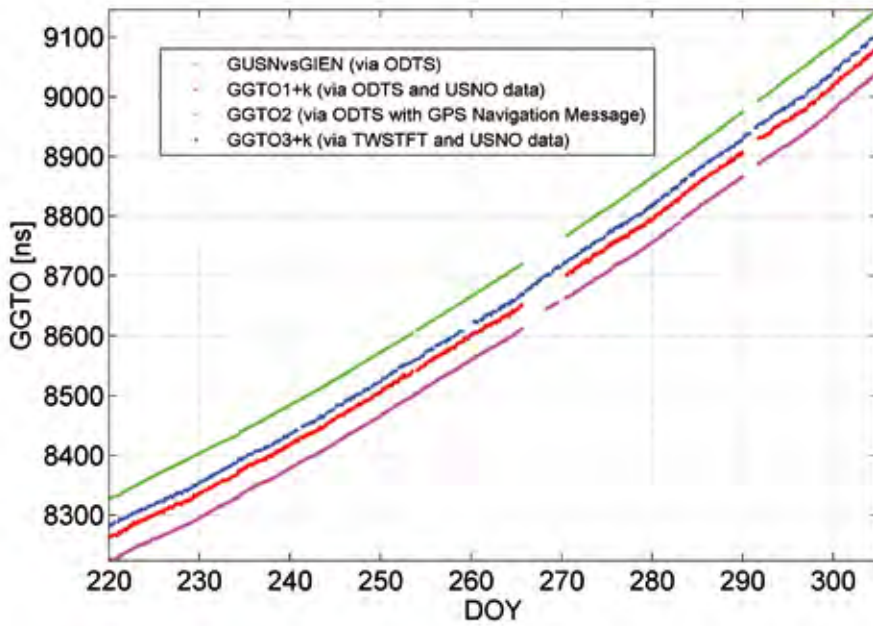


Figure 5.38. Comparison of the three GGTO estimation methods for the experimentation period 8 August to 31 October 2007.

Table 5.4. Overview of GGTO determination methods.

GGTO method	Origin of GPS time	Origin of E-GST	Input data	Sampling rate	Facilities involved	Latency	Stability ( $\tau = 1$ day)	Uncertainty (on daily average value), $1\sigma$	Calibration items
1	USNO measurements	GIEN H-maser	ODTS results/ USNO measurements	15 min	USNO OSPF	$\geq 1$ week (offline)	$1.5 \times 10^{-14}$	$> 6$ ns	USNO P/Y receiver, GUSN station
2	GPS SIS navigation message	GIEN H-maser	ODTS results/ GPS navigation message	5 min	OSPF	Almost real time	$3 \times 10^{-14}$	About 2.4 ns (excluding ISB)	None in GIOVE/ in FOC PTF GESS station
3	USNO measurements	GIEN H-maser	TWSTFT measurements/ USNO measurements	2 h	USNO TWSTFT community	$\geq 1$ week (offline)	$3 \times 10^{-14}$	$> 6$ ns	USNO P/Y receiver, TWSTFT link, GIEN station



**→ GIOVE-B: THREE YEARS  
OF EXPERIMENTATION  
RESULTS**



## 6. GIOVE-B: Three Years of Experimentation Results

Even in the early phases after launch, interest in GIOVE-B has been very high due to the payload carried by the satellite, the Navigation Signal Generation Unit (NSGU) capable of generating the MBOC signal, and the Passive Hydrogen Maser.

Early measurements on the clocks were performed during the GIOVE-B in-orbit test phase, when GIOVE-A had been transmitting the E1 + E5 signals. Whenever possible, data from the two GIOVE satellites were processed together in ODTS, in addition to the GPS satellites. When processing GIOVE + GPS data together in ODTS, a so-called inter-system bias must be estimated for each GESS station to account for the different delays in the GIOVE and GPS signals between stations.

Table 6.1 shows the most relevant measurement pre-processing configuration parameters used in ODTS, as extracted from its configuration file. The characterisation of orbits and clocks has continued since shortly after launch.

### Summary of typical ODTS arcs

Several ODTS data arcs were processed during and after the IOT period. Some of them would have benefited from the presence of SLR measurements.

Table 6.2 shows statistics of pseudorange (code) and phase residuals from ODTS (i.e. the typical differences between the actual and reconstructed measurements). The global rms residual, including all GESSs and elevation angles, is also shown.

A 10° cutoff elevation angle is used in ODTS. The residuals include most effects not absorbed by ODTS models, like GESS noise, interference or multipath (however, part of the mis-modelling can be absorbed by the satellite or station

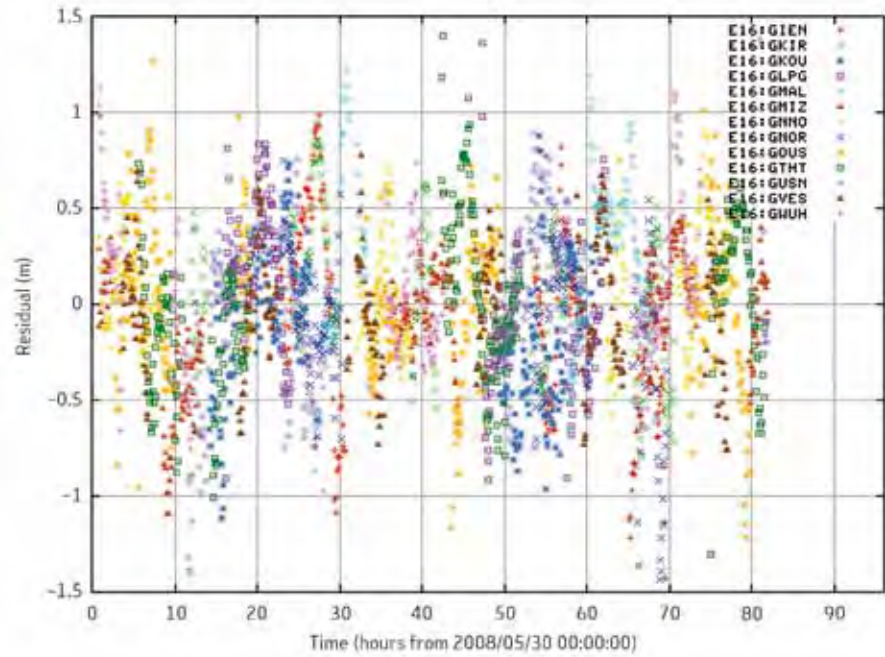
Parameters	
GIOVE raw observables	E1 + E5 → code: C1C–C7Q; phase: E1C–L7Q E1 + E6 → code: C1C–C6C; phase: E1C–L6C
GPS raw observables	Code: P1–P2; phase: E1–L2
Basic observables	Undifferenced iono-free code + phase
Sampling rate of raw observables	1 s
Code smoothing	yes
Type of code smoothing	Hatch filter
Code smoothing time interval	1000 s
Sampling rate after pre-processing	5 min
GPS a priori orbits	from IGS
GPS a priori clocks	from IGS
GIOVE a priori orbit	from two line elements
GIOVE a priori clock	none
SLR for GIOVE-A and GIOVE-B	yes (when available)
GESS meteo data	no
SLR meteo data	yes
SLR tropo correction	Marini–Murray

Table 6.1. ODTS configuration parameters (pre-processing).

	GIOVE E1 + E6	GIOVE E1 + E5	GPS E1 + L2	GPS E1 + L2 (IGS scenario)
Smoothed code (cm)	50.0	40.0	40.0	27.0
Phase (mm)	13.0	13.0	9.0	7.0

Table 6.2. Code and phase residuals from ODTS.

Figure 6.1. Smoothed ODTS pseudorange residuals pattern (PRN: E16, GSS: all).



apparent clock estimates). For comparison, the ODTS residuals of an ‘IGS scenario’ (i.e. ODTS processing of around 30 IGS stations worldwide) are shown in Table 6.2. It can be seen that the number and quality of stations have an impact on the ODTS residuals and hence on the quality of the ODTS products.

When each GESS is analysed separately in detail, an unexpected linear elevation-dependent pattern is observed in the code residuals (see Figure 6.1). This pattern is also observed when analysing multipath from the code phase data, although the effect has been demonstrated to have its origin at the GESS antenna. A modified antenna prototype has been developed that seems to mitigate this effect, and has been installed at the GNOR and in GIEN stations.

It should be noted that the code residuals for GPS measurements also show the same type of behaviour, as would be expected if the origin of the incoherence is the antenna (common to GPS and GIOVE).

### Use of Satellite Laser Ranging

Satellite Laser Ranging is a two-way optical tracking system that is widely used for precise orbit determination. Its use is limited by factors such as the size of the satellite retro-reflector, the meteorological conditions at the station (a clear sky is normally required, and some stations can only track at night), the availability of precise orbit predictions for station telescope pointing, and the priority of the satellite mission for the International Laser Ranging Service (ILRS), the institution that coordinates the SLR station activities.

Figure 6.2 shows the typical distribution of SLR residuals in time for some of the ODTS arcs for which SLR data were available. In general, the SLR residuals are of the order of 4 cm rms (one-way), which indicates a very good agreement between the L band measurements from the GESS network and the SLR measurements.

The SLR residual statistics for the different ODTS arcs range from 2.0 cm to 7.0 cm rms one-way. In general, it can be said that this technique is used both as a quality check system for the orbit, and as a means to improve the accuracy of orbit estimates when the measurements are sufficient.

It has in fact been demonstrated that the measured frequency stability of the GIOVE-B PHM improves when the SLR measurements are used in weighted mode.

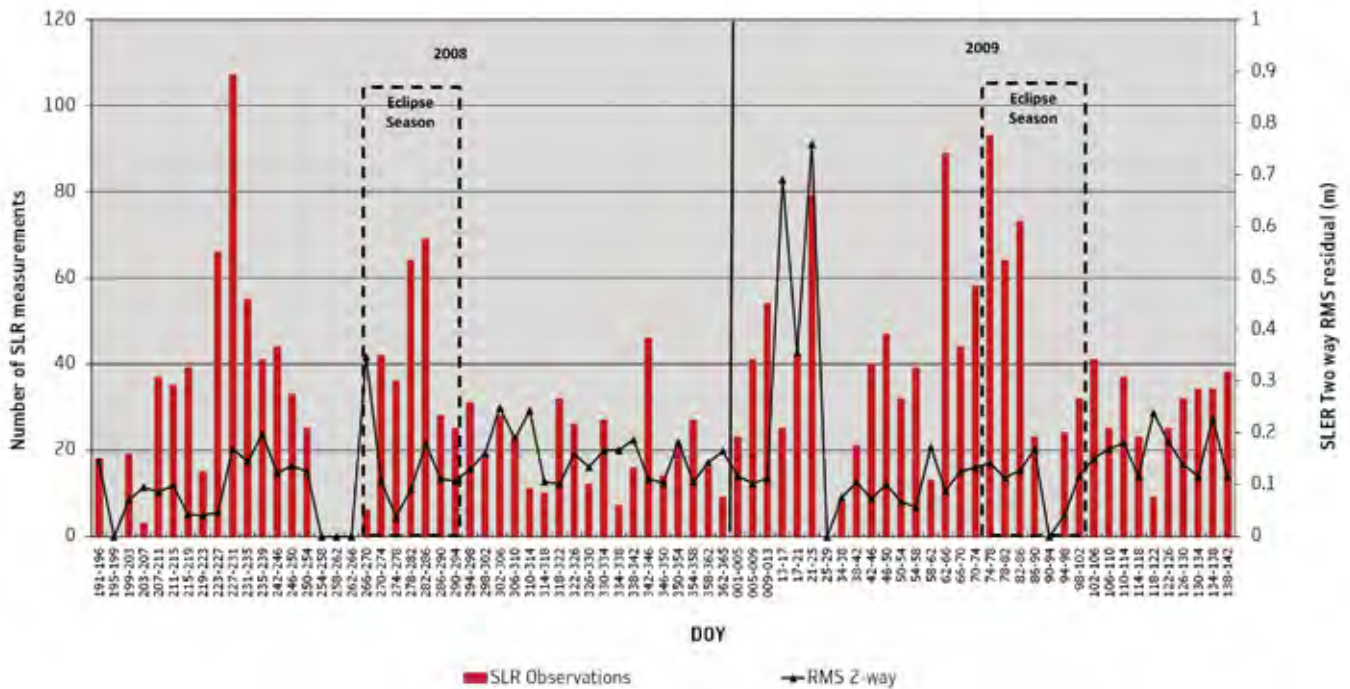


Figure 6.2. Two-way SLR residuals from ODTS for GIOVE-B.

## Evaluation of the Accuracy of Clock and Orbit Estimates

An assessment of the GIOVE (and GPS) estimated clock accuracy provided by ODTS is necessary in order to understand the clock characterisation results presented in the following sections. The restituted orbit accuracy is also interesting since the orbit and clock estimates are made together in ODTS from the same observables, and therefore the two are to some extent correlated.

For the GIOVE satellites, one way to assess the orbit and clock accuracy is to use so-called overlaps, which simply involves comparing the orbit and clock solutions generated by ODTS over two consecutive but overlapping ODTS arcs. Normally, the overlapping period used in the ODTS configuration is 1 day. The concept is depicted in Figure 5.6. Actually, the overlap comparisons do not really measure the absolute orbit and clock accuracy but rather the internal ODTS consistency.

Figure 6.3 shows the ODTS typical overlap differences for ODTS arc 06 for GIOVE-B. The clock difference has been converted to distance (m) in order to provide a better comparison with the (radial) orbit difference. As can be seen, the clock overlap difference is normally in opposition to the radial orbit error, and is roughly of the same magnitude. This indicates that there is some correlation between the orbit error and the clock error, which is a normal feature of a process like ODTS. Figure 6.4 presents a summary of all the arcs analysed. The global rms for GIOVE-B arc overlap is 14.5 cm (17.8 cm during the eclipse period).

Figure 6.5 shows the clock arc overlap over the same period, which is an indication of the precision of the clock estimation. In this case the overall rms is 0.5 ns (0.52 ns during the eclipse period).

During the GIOVE experimentation, the E-OSPF generated 1-day long orbit predictions in each ODTS arc. Similar to the orbit estimation, the orbit predictions have been projected into the WUL in order to derive a performance indicator. Figure 6.6 shows that, for GIOVE-B, the overall rms error is 20.3 cm (28.2 cm during and 17.5 cm outside the eclipse period).

Figure 6.3. ODTS overlaps for arc 06.  
Orbit and clock difference for E16.

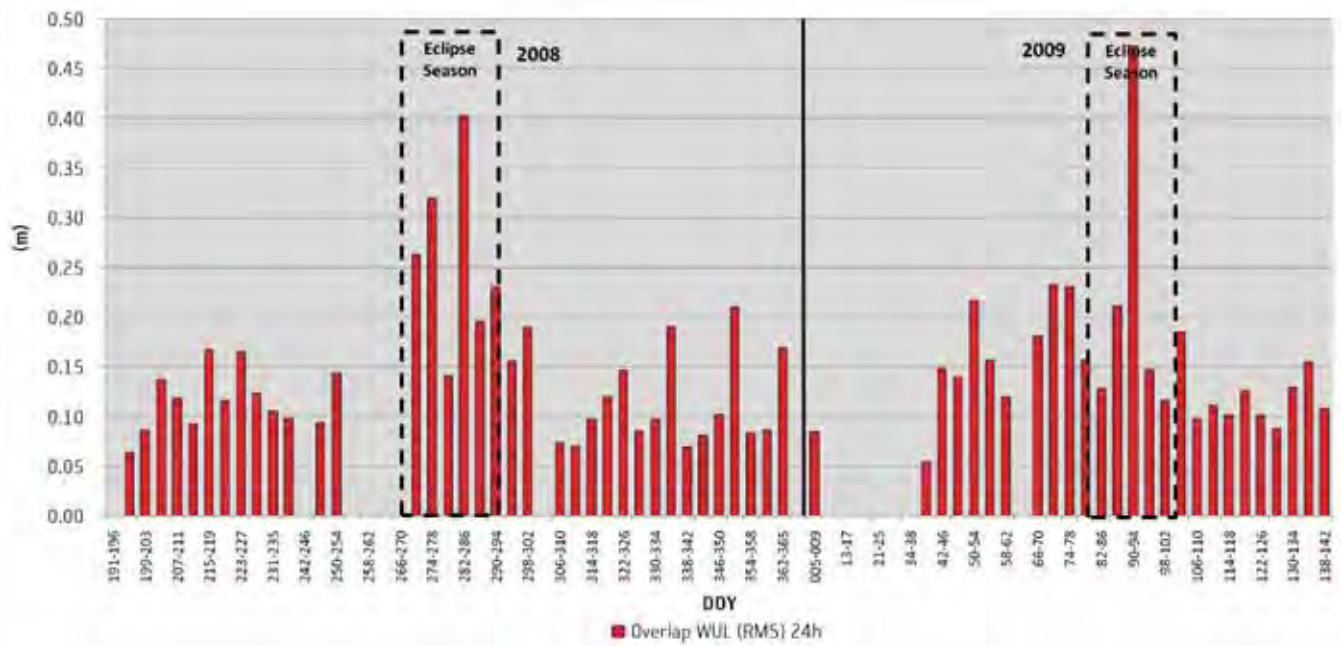
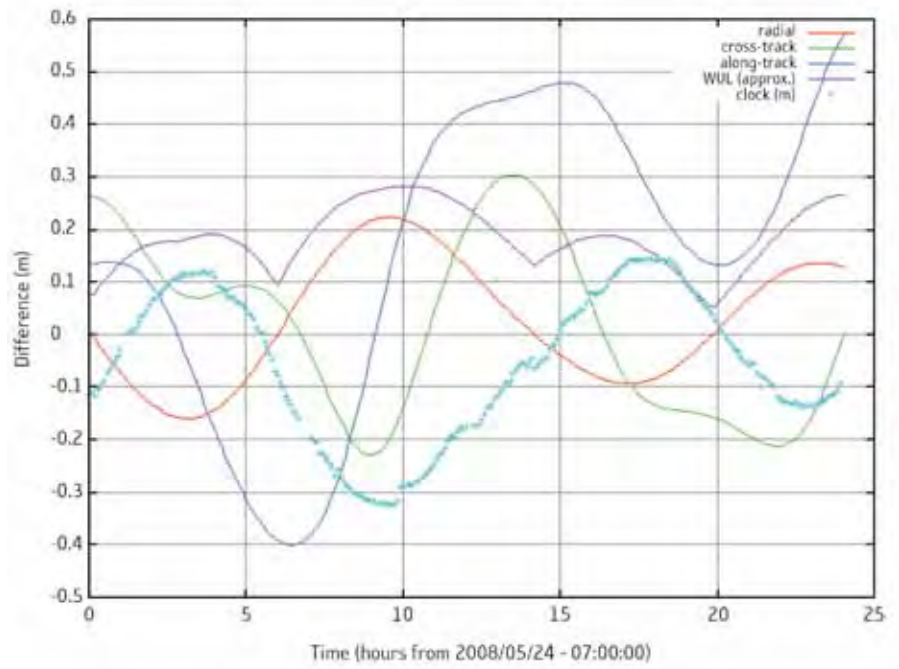


Figure 6.4. GIOVE-B orbit overlap consistency.



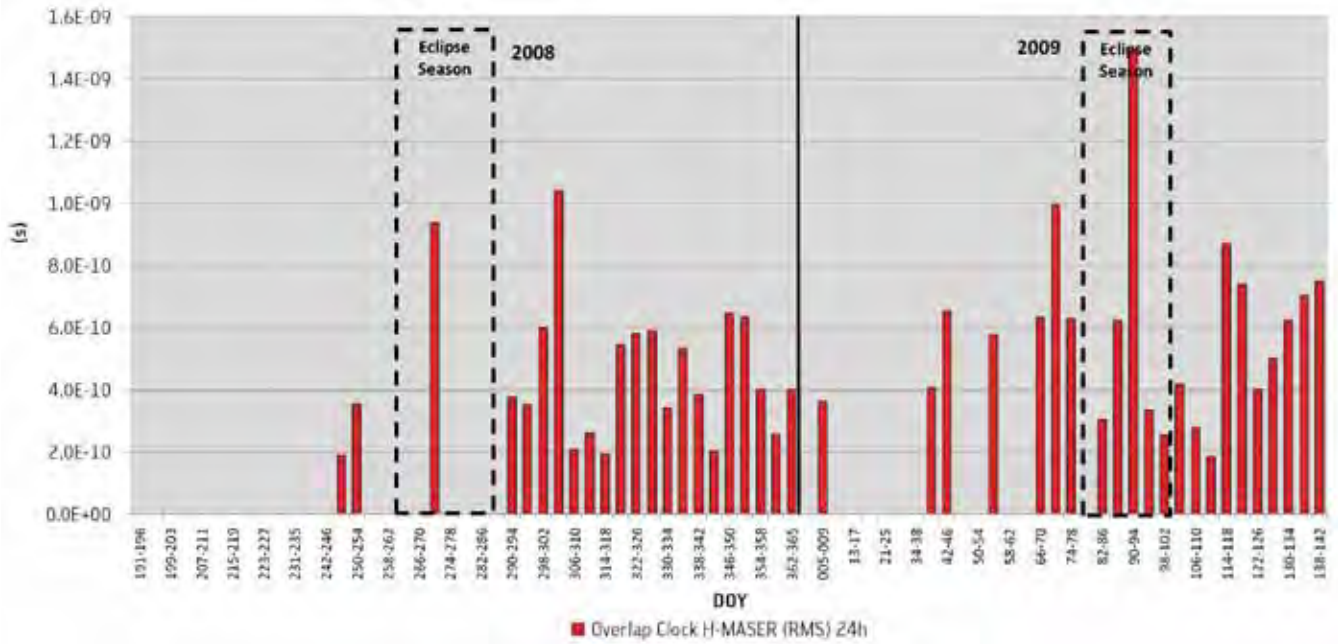


Figure 6.5. GIOVE-B clock overlap consistency.

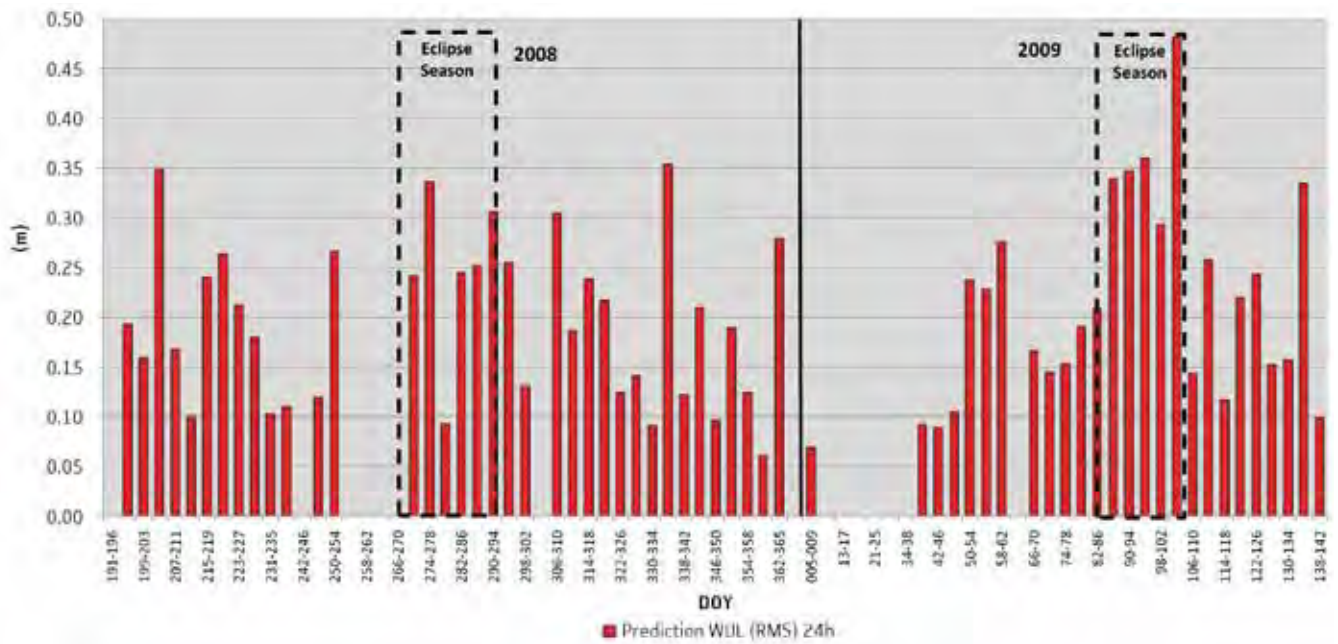


Figure 6.6. GIOVE-B orbit prediction accuracy.

Clock predictions have also been generated over 1 day. However, an additional campaign has been performed with the IOV configuration, which implies performing clock predictions at 100 min in the worst case.

Figure 6.7 shows that for GIOVE-B the mean clock prediction error is 0.18 ns and the 95% percentile is 0.40 ns.

An additional means to evaluate the quality of the GIOVE-B orbit (and hence the clock) estimated by ODTS is to analyse the stability of the satellite Solar Radiation Pressure parameters. On each ODTS arc a total of 15 dynamic parameters are estimated for the satellite orbit: the six components of the initial state vector (position and velocity), plus nine SRP parameters. There are three SPR parameters in three orthogonal directions, with a constant, sine and cosine term in each direction.

Figure 6.7. GIOVE-B clock prediction accuracy at 100 min with an FOC fitting strategy.

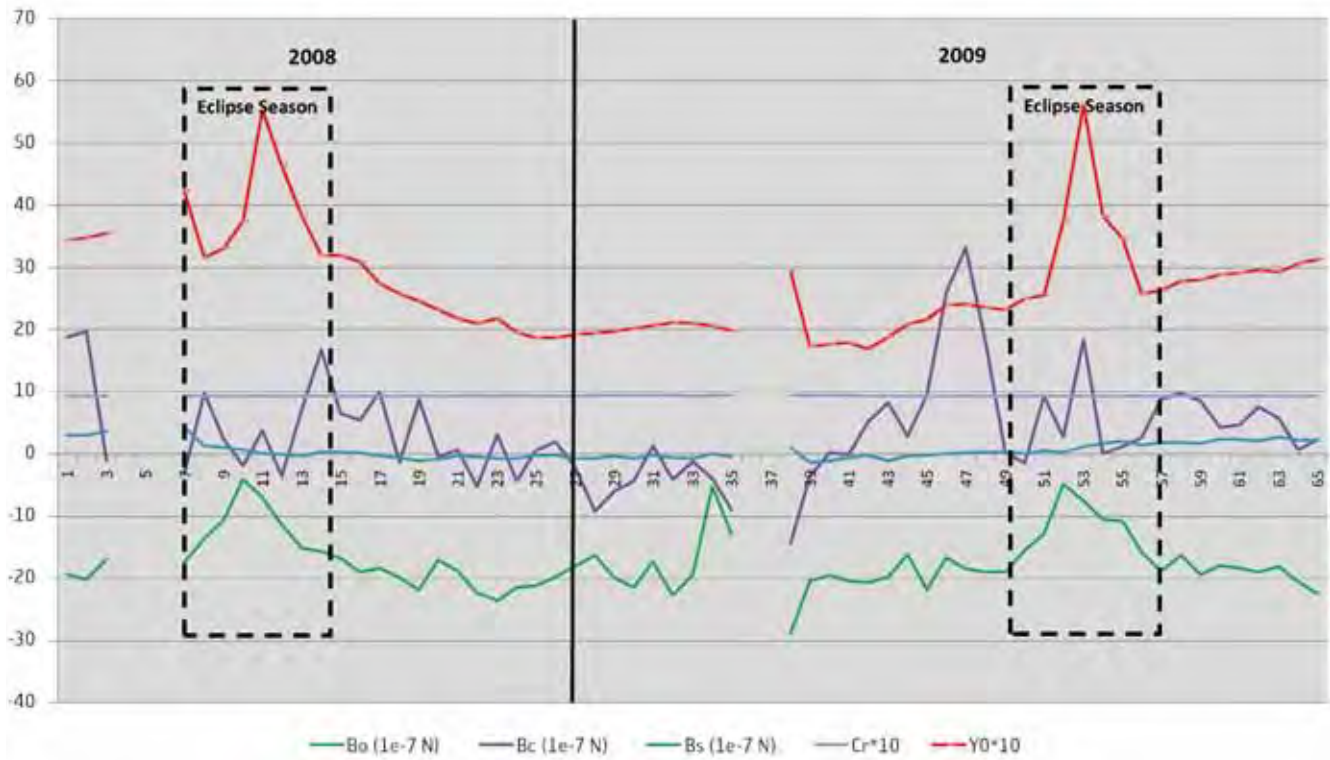
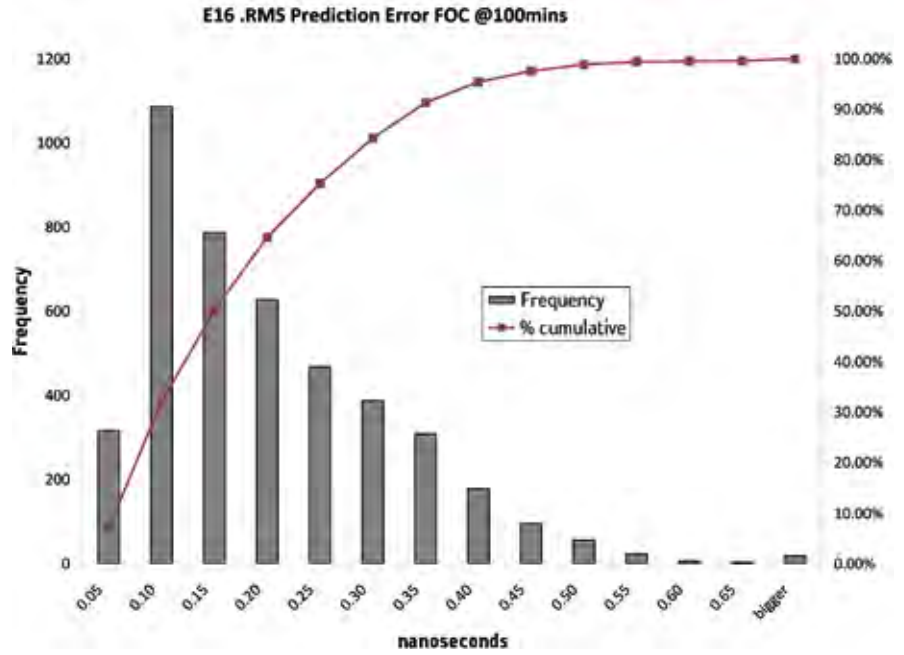


Figure 6.8. Evolution of GIOVE-B SRP parameters.

Figure 6.8 shows the values of the SRP parameters estimated for the different ODT arcs (units are  $10^{-7}$  N). The main SRP term (constant in the Sun–satellite direction) is not shown in the figure because its magnitude is much larger than those of the other coefficients.

As can be seen from Figure 6.8, the stability of the SRP parameters is good over the ODT arcs outside the eclipse period, but it becomes worse for the period in eclipse. This result will be used to refine the fine positioning and station-keeping procedures for the IOV and FOC phases.

Clock, orbit and SRP estimates for 2010 and 2011 are consistent with those shown in this section.

## Evaluation of Overall System Noise

The PHM performance onboard stretch the capabilities of the Ground Mission clock estimation to their limits. As a synthesis of the previous sections, it can be said that the satellite clock observability from the ground is conditioned by the following limitations in the GIOVE Mission ground infrastructure:

- the small number of GESS stations (13);
- the sub-optimal quality of the GESS station data (compared with those from IGS stations); and
- the small number of SLR measurements to improve the satellite orbit (and hence the clock) estimation.

One possible way to evaluate the limit of observability imposed by the GIOVE Mission infrastructure on the satellite clock estimation is to calculate the relative stability of the GIEN and GUSN clocks as seen by the ODTS process. The GIEN and GUSN stations are both connected to a very stable Active Hydrogen Maser clock. These are the most stable clocks that can be operationally used nowadays, and are more stable than the GIOVE-B PHM and RAFS clocks to be characterised. Since both GIEN and GUSN data are processed in ODTS, and GIEN is generally the reference for all estimated clocks, it is then possible to obtain and evaluate the GUSN–GIEN clock difference.

Figure 6.9 shows the Allan deviation (ADEV) plot associated with the GUSN–GIEN clock difference as obtained by ODTS in arc 06. The plot line (shown in pink) is labelled ‘GPC measurement noise level’. This ‘system noise’ ADEV plot must be understood as the best (lowest) Allan deviation that can be obtained with the GIOVE Mission infrastructure for any clock to be characterised (on the ground or in space). This means that even if the clock in question is very stable, its stability cannot be observed below the ‘system noise’ ADEV plot.

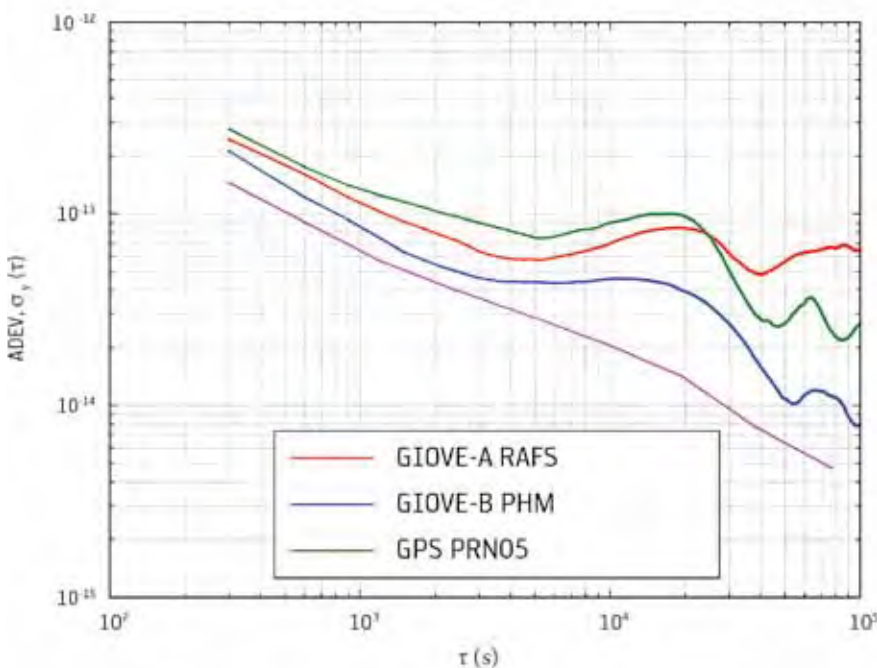


Figure 6.9. GIOVE ‘system noise’ evaluation. Frequency stability Allan deviation.

## 6.1 GIOVE-B Clock Characterisation

### Operation of GIOVE-B Clocks

Shortly after the launch of GIOVE-B, the PHM was switched on and subsequently underwent several on–off sequences, all of which appeared to be perfectly nominal. As of 31 August 2011, the PHM had accumulated more than 1047 days of operation. Table 6.3 summarises the operation of the PHM on GIOVE-B.

### Overview of PHM performance

As soon as the first GIOVE-B signals were transmitted, the GIOVE Ground Segment was able to track and record relevant observables and to run the ODTs process with GIOVE-B data. This is illustrated in Figure 6.10, which depicts the operational and estimated fractional frequency offset of the PHM on GIOVE-B over the full mission up to the end of March 2009. As for GIOVE-A, the data gaps correspond to missing data or interruptions in signal transmission.

Figure 6.10 shows that for most of the time the PHM fractional frequency offset estimated against the free-running AHM located at the GIEN station showed extremely flat behaviour, with a frequency drift below  $5 \times 10^{-15}$  per day almost immediately after switch-on. During the first week of operation (May 2008), one can notice a slightly higher level of noise that corresponds to the GIOVE-B in-orbit test campaign during which the signal configuration was changed intermittently. A similar increase in noise is evident during the second half of January 2009, which corresponds to periods of intermittent signal configuration changes (including in-orbit test repeat campaigns), combined with some limitations of the GESS receivers in the tracking of the E6 signal.

Apart from these slight noise increases, as shown in Figure 6.11, the estimated PHM fractional frequency offset has a periodic oscillation of the orbital period, with an amplitude significantly lower than that observed on GIOVE-A.

The PHM on GIOVE-B is operating well within its nominal temperature range and the temperature at the PHM location is extremely stable. Similarly, the magnetic field variation at PHM location cannot explain such behaviour.

Table 6.3. Operation of the PHM on GIOVE-B.

	PHM
No. of on–off sequences	11
Accumulated operation (days)	1047
Longest uninterrupted period (days)	406

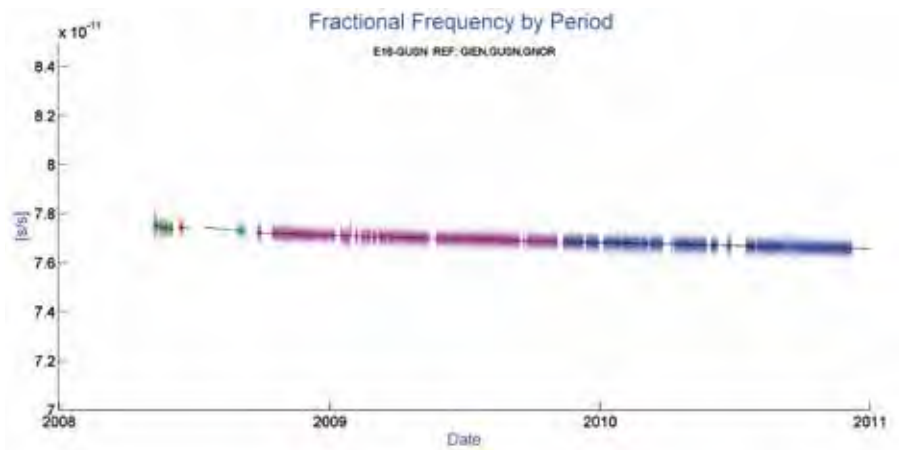


Figure 6.10. Operational and estimated fractional frequency offset of the PHM on GIOVE-B.

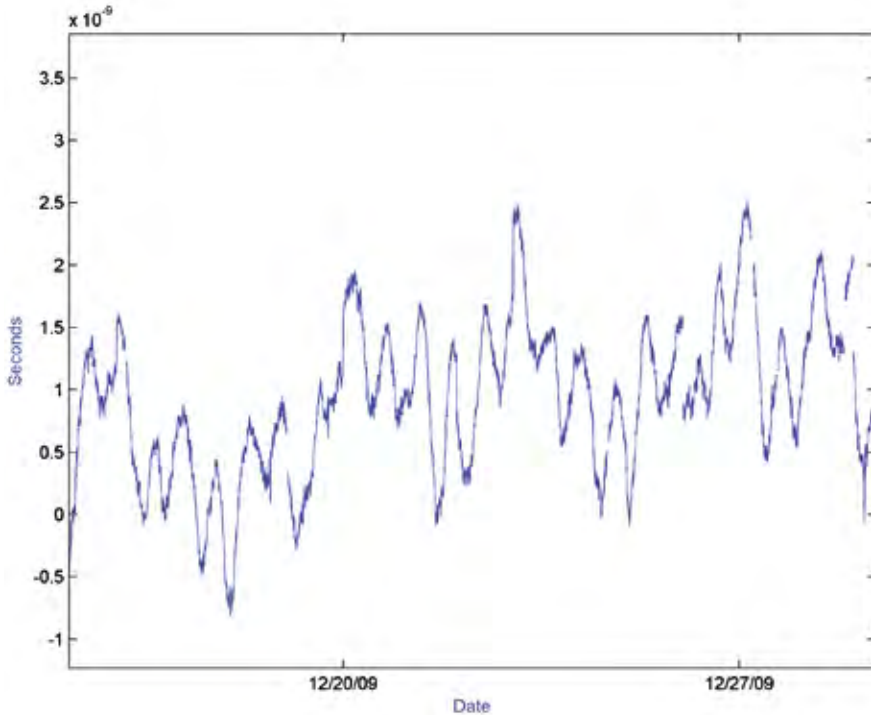


Figure 6.11. Estimated fractional frequency offset of the PHM on GIOVE-B (PHM phase trend removed).

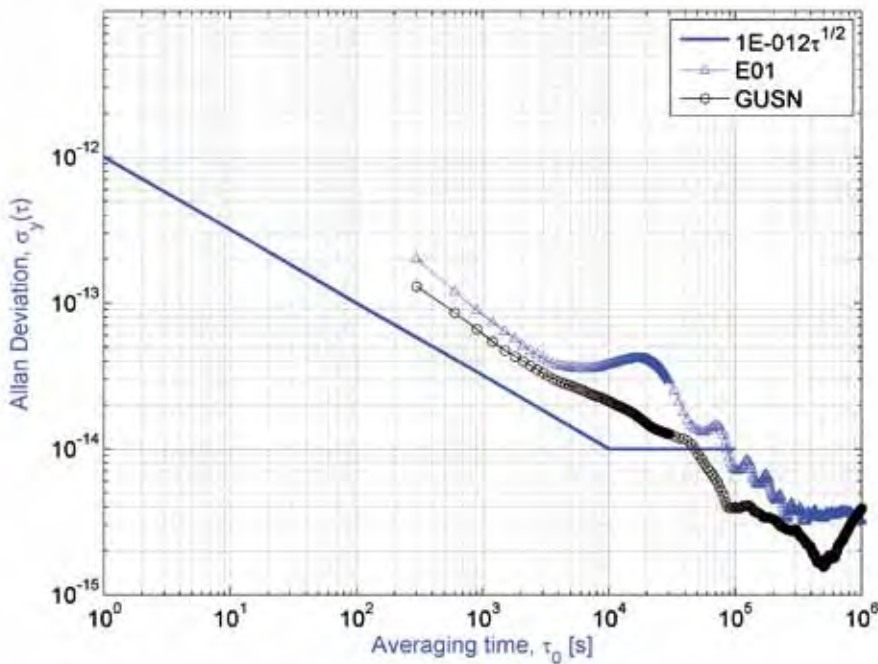


Figure 6.12. Typical Allan deviation of the estimated fractional frequency offset of the PHM on GIOVE-B, 4 November 2010 – 10 April 2010.

It is therefore assumed that the main cause of this oscillation is not the PHM itself. Rather, this is expected to be due to a combination of onboard phase variations due to temperature changes, and the effects of orbital residual oscillations due to limitations in the orbital models.

Finally, Figure 6.12 reports a typical Allan deviation computed on the estimated PHM fractional frequency offset after removal of the linear frequency drift. Also depicted is the level of system noise estimated over the same period. This plot clearly shows that, as anticipated, the estimation of PHM on GIOVE-B is limited over the short term by the system noise. At higher integration times, the oscillation in the Allan deviation illustrates the oscillation at the orbital period. It is remarkable to note that the Allan deviation reaches a few  $10^{-15}$  after few days of integration.

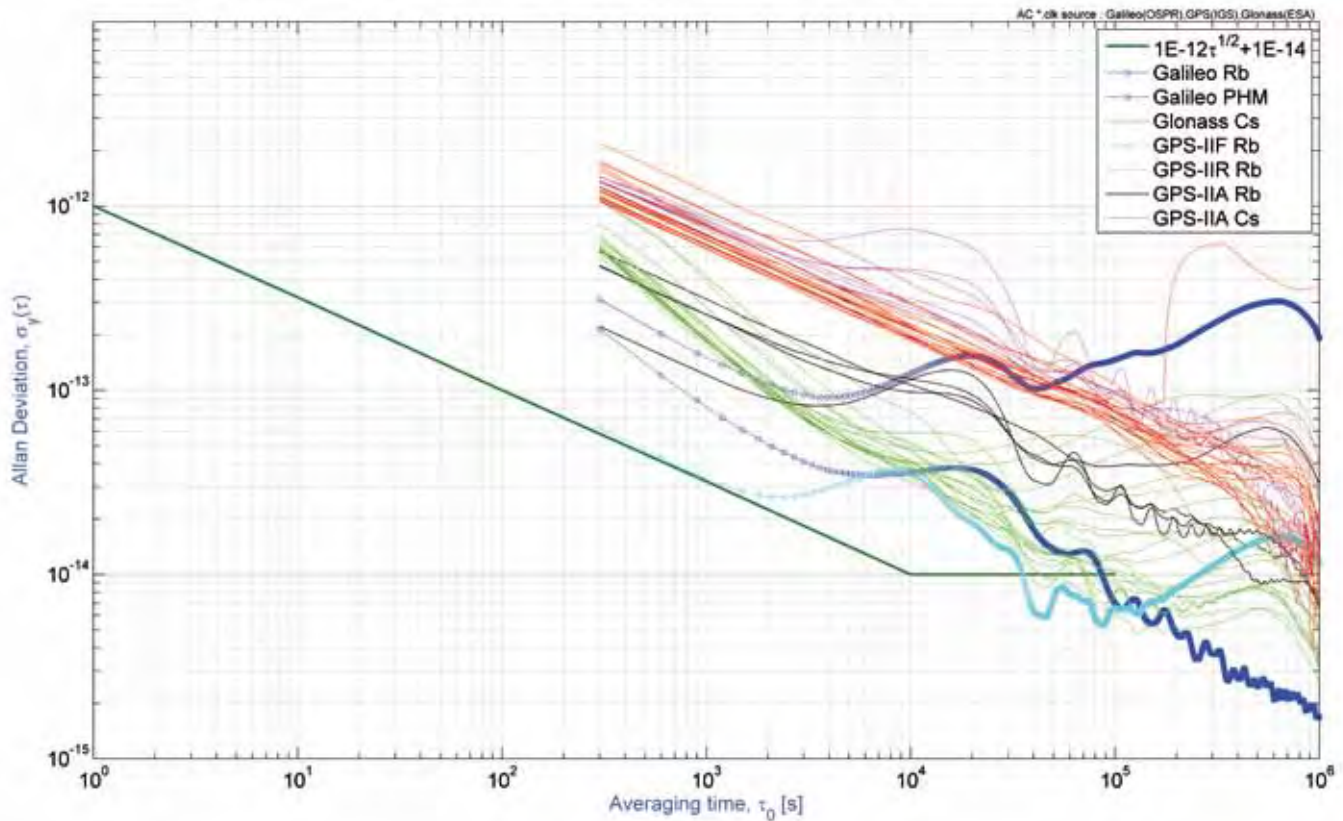


Figure 6.13. Estimated Allan deviation of the GIOVE and GPS clocks. GNSS ADEV 20091210T000000–20100125T000000.

Overall, the GIOVE clocks show excellent short- and medium-term stabilities compared with other in-orbit clocks, as depicted in Figure 6.13, which shows the Allan deviation of GIOVE-A (RAFS), GIOVE-B (PHM) and GPS clock estimates obtained from ODTS processing.

### Direct Verification of the Relativistic Effect through the PHM

Due to its excellent retrace capability, the PHM has allowed direct verification of the relativistic effect at the Galileo orbit altitude by comparing the frequencies measured on the ground and in space, with an error of the order of  $10^{-12}$ .

### GIEN Clock Stability Monitoring Based on PPP

In order to guarantee that the onboard clock characterisation results are not affected by the reference clock at GIEN, its behaviour was monitored continuously using two independent techniques: NRCan Precise Point Positioning (PPP) and ODTS. In both cases, it is possible to estimate independently the behaviour (and stability) of the reference AHM.

Figure 6.14 compares typical phase estimates of the GIEN and GUSN clocks with respect to the IGS time scale, and then GIEN versus GUSN, as obtained by the ODTS and by the NRCan PPP, with an indication of an identified anomaly, especially for the NRCan PPP clock solutions, for both the GIEN and GUSN GESS stations, versus the IGS time scale.

The continuous monitoring of GIEN by means of independent techniques such as PPP is very useful because it allows us to understand problems that may arise at the level of the GIEN H-maser local clock, at the level of the complete

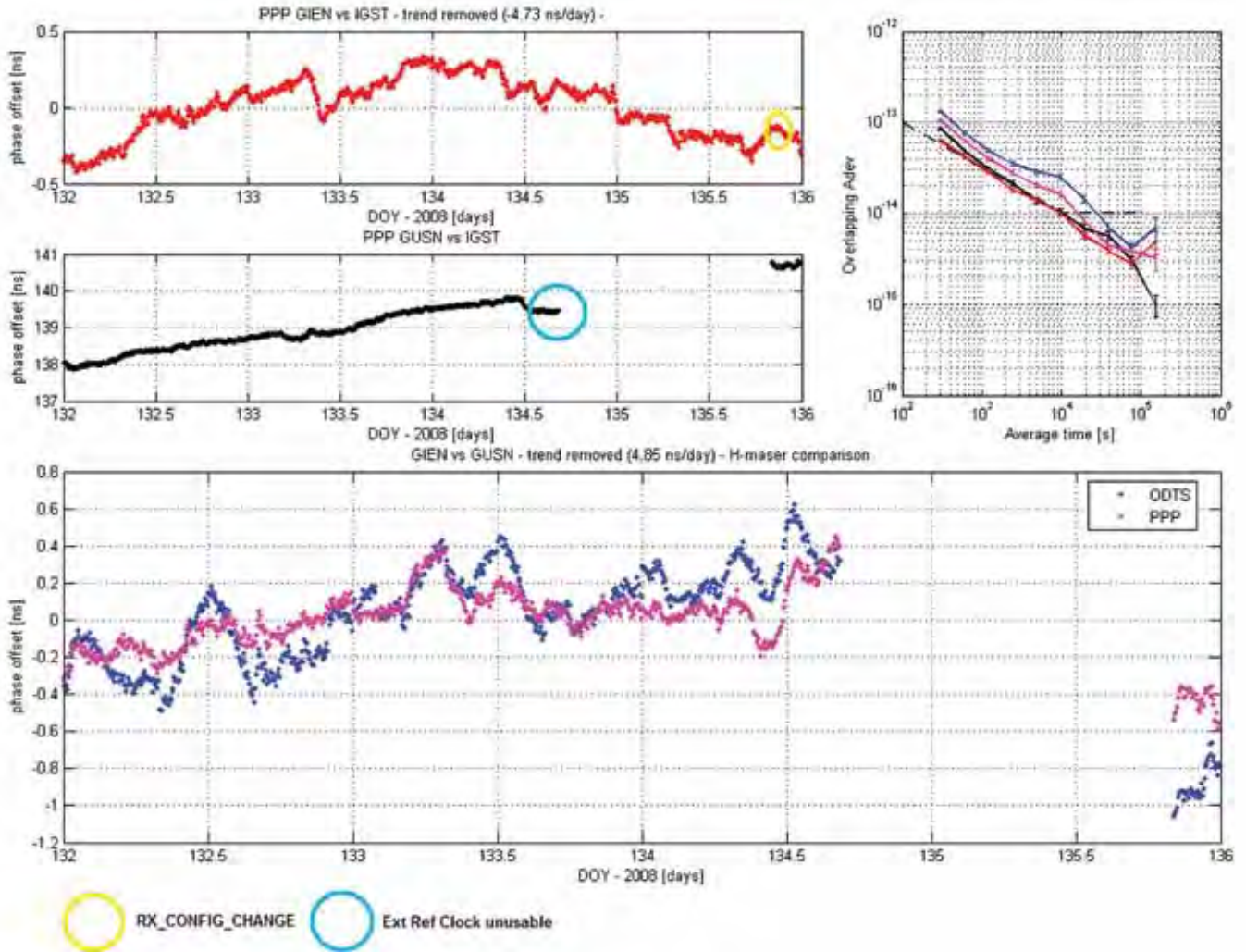


Figure 6.14. GIEN and GUSN monitoring by means of PPP and a comparison of GIEN and GUSN by means of ODTS and PPP (arc 2).

GIEN GESS station (missing data, interference, etc.), or at the level of ODTS as a complex global system for clock comparison. In addition, in the absence of any detected anomaly, it allows for the identification of the state-of-the-art time and frequency transfer capabilities using these two independent techniques.

## 6.2 GIOVE-B MBOC Characterisation

The Multiplexed Binary Offset Carrier (MBOC) is a new modulation derived from the regular BOC modulation, intended to optimise the performance of Galileo E1 Open Service (OS) and GPS L<sub>1C</sub> signals. Theoretically, the features implemented in this modulation allow better tracking accuracy and better multipath rejection.

GIOVE-B has the capability to broadcast this modulation, and a dedicated experiment was therefore executed. Figure 6.15 shows the specificity of the Power Spectral Density (PSD) of this signal, compared with the BOC one.

The MBOC signal combines two different BOC modulations: BOC(1,1) (10/11 of the overall signal power), and BOC(6,1) (1/11 of the overall signal power).

Composite BOC (CBOC) is one possible implementation of this combination, and has been assessed in the frame of GIOVE experimentation because it is the preferred solution for the possible baseline SIS evolution for the Galileo FOC Open Service.

Figure 6.15. Power Spectral Density (PSD) of BOC and MBOC signals.

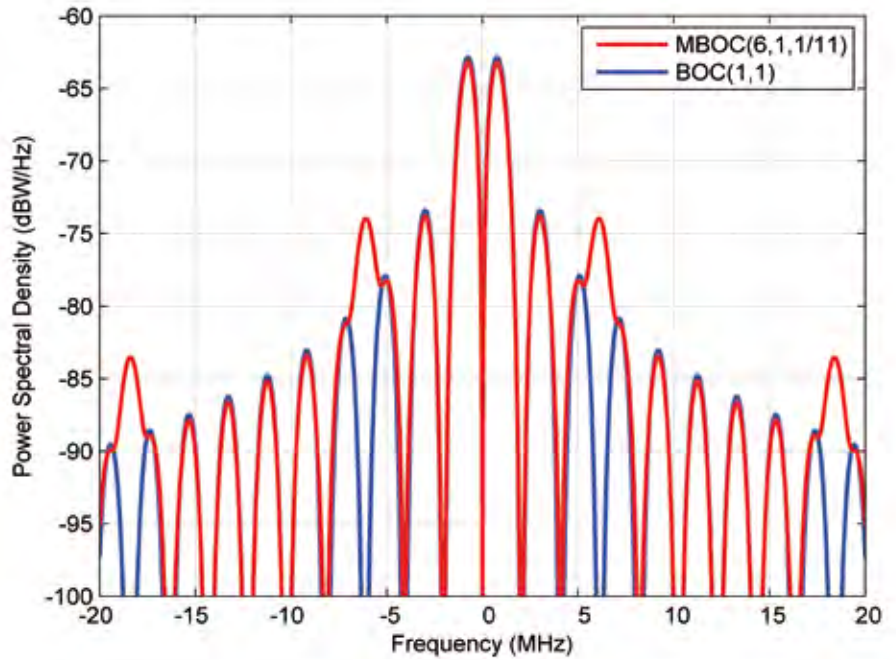
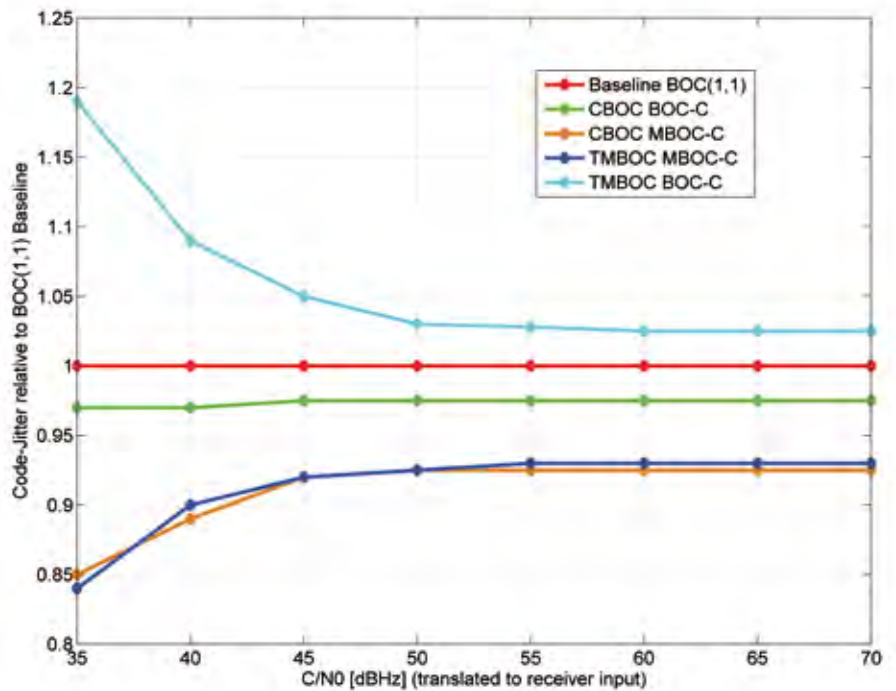


Figure 6.16. Comparison of BOC and MBOC tracking.



The objectives of the MBOC experimentation are to assess the gain brought about by this modulation at the MBOC-compatible stations (compared with the BOC case), and to characterise the performance of a BOC-compatible receiver when tracking an MBOC signal.

Theoretical tracking code noise jitter ratios are proposed in Figure 6.16 as functions of the signal-to-noise ratio. In the figure, the transmitted signal (CBOC or TMBOC) and the receiver compatibility (BOC or MBOC) are indicated as follows:

- red curve – reference performance of the BOC/BOC tracking configuration;
- orange curve – relative performance of the CBOC/CBOC configuration, which brings about a 14% improvement over BOC/BOC;
- green curve – relative performance of the CBOC/BOC configuration, which brings about a 4% improvement on BOC/BOC.



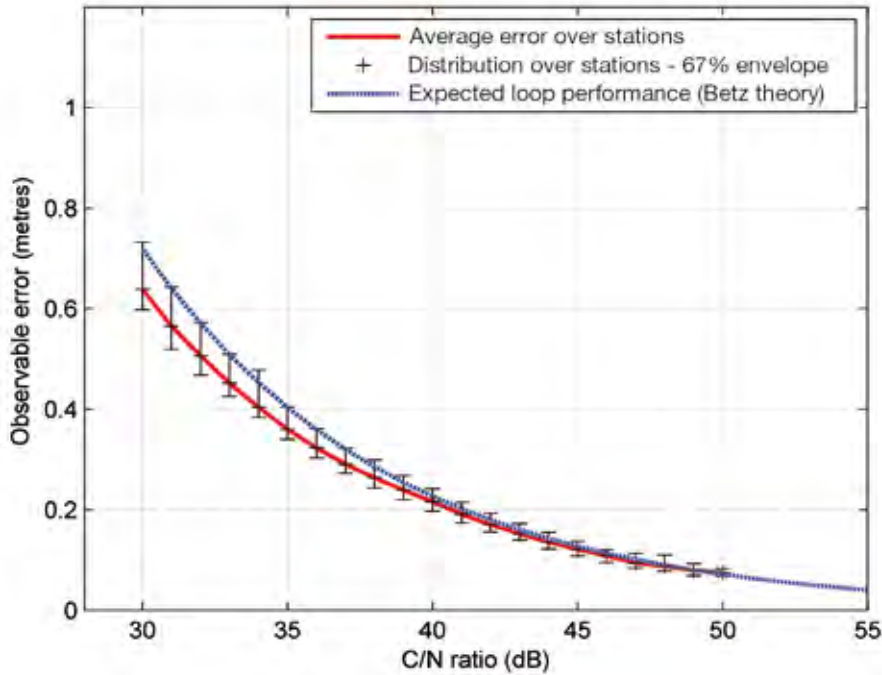


Figure 6.17. Uncorrelated tracking noise – Tx CBOC/Rx CBOC. Standard deviation  $L1_C$

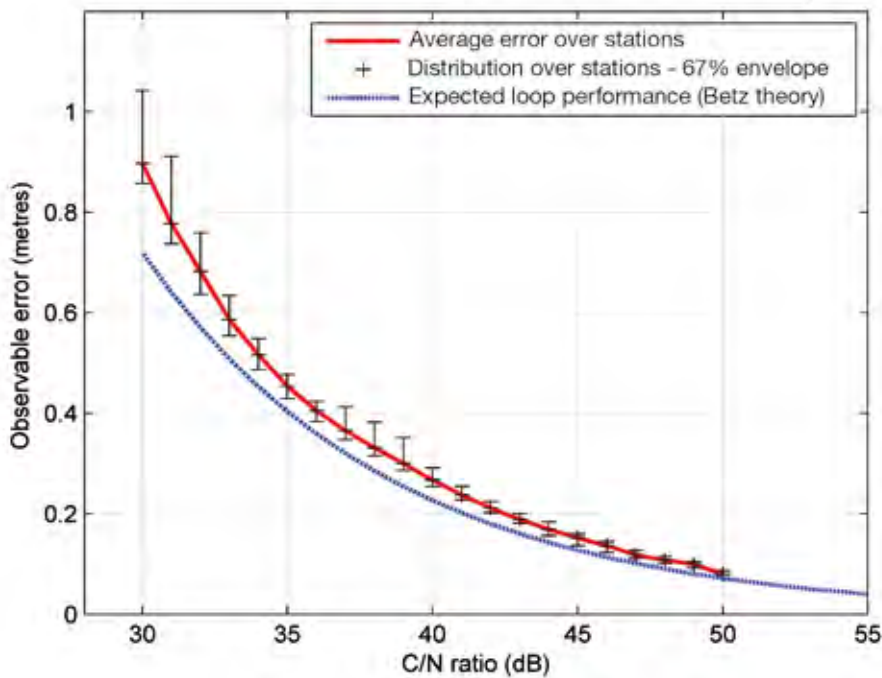


Figure 6.18. Uncorrelated tracking noise – Tx CBOC/Rx BOC. Standard deviation  $L1_B$

In the frame of the GIOVE experimentation, the code phase measurement uncorrelated noise was determined and is shown as a function of the signal C/N ratio in Figures 6.17 and 6.18.

The following trends are therefore extracted:

- the CBOC/CBOC configuration shows a gain in the code jitter of between 10% and 15%;
- with regard to the CBOC/BOC configuration, although an improvement of around 4% was expected, the experimental results did not allow confirmation of this trend. Note, however, that a theoretical improvement of 4% in the code jitter is small enough to be difficult to be identified through experimentation.

Both these effects could be examined by users tracking CBOC signals with CBOC or BOC local replicas.

Figure 6.19. BOC and MBOC multipath error envelopes (relative reflective power = -6 dB,  $\delta = 0.04$  chips, RX-BW = 28 MHz, non-coherent early-late discriminator).

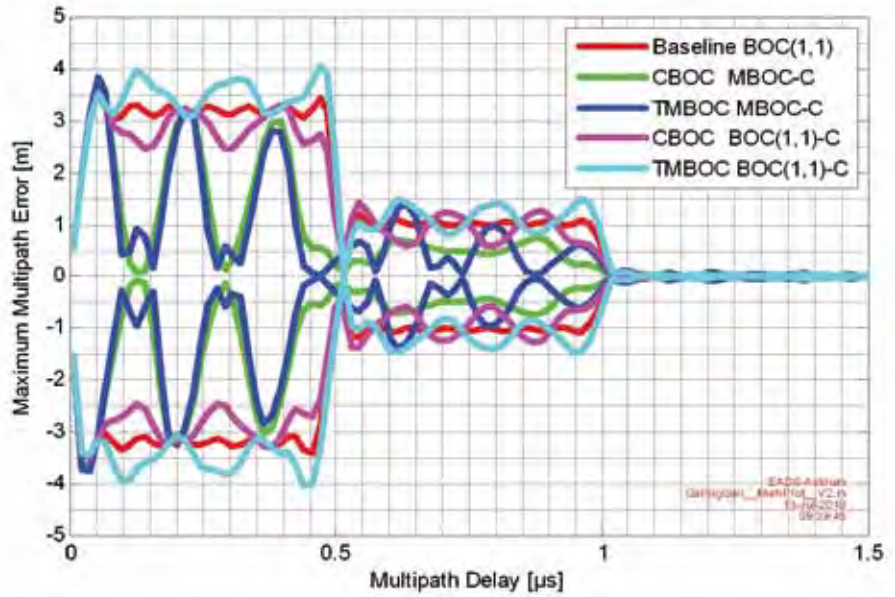
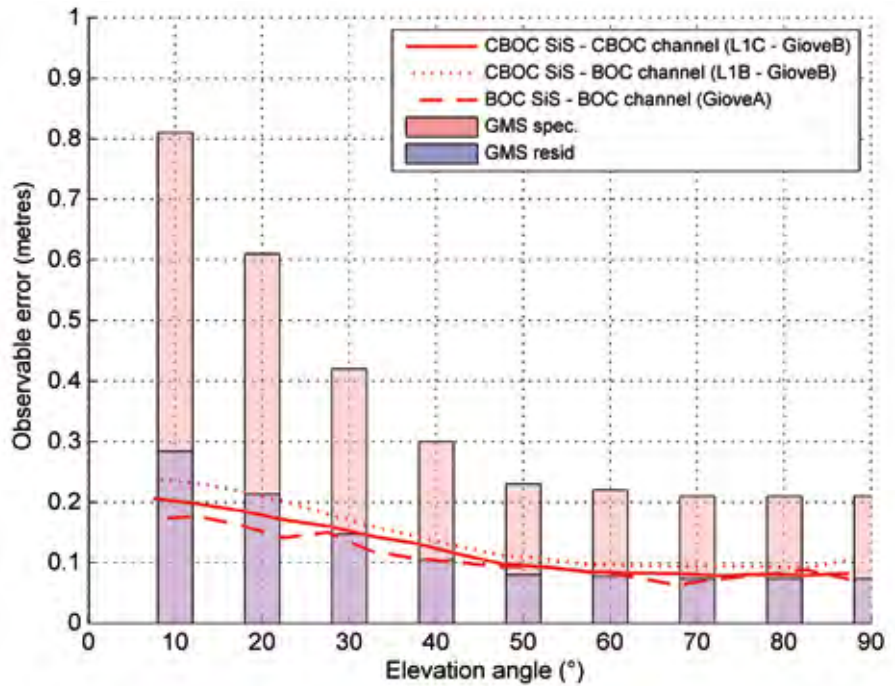


Figure 6.20. Experimental code phase residual errors.



The theoretical multipath or correlated error envelopes of the various modulations are shown in Figure 6.19.

From an experimental point of view, it was decided to characterise the multipath error component using the ‘residual’ code phase error.

In fact, at the IPF the station observables are filtered (Hatch filter with a 600 s time constant) in order to reduce the noise level. The ‘residual’ code phase error is the noise level at the output of this integrity pre-processing filter. It is well known that even if such a filter mitigates the uncorrelated error terms, its efficiency is actually driven by the level of correlated error components (such as multipath). The results are shown in Figure 6.20.

It can be concluded that the filtering process applied on the raw observables mitigates the ‘long-delay’ MP, and is less effective on the ‘short-delay’ MP, for which very little specificity exists among the modulations. The driving parameters are the environmental conditions (in particular the multipath power) rather than the signal structure.

**→ GIOVE: ADDED VALUE OF  
THE EXPERIMENTATION  
AND RISK MITIGATION  
FOR THE IOV PHASE**



## 7. GIOVE: Added Value of the Experimentation and Risk Mitigation for the IOV phase

### 7.1 Navigation Assessment and Orbit Models

The GIOVE experimentation has allowed the confirmation of basic assumptions in the development of the Galileo system related to the navigation message loop, the accuracy of the orbit and clock predictions by the GIOVE Mission Segment and the suitability of orbit models in the ODTS process.

The process of routinely generating navigation messages has proven to be adequate, as routine ODTS accuracy does not present excessive degradation due to the reduction of the ODTS arc length from 5 to 2 days.

After an initial experimentation, the GIOVE-A and GIOVE-B clocks have been kept synchronised with EGST. This has allowed a reduction in acquisition problems from ground receivers. Moreover, the navigation message closed-loop performance has been monitored more closely and more regularly.

Onboard clock performances are sufficient to meet the needs of the Galileo mission as the clock prediction error at 100 min is comparable with the target of the contribution to the User Equivalent Ranging Error (UERE) from orbits and clocks for Galileo IOV.

Dynamic models implemented using the ODTS software have proven to be reliable as the orbit accuracy has met expectations, although the higher carrier phase residuals compared with GPS are still under investigation. Attention has focused on two relevant models, the GIOVE attitude laws, and the SRP model:

- It has been determined that the implemented GIOVE attitude laws are sufficient to achieve the required accuracy. In addition, it has been confirmed that the reconstructed law is nearly identical to the one implemented.
- During the experimentation, a five-coefficient SRP model has been used, which has shown reasonable performance, especially outside the eclipse period. The proposed SRP model is therefore believed to be well suited to GIOVE.
- In parallel, other SRP models have been tested and the most promising one is an empirical second harmonic model where 15 parameters are estimated. Nonetheless, the general observed improvements are not always consistent between arcs and it is therefore recommended that the model is used in future experimentation phases, so that more definitive conclusions can be derived.
- Due to the performance and characteristics of the ground station network, it is believed that the observability of the SRP parameters is limited during eclipse periods, which in turn impacts the predictability of the satellite orbit. In addition, it has been found that SRP modelling (especially in eclipse periods) is highly dependent on the availability of SLR data.
- A new method has been implemented that smooths solar radiation forces across eclipse entry/exit in order to improve the orbit integration process.

Satellite Laser Ranging has been included in the processing as a means to improve the orbit and clock determination process (weighted measurements). Moreover, SLR residuals have been used to verify the reference points of the GIOVE satellite. During the experimentation, it has been confirmed that the use of SLR data improved the clock characterisation process by decoupling the orbit from the clock, and that the observed degradation in frequency stability at around half the orbital period almost disappeared when sufficient SLR measurements were available.

## 7.2 GIOVE Clock Characterisation

After more than five years and three years, respectively, GIOVE-A and GIOVE-B, together with their associated ground segments, have undergone extensive characterisation of their onboard clocks. Both the RAFS clocks on GIOVE-A and the PHM on GIOVE-B have demonstrated their survival of launch and fully nominal prolonged operation in medium-Earth orbit.

In terms of performance, the RAFS clock (GIOVE-A) has demonstrated short-term frequency stability that is fully in line with expectations. The medium-term stability is affected by a periodic oscillation that is directly related to temperature sensitivity. The long-term behaviour is affected by non-monotonic variations expected to be mainly due to the high-temperature operation. The short-term stability of the PHM (GIOVE-B) is limited by the noise of the clock estimation process (system noise). In the medium term, the stability of the PHM is affected by periodic oscillations that are not due to the PHM itself.

Overall, the PHM has shown the best performance ever of an onboard clock used for navigation purposes. Some degradation in the performance of the RAFS clocks on GIOVE-A was observed, investigated and addressed for future improvement. For example:

- the clock frequency may present sudden changes of the order of  $5\text{--}10 \times 10^{-13}$  in relative value;
- the frequency variation over time may not always be constant and linear (linear frequency drift); and
- some periodic fluctuations in clock behaviour appear due to the temperature environment, which is outside the specified values, although no impact of the radiation environment on the clock has been observed.

The RAFS clocks on GIOVE-B have not been completely characterised because priority has been given to the PHM.

The clock estimation system of the GIOVE Mission, based on 13 stations, has proven to be effective for the Galileo RAFS characterisation. This means that:

- the reference clock used on ground, which was continuously monitored, was stable enough to provide a good reference; and
- the network of stations, the quality of measurements and the operations were effective for the RAFS characterisation purposes.

However, the operation and monitoring of this network showed some limitations:

- The GESS stations may be affected by local interference signals that need to be suitably evaluated. Interference problems were experienced at the INRiM sensor station (the reference for the ODTS) that impacted the GESS received signals. It is recommended that the site hosting the receiver that feeds the PTF be monitored continuously for radio-frequency interference (RFI) cleanliness.
- The maintenance of the system and the complexity of realtime network management can generate some issues during operations.
- The limited number of GESS stations, the overall noise of the receivers and antennas, and limitations in the ODTS models make it difficult to appreciate fully the performance of the PHM on GIOVE-B, even if the ODTS process is almost the state-of-the-art in clock comparison with this type of receiver.

Recommendations from the experimentation campaign include the following:

- Telemetry measurements are necessary to evaluate the ‘global’ clock behaviour.
- Interactions with the radiation experts are recommended in order to evaluate any clock sensitivity to radiation, particularly in view of the expected increase in solar activity related to upcoming solar cycle.
- Pre-flight tests on space clocks on the ground are important in order to understand the behaviour that may be expected on board. A large number of repeated ground tests under different environmental conditions would be advisable.

### 7.3 IONO and BGD Experimentation

The experimentation in the IONO area provided confirmation of the plausibility of the Galileo assumption of the stability of the satellite inter-frequency bias. Moreover, it also allowed the refinement of the criteria for Galileo single-frequency user performance characterisation. In particular:

- The temporal stability of the GIOVE code IFB was remarkably good during the whole period analysed.
- The absolute GIOVE IFBs (BGDs), to be included in the navigation message, must also be computed. If a calibration of one GESS is available, this can be selected as the reference station and then all the estimated IFBs can be corrected.
- The stability of the GESS IFBs does not guarantee their accuracy. It is therefore recommended that in future the IFB estimation algorithms be investigated further in order to improve their accuracy.
- The vTEC values derived directly from the IONO algorithm and the vTEC IONEX values interpolated at the GESS locations have been compared, with errors typically below 10 TECUs. Nonetheless, equatorial stations show the greatest differences, which translate into larger errors when the NeQuick algorithm is used at these latitudes.
- The NeQuick algorithm has shown adequate internal coherence, and compliance targets have largely been met for all regions. NeQuick was tested using two methods, with similar results. A more recent version of NeQuick was also tested and found to provide similar end-user performance compared with the Galileo baseline version.
- The years 2008–2010 were very quiet in terms of solar activity. The IONO algorithm behaviour was assessed at the beginning of 2011, especially as regards the scintillation phenomenon, and will be verified also for the future in light of the increase of the solar cycle.
- The reduced network of 13 GESS stations used during the GIOVE Mission and their distribution had an impact on estimates of Az, and hence on the performance of the single-frequency IONO algorithm.
- The IDF algorithm should be improved by setting more adequate conditions for raising the IDF flag. For instance, one could combine all error observations for each region, and not only take into account the disturbance conditions for each station individually.

## 7.4 Sensor Station Characterisation

Several conclusions and recommendations can be derived from the experimentation in the area of sensor station characterisation. The E1 signal performance can be extrapolated to the IOV GSS case, allowing future station performance to be anticipated. This could be done by compensating as much as possible for the GESS antenna behaviour.

With regard to the RFI surveys at IOV sites, the validity of the overall approach has been demonstrated, but based on on-site trials of the procedure the following recommendations can be made:

- The noise floor of the measurement chain should be between  $-191$  dBW/Hz and  $-186$  dBW/Hz.
- If the noise floor is higher, the noise introduced by the equipment alone will be sufficient to exceed the site acceptance threshold, leading to the improper rejection of the site.
- The interference environment at a given site is likely to change. Consequently, since the site selection process is based on a snapshot of the RF environment (at the time of the survey), this constitutes a risk for the Galileo Mission Segment performance, because the performance of a station can be suddenly degraded.

As far as IOV GSS design is concerned, the antenna has received specific attention. In particular, the work performed at the GIOVE Mission level in order to compensate for and fix the antenna behaviour has been taken into account.

Finally, with regard to IOV GSS performance analysis tools, the various tools/algorithms used provided detailed insight into sensor station performance.

## 7.5 GGTO Experimentation

The Galileo and GPS reference timescales – Galileo System Time (GST) and GPS Time, respectively – will be generated independently. GST will be steered to UTC modulo 1 s, based on collaboration with European laboratories, and GPS Time to a real-time representation of UTC produced by the US Naval Observatory (USNO).

The difference between the GPS Time and GST – the GPS to Galileo Time Offset, GGTO – (as well as the inter-system bias) will cause an additional error in the user's navigation solution since the clock parameters broadcast in the navigation message will correct the measured Galileo and GPS pseudo-ranges to different references (GST and GPS Time). To mitigate this effect, Galileo and GPS will determine, coordinate and broadcast the GGTO in the navigation message (see Figure 7.1).

The GIOVE activity has allowed a representative evaluation of the GGTO determination. According to the GGTO Preliminary Interface Definition Document, the GGTO is to be determined using two methods: a connected clock approach between Galileo PTF and UTC (IOV), and a combined GPS/Galileo receiver (the primary method in FOC). The connected clock approach was tested by determining the GGTO via GIOVE ODTS clock products for the GIEN and USN3 (GGTO1) stations, and via the two-way satellite time and frequency transfer between INRiM and USNO (GGTO3). The combined receiver approach has been evaluated by comparing the GPS navigation message and the GIOVE ODTS (GGTO2).

The experimentation results show that the combined receiver approach (GGTO2) seems a promising technique, offering very good performance, and is also suitable for near-real-time implementation in an operational system.



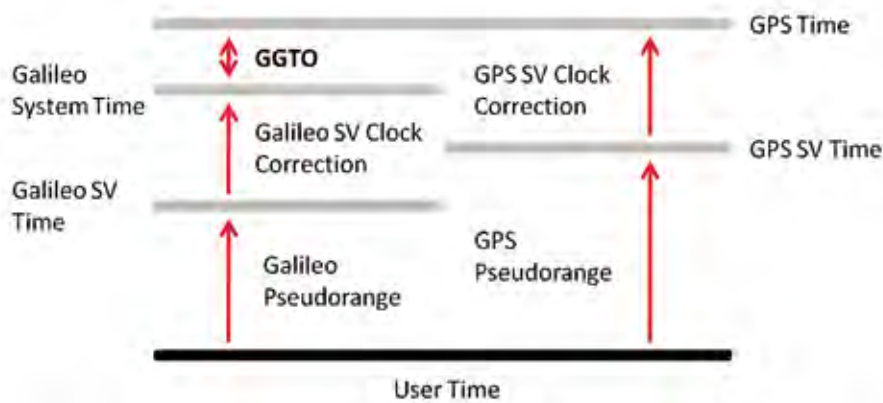


Figure 7.1. Measurement bias due to the GGTO.

Unlike the GIOVE implementation, the Galileo sensor stations will not include GPS receivers, and dedicated combined GPS/Galileo receivers will therefore be installed at Galileo PTF and USNO, as foreseen in the GGTO Preliminary Interface Definition Document.

Based on the GIOVE experiences, the recommendations for Galileo are as follows:

- The combined receiver approach should be maintained as the FOC baseline, considering as an option the deployment of more than one combined receiver in Galileo in order to increase the redundancy and reliability.
- The baseline on the GGTO model (linear model) and validity period (24 h) should be maintained.
- Calibration aspects should be carefully studied and inter-system biases accounted for by determining the GGTO via the combined receiver and also at the user level.



**→ GIOVE: A VERIFICATION  
STEP IN THE  
DEVELOPMENT OF  
GALILEO**



## 8. GIOVE: A Verification Step in the Development of Galileo

### 8.1 Key Performance Parameters

The Galileo system requirements have been detailed in a set of specifications, starting from the Galileo System Requirement Document and going down to the elements within the segments. It is the specific task of the System Engineering and Performance team to drive and monitor the flow-down process, ensuring the overall consistency of the set of requirements.

In the frame of this task, several requirements have been identified that are considered of paramount importance in ensuring the effective performance of the Galileo system. Some of these key performance parameters can already be investigated in the GIOVE Mission from two perspectives:

- summary from historical data in order to compare the Galileo requirements and provide the verification status with the GIOVE Mission; and
- continuous monitoring to evaluate the functional and performance behaviour of the GIOVE Mission.

### Summary of Performance Parameters

From the historical data of the GIOVE Mission a summary of the verification status of few Galileo requirements can be determined, bearing in mind that strict comparisons are not possible as the GIOVE Mission is a greatly downscaled version of the Galileo system.

One of the most important performance parameters is the ranging accuracy, which is monitored continuously by the GIOVE Mission Segment (see Table 8.1).

### Navigation Message Generation

The signals transmitted from GIOVE-A/GIOVE-B and GPS satellites are received by the network of GESS stations and processed to provide 1 Hz code/carrier phase pseudo-range observations to the GIOVE Processing Centre.

These observations are then used by the E-OSPF to reconstitute the orbits and clocks of the satellites over the previous 48 h and then to project these parameters into the future. The orbit predictions are segmented and simplified into 3 h ephemeris parts and then combined with the almanacs and clock and ionospheric corrections to form the navigation message. Once this navigation message has been uploaded, each ephemeris part will be transmitted for only a relatively short time (up to 3 h).

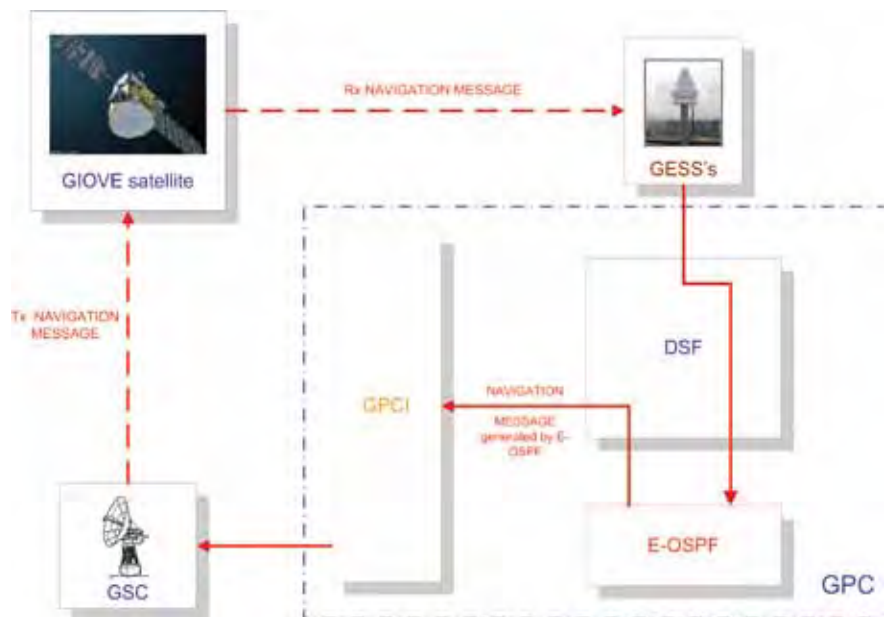
The navigation message is currently generated at hourly intervals at the GPC (Figure 8.1). The operational Galileo system will provide a high upload frequency with a new message upload per satellite at least every 100 min. However, the current GIOVE Mission Segment has been designed to guarantee at least one upload per day, similar to the nominal GPS operations scenario.

The strategies for GIOVE-A and GIOVE-B differ slightly due to their different operational setups and onboard Navigation Signal Generation Units (NSGUs). For GIOVE-A, the only navigation messages sent from the GPC are those whose times of ephemeris line up with an activation time of one of the onboard memory slots where the ephemeris parts are stored. These are then uploaded by GSC-A as soon satellite contact is achieved, and then throughout the period of visibility as soon as new messages are received.

Table 8.1. Summary of performance parameters.

Requirement	Galileo	GIOVE	Comment
Ranging accuracy (95%)	1.3 m	PHM 0.66 m (0.33 m, 1 $\sigma$ ) RAFS 0.84 m (0.42 m, 1 $\sigma$ )	GIOVE: orbit and clock predictions (PHM 22 cm/24 cm, 1 $\sigma$ ) (RAFS 26 cm/35 cm, 1 $\sigma$ )
GSS code phase error	0.81–0.21 m	0.87–0.40 m	Partially compliant at elevations >40°
GSS carrier phase error	10 mm	2 mm	
Single-frequency IONO algorithm	30% or 20 TECUs	<14 TECUs	Deviation at zenith direction
GPS to Galileo Time Offset (GGTO)	5.0 ns (2 $\sigma$ ) (86 400 s)	4.5 ns	Galileo: TWSTFT GIOVE: broadcast navigation message
SV differential group delay stability of ranging signals	0.3 ns/24 h (payload specifications only)	0.4 ns/24 h (overall process performance)	E1 user
RAFS frequency drift	1e-12/day	3e-13/day	
RAFS frequency stability	1 s: 5.1e-12 10 s: 1.64e-12 100 s: 5.1e-13 1000 s: 1.64e-13 10 000 s: 5.1e-14	300 s: 2.5e-13 1200 s: 1e-13 10 200 s: 8e-14 86 400 s: 4.7e-14	Compliant if drift removed
PHM frequency drift	8.2e-15/day	1e-14/day	Partially compliant due to limitations in the measurement system
PHM frequency stability	1 s: 1.1e-12 10 s: 3.5e-13 100 s: 1.1e-13 1000 s: 3.5e-14 10 000 s: 1.1e-14	300 s: 2e-13 1200 s: 7e-14 10 200 s: 4.0e-14	Partially compliant due mostly to measurement system noise

Figure 8.1. Navigation message closed-loop analysis



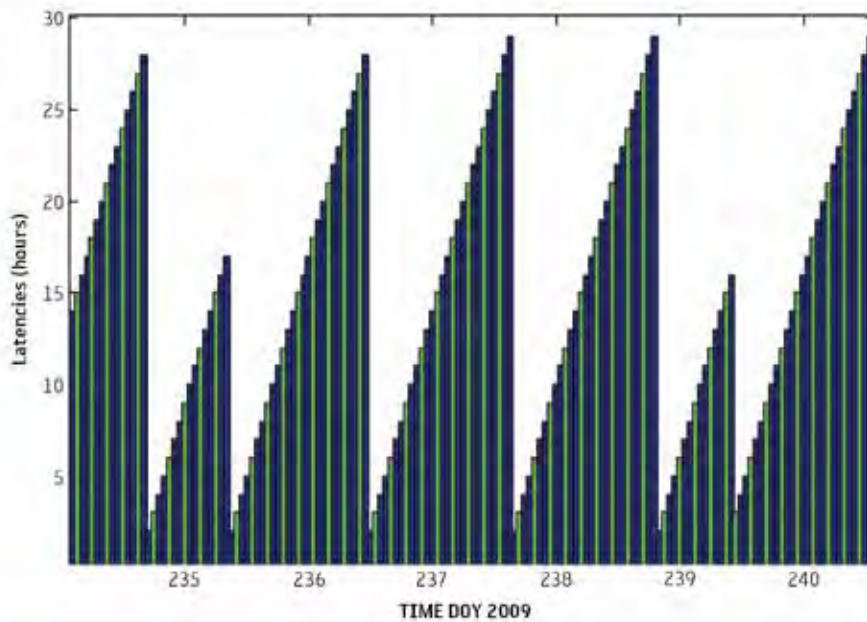


Figure 8.2. GIOVE-B navigation message latency, 22-28 August 2009

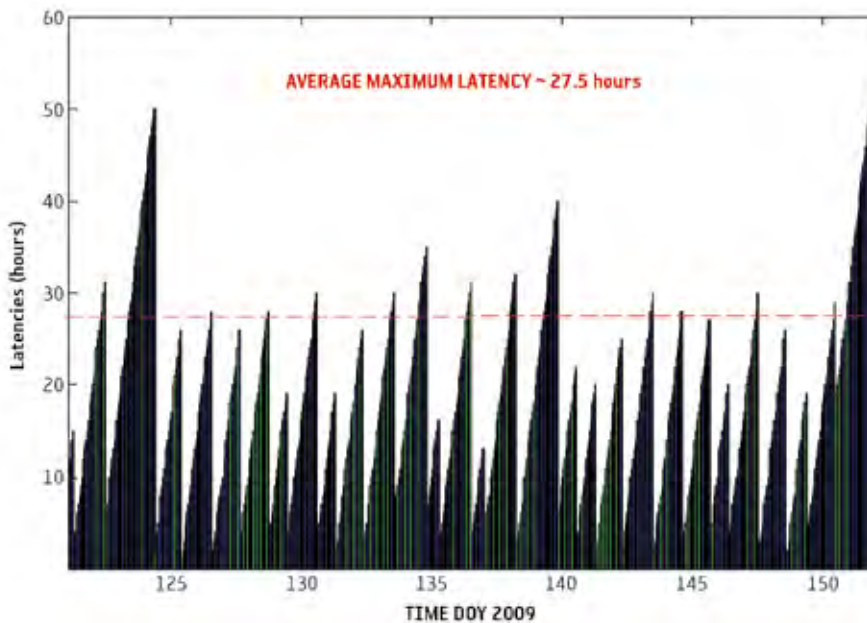


Figure 8.3. GIOVE-B navigation message latency, May 2009.

For GIOVE-B, the uploading is largely manual, nominally performed once per day, and taking the most recently generated message sent by the GPC.

The operations team at GPC continuously monitors the age of data transmitted to users, and checks the daily uploads.

The navigation message latency plots show a sequence of hourly bars characterised by different colours and heights (Figure 8.2). The green lines indicate the receipt of a new message data set, whereas blue refers to older data sets already transmitted in the previous few hours.

In particular, GIOVE-B transmits a sequence of 15 data sets that are part of the same uploaded navigation message. Each data set (or ephemeris) is transmitted for 3 h and is valid for 4 h starting from the time of its clock.

Typically, during nominal operations, the latency ranges from a few hours up to 30 h. During May 2009, the maximum latency was estimated to be similar, around 27.5 h (Figure 8.3). For reference, the GPS average maximum age of data (AOD) at upload for the entire constellation is 29.4 h.

## Navigation Message Data Accuracy

The accuracy of the Signal-in-Space User Ranging Error (SISRE) is a key performance indicator for the overall GIOVE Mission, including for measuring the performance of the ODTS algorithm, assessing the timeliness of ground operations and validating the uplink strategy. The SISRE can be defined as the difference between the satellite position based on the broadcast navigation data (position and clock) and the truth, projected along the line-of-sight to the user.

To obtain the orbit error components – radial, along- and cross-track errors – the difference vector between predicted and estimated positions has to be projected along the satellite reference frame.

The orbit and clock error components can be combined using a simple formula to estimate the SISRE at the Worst User Location (see Figure 8.4):

$$SISRE_{WUL} = \sqrt{(R - CLK)^2 + 0.215^2(A^2 + C^2)}$$

where  $R$  is the radial orbit error,  $A$  is the along-track orbit error,  $C$  is the cross-track orbit error, and  $CLK$  is the clock error.

A different geometric coefficient, 0.215, has been adapted for GIOVE (for GPS it is 0.204), due to the higher altitude of the satellites and the consequently smaller aperture of the view cone between the satellite and Earth. Figure 8.5 shows a sample plot of typical broadcast message errors for GIOVE-B over 2 days of nominal operations, when at least one upload per day was guaranteed. The instantaneous SISRE shows very good performance, never exceeding 1 m of error.

The discontinuities in the error are caused by the successive 3 h ephemerides transmissions (data set cutovers) and by the entire new message upload (upload cutovers).

It can be clearly seen that the broadcast accuracy is strictly related to the message latency. Using the available data, it is interesting to correlate the information contained in the previous plots, namely, the navigation message latencies and the broadcast accuracy, and to estimate the relationship between them.

It could be shown that that the radial error is substantially less affected by the message latency than are the along- and cross-track components. On the other hand, the correlation between the clock error and message latency is very pronounced, much higher than in the case of the orbital errors. This confirms that the clock prediction is more sensitive to the navigation message upload frequency.

The SISRE trend as a function of the message latency (Figure 8.6) shows good average performance within the first 24 h of latency, with an average error of around 1 m.



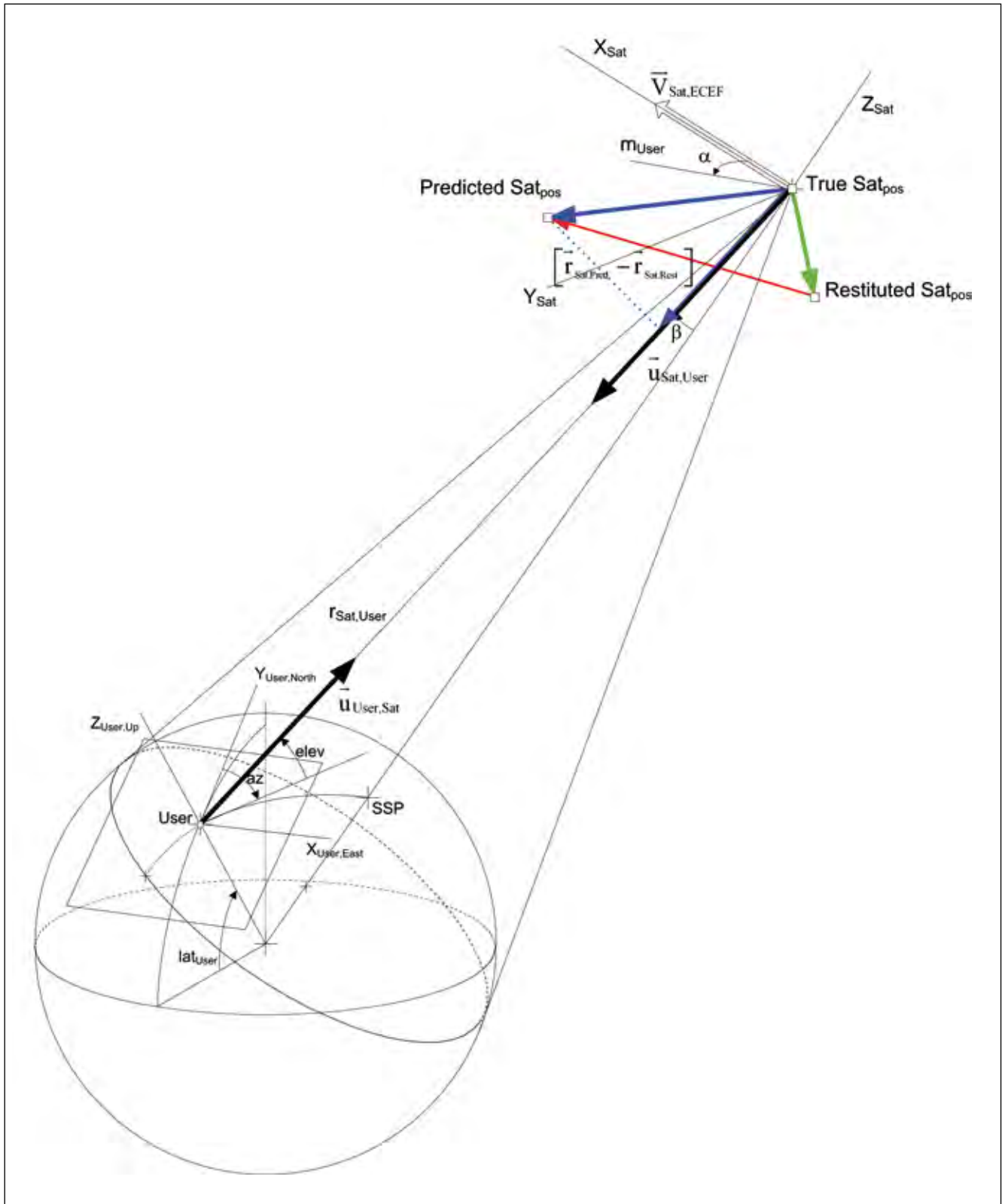


Figure 8.4. Satellite to user geometric conditions and prediction error projection.

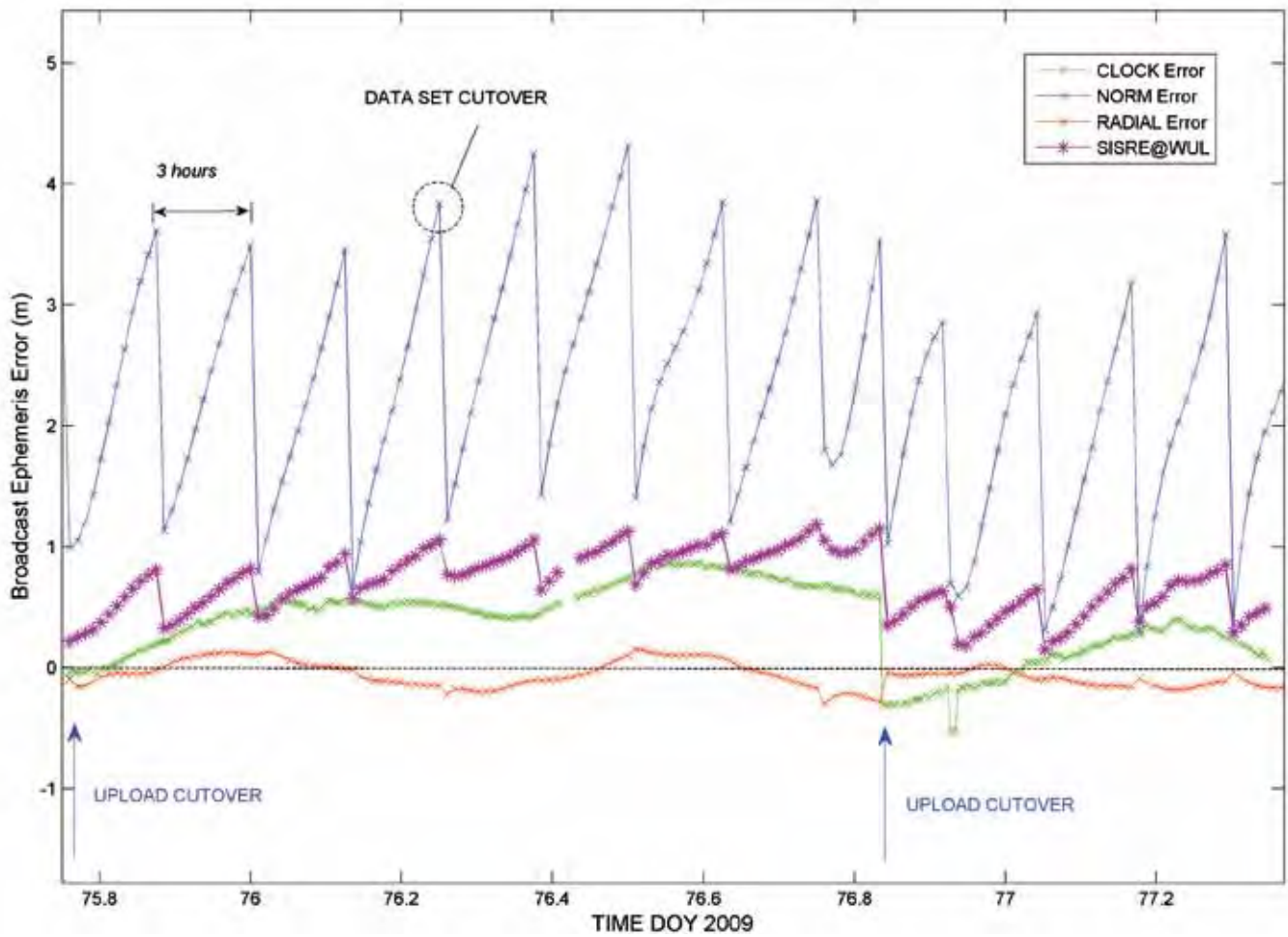


Figure 8.5. GIOVE-B broadcast navigation message accuracy – instantaneous SISRE, DOY 75–77 2009.

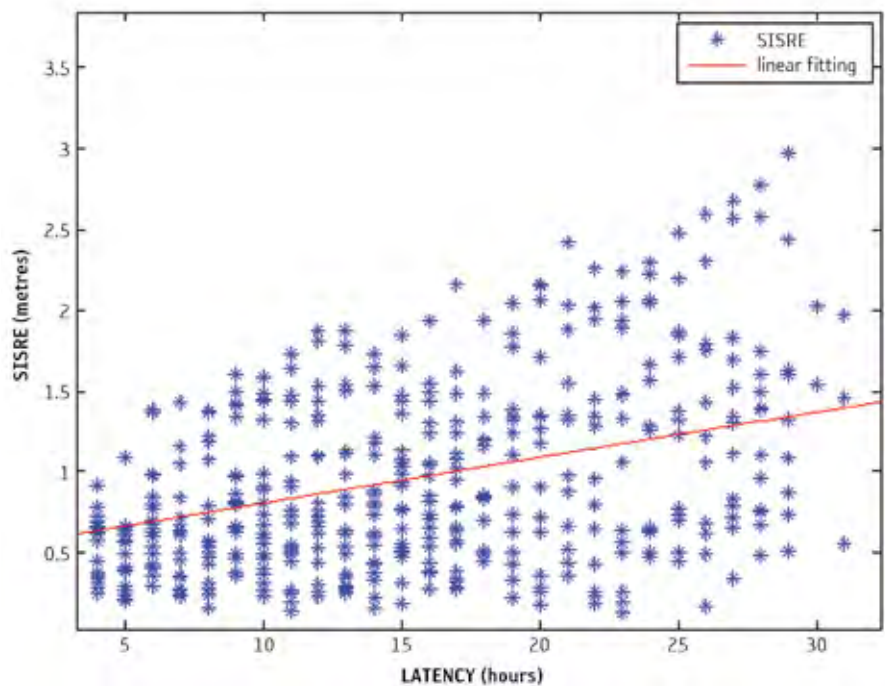


Figure 8.6. GIOVE-B navigation message latency – SISRE correlation plot (DOY 110–122 and 234–243 2009).

## 8.2 Use of GIOVE Results at the System Level

The GSTB-V2 experimentation activities have yielded several results that can be used to analyse the system performance. In the corresponding GIOVE experimentation, the areas of interest for system performance analysis using a Service Volume Simulator (SVS) include sensor station characterisation, orbit models and BGD results.

The results of the GIOVE experimentation in the areas of sensor station characterisation and orbit models are being used to update the ground segment parameters, in particular SISA and the contributions to the GSS error budget for the SISMA computation. Moreover, the results in the areas of orbit models and the BGD are being used to update user segment parameters, in particular the ODTS error contribution to the UERE budgets and the SISA value, as well as BGD uncertainty (Figure 8.7).

The GIOVE experimentation results of the system performance analysis using the SVS are being implemented as follows:

- Generation of adequate input parameters for the simulations from the experimentation results.
- Updates of UERE budget contributors based on GIOVE experimentation results.
- Analysis of system position accuracy and availability of accuracy based on updated UERE budgets.
- Update of GSS error budget contributors and GSS masking angle based on GIOVE results for SISMA computation.
- Determination of SISMA maps to identify the worst SISMA for performance simulations with fixed SISMA.
- Analysis of system integrity and availability of integrity based on updated UERE budgets and fixed SISMA.
- Analysis of system integrity and availability of integrity based on updated UERE budgets and SISMA maps.

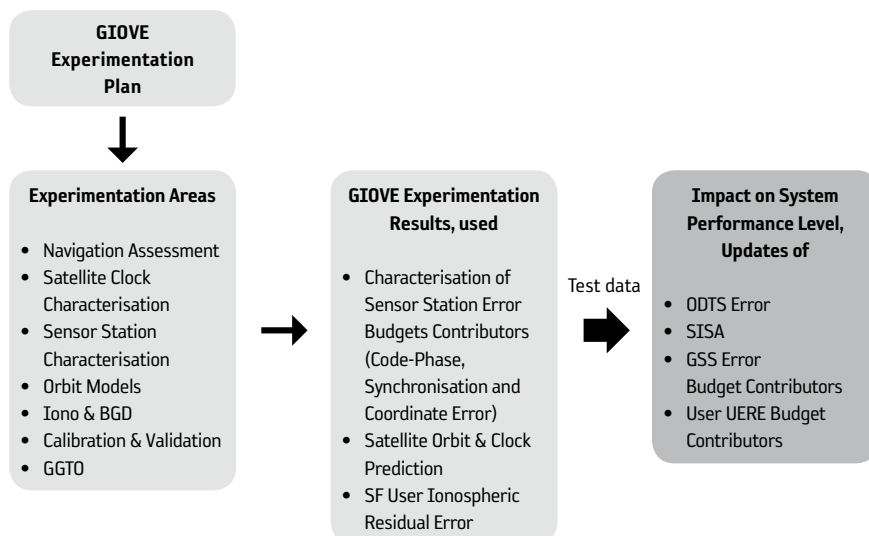


Figure 8.7. Overview of the impacts of the GIOVE experimentation at the system level

The System Performance team is contributing to this process by helping to define appropriate test cases in order to derive – as far as possible – all the appropriate performance figures of merit from GIOVE experimentations. For this activity the focus of the experimentation test cases should be on testing the performance of the key drivers that contribute to SVS input parameters (e.g. clock prediction error), are SVS input parameters themselves (e.g. state probabilities), or drive the system performance even if they are not direct inputs to the SVS (e.g. GGTO stability).

### Error Budget Update

Based on the GIOVE experimentation, the following UERE contributors have been adapted:

- ODTS error;
- SISA value;
- satellite BGD error (single frequency only);
- code carrier ionospheric divergence error (single frequency only); and
- residual ionosphere error (single frequency only).

The ODTS error is applicable for all accuracy simulations of the scenarios OS and SoL. For integrity simulations, the Signal-in-Space accuracy – the statistically overbounded ODTS error – is relevant instead. The derived UERE budgets for the dual-frequency test cases are presented in Figure 8.8.

### System Performance Analysis Results

For the system performance analysis using the GIOVE experimentation results several simulation scenarios (or services) have been selected. For the system performance simulations based on GIOVE Mission results, the Galileo System Simulation Facility (GSSF) has mainly been used.

The GSSF is a software simulator tool that reproduces the functional and performance behaviour of the Galileo system in order to support the simulation needs during the Galileo programme. The Service Volume Simulator capability of the GSSF allows analysis of the navigation and integrity performance. Considering the scenarios OS, Rural Vehicle, Dual Frequency without integrity, and E5a–E1 User, the achieved horizontal availability of accuracy with a nominal space segment is 100%, i.e. the horizontal position accuracy is 100% below the specified maximum horizontal position of 4 m. Even using a degraded space segment (one satellite not available) the horizontal availability of accuracy is between 99.3% and 100% (see Figure 8.9).

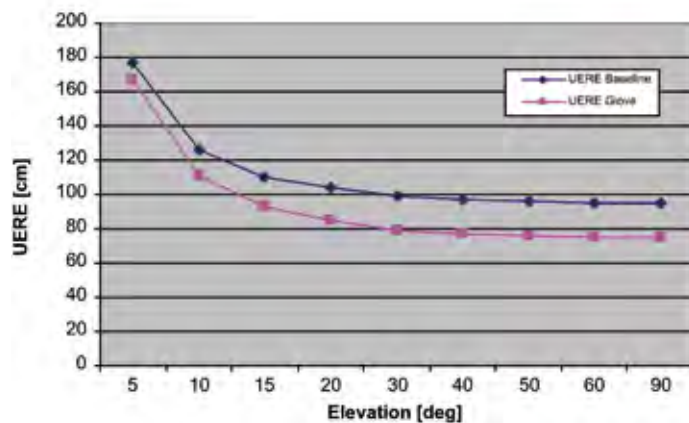


Figure 8.8. Comparison of UERE budgets IOV baseline and GIOVE (E5a–E1).

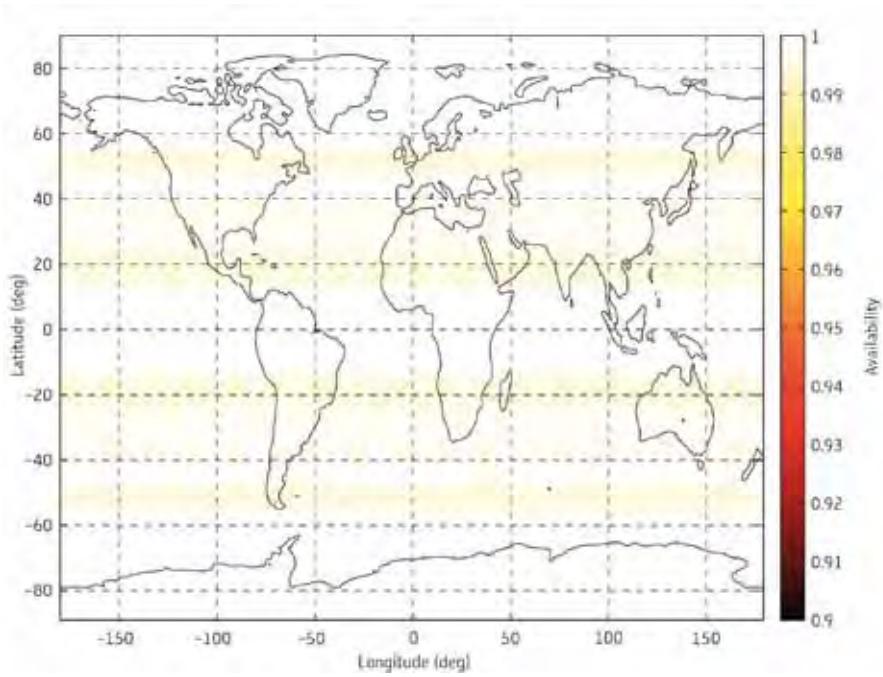


Figure 8.9. Availability of horizontal position accuracy, GIOVE, degraded space segment.

E5a-E1	Average	WUL	GSRD requirement
System availability of accuracy (%)	99.73	99.71	99.50

Table 8.2. System availability of accuracy.

The system availability of accuracy and integrity is then determined with the system state probabilities for the Worst User Location and the global average, as shown in Table 8.2.



**→ CONCLUSIONS**





## 9. Conclusions

### 9.1 GIOVE-A

Following an in-orbit test campaign performed in early 2006, GIOVE-A has proven to be an invaluable asset for the Galileo Programme and the wider navigation community. The availability of representative Galileo Signals in Space has enabled ESA to validate the GIOVE Mission Segment and associated operating procedures and analysis algorithms, such as orbit determination and clock modelling. This is an important step in preparing for the operation of the full Galileo Ground Segment. In addition, with the publication of the GIOVE-A SIS Interface Control Document, many receiver manufacturers have developed GIOVE capable receivers and have been able to verify their functionality using broadcast signals rather than simulations.

Operational Galileo satellites have more stringent requirements than the GIOVE satellites, in particular much longer lifetimes, higher performance specifications and additional services. However, the main payload units flown on GIOVE-A were pre developments for the final constellation and are quite similar to those to be flown on the operational satellites. The SSTL platform units flown on GIOVE-A were a mix of heritage commercial off-the-shelf (COTS) units and radiation-tolerant modules developed under a GEO development programme. The longer mission lifetimes specified for the full Galileo satellites mean that careful analysis of the environment is needed before proposing unit designs that will meet the environmental requirements, but which are still compatible with a tight schedule and are cost effective.

### 9.2 GIOVE-B

In the months following the launch of GIOVE-B on 26 April 2008, ESA coordinated an intensive in orbit test campaign involving several IOT stations and early orbit phase and platform commissioning activities.

ESA used the Chilbolton IOT station to carry out complementary IOT measurements in parallel to the main IOT station at Redu. The performance of the measurement system at Chilbolton had been proven during earlier GIOVE-A IOT campaigns. As a result, the combined STFC/SSTL team, working in collaboration with the ESA team, had already gained considerable experience in measuring and analysing satellite navigation signals.

The GIOVE-B satellite has joined GIOVE-A in routine operations. With the exception of specific future IOT activities or spacecraft maintenance, both satellites are now continuously broadcasting prototype Galileo navigation signals that can be used for several experimental purposes.

### 9.3 GIOVE Mission Segment

The GIOVE Mission is an integral part of the Galileo In-orbit Validation and has accomplished its objectives with the GIOVE satellites in the areas of payload technology validation (of signal, clocks and navigation message), Signal-in-Space experimentation (including receivers and antennas) and MEO radiation characterisation.

The GIOVE Mission infrastructure is fully deployed and has been operational since April 2007. Following the launch of GIOVE-B in 2008, the GIOVE Mission experimentation and operations were extended until mid-2011.

A number of upgrades to the GIOVE Mission core infrastructure have been implemented. The GIOVE Processing Centre facilities have been renewed and migrated to a new platform that provides improved processing capabilities to

cope with two GIOVE satellites and additional ground stations. An upgraded version of the GESS (GESS+) has been developed and integrated into the GIOVE Mission core infrastructure. Furthermore, the GPC has been fitted with capabilities to generate a set of key performance indicators in order to measure continuously the quality of the processing.

## 9.4 GIOVE-A: Five Years in Orbit

RAFS-A and RAFS-B have now accumulated more than 41 000 h in operation. The experimentation on GIOVE-A allowed the anticipation of several design, development and verification topics that are being encountered in Galileo IOV and that will also be experienced in Galileo FOC. These topics include:

- orbit estimation and prediction accuracy and the applicability of related models for navigation assessment and orbit models;
- extensive experimentation on the frequency accuracy and stability of the RAFS clocks for clock characterisation;
- estimation accuracy and the stability of the satellite and station inter-frequency biases for ionospheric and BGD experimentation;
- critical evaluation of the sensor station error budget and the derivation of site survey procedures for the sensor station characterisation; and
- derivation of operational methods for the GGTO estimation and prediction in the GGTO experimentation.

Also, the capability to generate and broadcast routinely the navigation message has been implemented, so that potential users can benefit from the presence of GIOVE-A and GIOVE-B to perform navigation solutions.

## 9.5 GIOVE-B: Three Years in Orbit

The PHM has accumulated more than 25 000 h of operation in orbit and has undergone several successful switch-on sequences.

The short-term stability of the PHM apparent clock is the best ever measured in space. The medium-term stability is affected by a periodic oscillation at the orbital period. Such oscillations have also been observed on the GPS satellites. In the long term, the PHM frequency drift is extremely low and no frequency jumps have been detected.

As of 15 June 2011, RAFS-A has been operating continuously for ~1000 h in orbit as a primary clock, with all telemetry fully nominal, while RAFS-B has been operating continuously for ~3200 h in orbit as a primary clock, the priority being given to experiments with the PHM.

## 9.6 GIOVE: Added Value of the Experimentation and Risk Mitigation for the IOV Phase

The experimentation with GIOVE has proven to be extremely useful in the early characterisation of payload critical technologies such as the RAFS, the PHM, the NSGUs and the navigation antenna. Moreover, it has provided and is still providing important results that can be used in the development of Galileo in all seven areas defined in the experimentation plan. For example, it will provide important feedback on the ionosphere behaviour over the coming years while solar activity is increasing.

## 9.7 A Verification Step in the Development of Galileo

The results of the GIOVE experimentation have been actively used by the System Performance team to update the assumptions on the errors of the User and Ground Mission Segment, especially in the areas of orbit determination, time synchronisation and Signal-in-Space accuracy. This has enabled an indirect step towards the verification of the main capabilities of the Galileo system, by extrapolating the performance of users receiving the ranging signals and the navigation message from GIOVE satellites. This has been possible due to the similarity between the GIOVE and Galileo IOV spacecraft and to the commonalities between the ground receivers deployed in the GIOVE Mission and those in the Ground Mission Segment of Galileo.

The GIOVE mission is planned to be instrumental in the maintenance of the Galileo system performance budget file until the advent of the IOV satellites.



**→ ANNEXES**



## Bibliography

The information contained in this publication has been presented at various public conferences and workshops. This bibliography lists the papers on GIOVE presented between 2006 and early 2010.

### PTTI 2010 Conference

Proceedings of the 2nd Annual Precise Time and Time Interval Systems and Applications Meeting, Reston, VA, USA, 15–18 November 2010:  
[www.pttimeeting.org/archivemeetings/ptti2010.html](http://www.pttimeeting.org/archivemeetings/ptti2010.html)

F. Gonzalez et al., Long-term Performance Analysis of GIOVE clocks

### ION GNSS 2009

Proceedings of the 22nd International Technical Meeting of the Satellite Division of the Institute of Navigation, Savannah, GA, USA (CD-ROM)

B. Bonhoure et al., GPS–GIOVE Mixed PVT Experimentation

G. Galluzzo et al., GIOVE-B Navigation Message Performance Analysis and Signal in Space User Ranging Error Characterization

J. Giraud et al., Latest Achievements in GIOVE Signal and Sensor Station Experimentations

V. Oehler et al., Galileo System Performance Status Report

A. Quiles et al., Development and Verification of Galileo Ground Mission Segment

G.J. Robertson et al., GIOVE-B Satellite Design and Performance Validation

G. Tobias et al., Building Galileo Navigation System: Two Years of GIOVE-M Experimentation

### ENC GNSS 2009

Proceedings of the ENC-GNSS 2009, Istituto Italiano di Navigazione, Naples, Italy (CD-ROM)

P. Durbà et al., Multi-Receiver GIOVE-M Sensor Station

M. Falcone, Galileo Status & Plans

N. Gerein et al., NovAtel's GIOVE Monitoring Receiver

M. Eleuteri et al., Detailed Analysis on GIOVE-B User Equivalent Range Error

G. Franzoni et al., Development of a MBOC Reference Receiver: Testing the Binary Offset-Carrier BOC Modulations Transmitted by the Second GIOVE Spacecraft, GIOVE-B

G. Galluzzo et al., GIOVE Navigation Message Validation through Key performance Indicators

I. Hidalgo et al., E-OSPF Experimentation Results in the Frame of the GIOVE-M Core Infrastructure

M. Kirchner et al., Results of the GIOVE Data Processing to Allow Evaluation of Principal System Performance Drivers

M. Malik et al., GIOVE-B Satellite & Payload Overview

A. Ostilio et al., Passive Hydrogen Maser (PHM): The Heart of the Galileo Navigation Payload

M. Soellner et al., One Year in Orbit: GIOVE-B Signal Quality Assessment from Launch to Now

### PTTI 2008 Conference

Proceedings of the 40th Annual Precise Time and Time Interval (PTTI) Systems and Applications Meeting, Reston, VA, USA, 1–4 December 2008

F. Gonzalez et al., In-orbit Performance Assessment of GIOVE Clocks  
R. Piriz et al., Estimation and Prediction of the GIOVE Clocks  
P. Waller et al., In-orbit Performance Assessment of GIOVE Clocks

### GIOVE Workshop, October 2008

GIOVE Workshop, October 2008: [www.giove.esa.int](http://www.giove.esa.int)

T. Burger, GIOVE-A and GIOVE-B Signal in Space Summary and SIS-ICD Publication  
M. Crisci et al., Galileo Receivers Experimentation  
C. Di Loreto, GIOVE-B Operations and Status  
J. Hahn et al., Galileo Performance Validation in Orbit with GIOVE  
M. Malik et al., In-orbit Test of the New Modulations  
D. Rodgers et al., Galileo MEO Radiation Environment: Summary of Results from GIOVE-A and GIOVE-B  
E. Rooney, GIOVE-A 2 years In-orbit Overview and Status  
A. Simsky et al., Early Experimentation with Sensor Station Characterisation  
R. Swinden et al., GIOVE Mission Segment and Website  
P. Waller et al., PHM and RAFS Clock Characterisation  
A. Woelker et al., GIOVE-B Overview and Status

### International Astronautical Conference (IAC), 2008

Space Communication and Navigation Symposium, Mobile communications and satellite navigation session, Glasgow, UK, 29 September–3 October 2008. IAC Papers Archive, IAC-08 (CD-ROM). [www.iafastro.net/iac/archive/browse/IAC-08/B2/](http://www.iafastro.net/iac/archive/browse/IAC-08/B2/)

G. Galluzzo et al., Development, Implementation and Integration of Key Performance Indicators within the GIOVE Mission Segment

### ION GNSS 2008

Proceedings of the 21st International Technical Meeting of the Satellite Division of the Institute of Navigation, Manassas, VA, USA (CD-ROM)

A. Simsky et al., Multipath and Tracking Performance of Galileo Ranging Signals Transmitted by GIOVE-B

### ENC GNSS 2008

Proceedings of the European Navigation Conference, Centre National d'Etudes Spatiales, Toulouse, France (CD-ROM)

M. Falcone et al., GIOVE Mission Processing Centre Modernisation and Operations  
A.M. Garcia et al., GIOVE Orbit and Clock Determination and Prediction: Experimentation Results  
J. Giraud et al., Station Measurement Quality with new Galileo Signals  
M. Tossaint et al., Galileo Initial Validation Step: GIOVE Navigation Message



### PTTI 2007 Conference

Proceedings of the 39th Annual Precise Time and Time Interval Systems and Applications Meeting, Long Beach, CA, USA, 27–29 November 2007

J.H Hahn et al., GIOVE-A Apparent Clock Assessment and Results

### ION GNSS 2007

Proceedings of the 20th International Technical Meeting of the Satellite Division of the Institute of Navigation, Manassas, VA, USA (CD-ROM)

M. Crisci et al., GIOVE Mission Sensor Station Performance Characterization: Overview of the Results

M. Falcone et al., An Incremental System Approach to Galileo In-orbit Validation

E. Rooney et al., Giove-A In-orbit Testing Results

A. Simsky et al., Multipath and Tracking Performance of Galileo Ranging Signals Transmitted by GIOVE-A

### Time Nav, 2007

European Frequency Time Navigation Forum, Geneva, Swiss Institute of Navigation, Switzerland, 29 May–1 June 2007

GIOVE-Mission, Signal Performance Characterisation Results

F. Droz et al., Galileo Rubidium Standard: Lifetime Data and GIOVE-A related Telemetries

P. Durbà et al., The Architecture of the Galileo System Test Bed (GSTB-V2) Mission Infrastructure

G. Gatti et al., GIOVE-A: Satellite Overview

G. Gatti et al., GIOVE-A Satellite & Payload Overview

J.H. Hahn et al., A Report on GPS and Galileo Time Offset Coordination Efforts

F. Mercier et al., CNES Contribution to GIOVE-A performance assessment

R. Piriz et al., Towards a Galileo Navigation Message

A. Simsky et al., Experience with Galileo Signal in the Field

### GALILEO One Year in Orbit Workshop, 2007

GALILEO One Year in Orbit Workshop, March 2007: [www.giove.esa.int](http://www.giove.esa.int)

C. Boulanger et al., CNES ODTS Cross Validation

M. Crisci, Sensor Station Characterisation Lessons Learned

M. Falcone, Experimentation Roadmap

M. Falcone et al., GIOVE-M Overall Architecture

J. Giraud et al., Sensor Station Characterisation Experimentation Results

F. Giuntini et al., GIOVE-M Core Infrastructure Overview

F. Giuntini et al., GIOVE-M Development

A. Hedqvist et al., GIOVE-M GPC Operations

M. Hollreiser et al., Galileo Receivers Lessons Learned

G. Mandorlo, GIOVE-A In-orbit Lessons Learned

R. Piriz et al., ODTS Methodology and Quality Control

P. Rochat et al., RAFS Assessment and Lessons Learned

E. Rooney, GIOVE-A Overview and Status

J.-M. Sleewaegen et al., Galileo Receivers Experimentation Results

P. Tavella et al., Apparent Clock Assessments

M. Tossaint et al., GIOVE-M Website and SIS ICD

### NAVITEC 2006

Proceedings of the 3rd ESA Workshop on Satellite Navigation User Equipment Technologies, ESTEC, European Space Agency, Noordwijk, the Netherlands, 11–14 December 2006 (CD-ROM)

M. Crisci et al., GIOVE Mission Sensor Station Receiver Performance Characterization: Preliminary Results

M. Spelat et al., Analysis and Validation of GIOVE-like SIS using ESTEC Laboratory Equipment

### ION GNSS, 2006

Proceedings of the 19th International Technical Meeting of the Satellite Division of the Institute of Navigation, Manassas, VA, USA, September 2006 (CD-ROM)

M. Falcone et al., GIOVE-A In-orbit Test Results Paper

G. Gatti et al., GIOVE-A Satellite: From Design to In-orbit Commissioning

R. Piriz et al., The Galileo System Test Bed V2 for Orbit and Clock Modelling

A. Simsky et al., Performance Assessment of Galileo Ranging Signals Transmitted by GSTB-V2 Satellites

M. Spelat et al., GIOVE-A Signal-in-Space Test Activity at ESTEC

## Acronyms and Abbreviations

<b>ACF</b>	Auto-Correlation Function	<b>GSTB</b>	Galileo System Test Bed
<b>ADEV</b>	Allan deviation	<b>GTRF</b>	Galileo Terrestrial Reference Frame
<b>AHM</b>	Active Hydrogen Maser	<b>GTR</b>	Galileo Test Receiver
<b>ANTEX</b>	ANTenna EXchange format files	<b>GVGA</b>	Galileo versus GPS analysis
<b>BGD</b>	Broadcast Group Delay	<b>IBUS</b>	In-band Unwanted Spurious
<b>BIPM</b>	International Bureau of Weights and Measures	<b>IDF</b>	IONO Disturbance Flag
<b>BOC</b>	Binary Offset Carrier	<b>IFB</b>	Inter-frequency Bias
<b>CAPE</b>	Carrier Phase Error Analysis	<b>IGS</b>	International GNSS Service
<b>CASM</b>	Coherent Adaptive Subcarrier Modulation	<b>ILRS</b>	International Laser Ranging Service
<b>CBOC</b>	Composite Binary Offset Carrier	<b>INRiM</b>	Istituto Nazionale di Ricerca Metrologica (Turin, Italy)
<b>CMCU</b>	Clock Monitoring and Control Unit	<b>IOT</b>	In-orbit Test
<b>CNA</b>	C/N analysis	<b>IOV</b>	In-orbit Validation
<b>COPE</b>	Code Phase Error Analysis	<b>IPF</b>	Integrity Processing Facility
<b>CV</b>	Common View	<b>ISB</b>	Inter-system Bias
<b>CW</b>	Continuous Wave	<b>ITU</b>	International Telecommunications Union
<b>CYSA</b>	Cycle Slip Analysis	<b>KPI</b>	Key Performance Indicators
<b>DME</b>	Distance Measuring Equipment	<b>MBOC</b>	Multiplexed Binary Offset Carrier
<b>DQT</b>	Data Quality Tool	<b>MEO</b>	Medium Earth orbit
<b>DSF</b>	Data Server Facility	<b>MODIP</b>	Modified Dip Latitude
<b>EGGTO</b>	Experimental GPS to Galileo Time Offset	<b>MP</b>	multipath
<b>EGST</b>	Experimental GIOVE System Time	<b>MUST</b>	Mission Utility and Support Tool
<b>EIRP</b>	Equivalent Isotropic Radiated Power	<b>M&amp;C</b>	monitoring and command
<b>E-IOT</b>	Extended In-orbit Test	<b>NAGU</b>	Notice Advisory to GIOVE Users
<b>E-OSPF</b>	Experimental Orbitography and Synchronization Processing Facility	<b>NAV</b>	Navigation
<b>E1/L1</b>	Carrier frequency designator 1575.42 MHz	<b>NRCan</b>	Natural Resources Canada
<b>E5a</b>	Carrier frequency designator 1176.45 MHz	<b>NSGU</b>	Navigation Signal Generation Unit
<b>E5b</b>	Carrier frequency designator 1207.14 MHz	<b>OASIS</b>	Offline Analysis of Signal In Space
<b>E6</b>	Carrier frequency designator 1278.75 MHz	<b>OBUS</b>	Out-of-band Unwanted Spurious
<b>FGUU</b>	Frequency Generation and Up-conversion Unit	<b>ODTS</b>	Orbit Determination and Time Synchronisation
<b>FOC</b>	Full Operational Capability	<b>PHM</b>	Passive Hydrogen Maser
<b>FPGA</b>	Field Programmable Gate Array	<b>POR</b>	Payload Operation Requests
<b>GCS</b>	Ground Control Centre	<b>PPP</b>	Precise Point Positioning
<b>GD</b>	Group Delay	<b>PPS</b>	pulses per second
<b>GDV</b>	Group Delay Variation	<b>PTF</b>	Precise Timing Facility (Galileo)
<b>GESS</b>	Galileo Experimental Sensor Station	<b>RAFS</b>	Rubidium Atomic Frequency Standard
<b>GETR</b>	Galileo Experimental Test Receiver	<b>RFI</b>	Radio-frequency Interference
<b>GGTO</b>	GPS to Galileo Time Offset	<b>RINEX</b>	Receiver Independent Exchange Format
<b>GIEN</b>	GESS Istituto Elettrotecnico Nazionale (now INRiM, Turin, Italy)	<b>RMS</b>	Root mean square
<b>GGTO</b>	GPS to Galileo Time Offset	<b>SISA</b>	Site Installation Sensitivity Analysis
<b>Glonass</b>	Global Navigation Satellite System (Russian Federation)	<b>SF</b>	Single Frequency
<b>GMS</b>	Ground Mission Segment	<b>SIRD</b>	Site Interface Requirement Document
<b>GNSS</b>	Global Navigation Satellite Systems	<b>SIS</b>	Signal-in-Space
<b>GPC</b>	GIOVE Processing Centre	<b>SISA</b>	Signal-in-Space Accuracy
<b>GPCI</b>	GIOVE Payload Control Interface	<b>SIS ICD</b>	Signal-in-Space Interface Control Document
<b>GSC-A/B</b>	Ground Satellite Control Centres, GIOVE-A/GIOVE-B	<b>SLR</b>	Satellite Laser Ranging
<b>GSS</b>	Galileo Sensor Station	<b>SRP</b>	Solar Radiation Pressure
<b>GSSF</b>	Galileo System Simulation Facility	<b>SSN</b>	Septentrio Satellite Navigation
<b>GSMU</b>	GSS model update	<b>SSPA</b>	Solid State Power Amplifier
<b>GST</b>	Galileo System Time	<b>SSTL</b>	Surrey Satellite Technology Ltd (UK)
		<b>STAA</b>	Station Availability Analysis
		<b>STEC/sTEC</b>	Slant Total Electron Content
		<b>STFC</b>	Science and Technology Facilities Council (UK)

<b>SVS</b>	Service Volume Simulator
<b>TAS-F</b>	Thales Alenia Space (France)
<b>TEC</b>	Total Electron Content
<b>TECU/TECu</b>	TEC unit
<b>TC</b>	Telecommand
<b>TM</b>	Telemetry
<b>TMBOC</b>	Time-multiplexed Binary Offset Carrier
<b>TT&amp;C</b>	Tracking, telemetry & command

<b>TWSTFT</b>	Two-way Satellite Time and Frequency Transfer
<b>USERE</b>	User Equivalent Ranging Error
<b>USNO</b>	US Naval Observatory
<b>UTC</b>	Coordinated Universal Time
<b>vTEC</b>	vertical Total Electron Content
<b>WUL</b>	Worst User Location





## ESA Member States

Austria  
Belgium  
Czech Republic  
Denmark  
Finland  
France  
Germany  
Greece  
Ireland  
Italy  
Luxembourg  
Netherlands  
Norway  
Portugal  
Romania  
Spain  
Sweden  
Switzerland  
United Kingdom

